

# Models and Methods for Tribology Across Scales: an Overview

A.I. Vakis, V.A. Yastrebov, J. Scheibert, L. Nicola, C. Minfray, A. Almqvist, M. Paggi, S. Lee, G. Limbert, J.F. Molinari, G. Anciaux, S. Echeverri Restrepo, A. Papangelo, A. Cammarata, P. Nicolini, R. Aghababaei, C. Putignano, S. Stupkiewicz, J. Lengiewicz, G. Costagliola, F. Bosia, R. Guarino, N.M. Pugno, G. Carbone, D. Dini, M.H. Müser and M. Ciavarella\*

## A.I. Vakis

Advanced Production Engineering, Engineering and Technology Institute Groningen, Faculty of Science and Engineering, University of Groningen, Nijenborg 4, 9747 AG Groningen, the Netherlands

## V.A. Yastrebov

MINES ParisTech, PSL Research University, Centre des Matériaux, CNRS UMR 7633, BP 87, F 91003 Evry, France

## J. Scheibert and C. Minfray

Laboratoire de Tribologie et Dynamique des Systèmes, UMR5513, CNRS/Ecole Centrale de Lyon/Univ Lyon/ENISE/ENTPE, 36 Avenue Guy de Collongue, F-69134 Ecully, France

## L. Nicola

Department of Materials Science and Engineering, Delft University of Technology, Mekelweg 2, 2628 CD Delft, The Netherlands; Department of Industrial Engineering, University of Padova, via Venezia 1, 35015 Padua, Italy

## A. Almqvist

Division of Machine Elements, Luleå University of Technology, Luleå, Sweden

## M. Paggi

IMT School for Advanced Studies Lucca, Multi-scale Analysis of Materials Research Unit, Piazza San Francesco 19, 55100 Lucca, Italy

## S. Lee

Department of Mechanical Engineering, Technical University of Denmark, DK-2800, Kgs. Lyngby, Denmark

## G. Limbert

National Centre for Advanced Tribology at Southampton (nCATS) | Bioengineering Science Research Group, Faculty of Engineering and the Environment, University of Southampton, Southampton SO17 1BJ, UK; Biomechanics and Mechanobiology Laboratory, Biomedical Engineering Division, Department of Human Biology, Faculty of Health Sciences, University of Cape Town, Anzio Road, Observatory 7925, South Africa

## J.F. Molinari and G. Anciaux

LSMS, ENAC, Swiss Federal Institute of Technology (EPFL), CH-1015, Lausanne, Switzerland

## R. Aghababaei

Department of Engineering, Aarhus University, Inge Lehmanns Gade 10, 8000 Aarhus C, Denmark

## S. Echeverri Restrepo

SKF Engineering & Research Centre (ERC), SKF B.V., Nieuwegein, the Netherlands; Department of Physics, King's College London, Strand, London WC2R 2LS, England, UK

## A. Papangelo

Hamburg University of Technology, Department of Mechanical Engineering, Am Schwarzenberg-Campus 1, 21073 Hamburg, Germany

## A. Cammarata and P. Nicolini

Department of Control Engineering, Faculty of Electrical Engineering, Czech Technical University in Prague, Karlovo náměstí 13, 12135, Prague 2, Czech Republic

## C. Putignano, G. Carbone and M. Ciavarella

Politecnico di Bari. V. le Gentile 182, 70125 Bari-Italy

## S. Stupkiewicz and J. Lengiewicz

Institute of Fundamental Technological Research, Polish Academy of Sciences, Pawinskiego 5B, 02-106 Warsaw, Poland

## G. Costagliola and F. Bosia

Department of Physics and Nanostructured Interfaces and Surfaces Centre, University of Torino, Via Pietro Giuria 1, 10125 Torino, Italy

## R. Guarino

Laboratory of Bio-Inspired & Graphene Nanomechanics, Department of Civil, Environmental and Mechanical Engineering, University of Trento, Via Mesiano 77, 38123 Trento, Italy

## N.M. Pugno

Laboratory of Bio-Inspired & Graphene Nanomechanics, Department of Civil, Environmental and Mechanical Engineering, University of Trento, Via Mesiano 77, 38123 Trento, Italy; Ket Lab, Edoardo Amaldi Foundation, Italian Space Agency, Via del Politecnico snc, 00133 Rome, Italy; School of Engineering and Materials Science, Queen Mary University of London, Mile End Road, E1-4NS London, United Kingdom

## D. Dini

Tribology Group, Department of Mechanical Engineering, Imperial College London, South Kensington Campus, Exhibition Road, London SW7 2AZ, UK

## M.H. Müser

Department of Materials Science and Engineering, Saarland University, 66123 Saarbrücken, Germany; John von Neumann Institut für Computing and Jülich Supercomputing Centre, Institute for Advanced Simulation, FZ Jülich, 52425 Jülich, Germany

\* Corresponding author. E-mail: mciava@poliba.it

## Abstract

This review summarizes recent advances in the area of tribology based on the outcome of a Lorentz Center workshop surveying various physical, chemical and mechanical phenomena across scales. Among the main themes discussed were those of rough surface representations, the breakdown of continuum theories at the nano- and micro-scales, as well as multiscale and multiphysics aspects for analytical and computational models relevant to applications spanning a variety of sectors, from automotive to biotribology and nanotechnology. Significant effort is still required to account for complementary nonlinear effects of plasticity, adhesion, friction, wear, lubrication and surface chemistry in tribological models. For each topic, we propose some research directions.

**Keywords:** tribology, multiscale modeling, multiphysics modeling, roughness, contact, friction, adhesion, wear, lubrication, tribochemistry

## 1. Introduction

The word tribology introduced in the famous Jost report of 1966 [1] was apparently coined by David Tabor and Peter Jost, deriving from the root tribo- (Greek τρίβος, meaning “rubbing”) and the suffix -logy (Greek -λογία, meaning “the study of”). The Jost report suggested that problems of lubrication in engineering needed an interdisciplinary approach –including chemistry and materials science, solid mechanics and physics. At that time, Jost suggested that the British industry could have saved £500 million a year “as a result of fewer breakdowns causing lost production; lower energy consumption; reduced maintenance costs; and longer machine life.” Fifty years later, frictional losses are often evaluated as costing more than 1 per cent of GDP [2], and tribology is therefore still flourishing.

There is no doubt that tribological interactions have a profound impact on many areas of engineering and everyday life. The widespread significance of these effects has been highlighted in many articles and reports over the years, which, however, until recently have mainly focused on lubrication and friction and wear-related energy and material losses for “traditional” industrial applications, such as manufacturing and automotive. The reader is referred to recent reviews, which have, for example, looked at the development of solid lubricant coatings [3], lubrication [4], and the interplay between surfaces and lubricants [5]. Other works have focused on how improvements in friction reduction technologies could significantly reduce frictional energy losses in passenger cars in the short, medium and long term [6]. Reducing wear can also improve long-term efficiency and performance of moving components, as well as reducing costs of maintenance and/or improving quality of life. Accordingly, much research into means of reducing friction and wear, together with the development of new additives, lubricants and functional materials to improve the performance of interfaces, has taken place, typically in the form of experimental studies for developing improved surface materials, topography/textures or lubrication. Most of these activities have been supported and accompanied by fundamental developments in contact mechanics, e.g. [7,8], as well as surface and material science, e.g., [9]. This has in turn improved our understanding of how surface roughness and surface modifications affect the response of components in various applications [10,11].

More recently, new areas of tribology have emerged, including nanotribology, i.e. the study of friction, wear and lubrication at the nanoscale as applied, for example, to micro- and nano-electromechanical systems (MEMS/NEMS), e.g., [12,13], and magnetic storage, e.g., [14,15], and biotribology, which deals with human joint prosthetics, dental materials, skin, etc., and ecological aspects of friction, lubrication and wear (tribology of clean energy sources, green lubricants, biomimetic tribology) [2,16-19]. Studies of superlubricity, i.e. the mechanisms responsible for extremely low friction [20-23], have created great expectations of energy savings, and the recent creation of graphene is also greatly

1 promising in this direction [24]. Insects' and reptile's adhesive performance inspired numerous studies  
2 on adhesive contacts (e.g. [25-29]) and resulted in improved understanding and successful mimicking  
3 of Nature-made feet [30-37]. Massive usage of tactile interfaces triggered multiple studies in  
4 understanding sensing through contact and friction [38], and in reproducing interactive haptic  
5 feedback to moving fingers [39-42]. In keeping up with and enabling such developments, new  
6 knowledge is necessary to describe complex multiscale and multiphysical phenomena within the  
7 context of tribology, both in the modeling and experimental domains.  
8

9  
10 In this contribution, we aim to summarize the presentations and discussions that took place during a  
11 Lorentz workshop on “Micro/Nanoscale Models for Tribology” in Leiden, the Netherlands, between  
12 30 January and 3 February 2017. It was found that one of the key issues facing the tribology  
13 community is the apparent disparity between the fields of expertise relevant to such an  
14 interdisciplinary topic, which leads to a lack of communication between engineers, material scientists,  
15 applied physicists and chemists who work to solve similar tribological problems: differences exist in  
16 notation, language, methods, the way in which problems are posed and how solutions are presented.  
17 Another finding is that new analytical models are necessary to understand the behavior at tribological  
18 interfaces, partly to avoid that numerical simulations become “black boxes” where the nuances of the  
19 phenomena involved are lost, and partly because full computational models often require prohibitively  
20 long computational times. At the same time, the industry would benefit from lightweight analytical  
21 models as long as those are sufficiently robust and able to predict critical quantities of interest with a  
22 priori known precision. Further adding to these challenges is the complexity of model validation: as  
23 the contact interface in most cases is not accessible to direct in situ observations, it is very difficult to  
24 carry out experiments aiming to access local near-surface states.  
25  
26  
27  
28

29  
30 Difficulties are further enhanced by divisions between modelers and experimentalists, as well as those  
31 working on analytical versus computational methods –and also between the proponents and users of  
32 different theories, computational methods and tools– and depending on the research applications.  
33 Since increased visibility and cooperation between tribologists from different backgrounds is  
34 necessary, the present review aims at providing a starting point for further collaboration and possible  
35 focal points for future interdisciplinary research in tribology. Accordingly, the paper is organized as  
36 follows: various modeling methods and tools are discussed in §2; research themes in tribology,  
37 including multiphysical aspects, rough surface representations, scale effects and the breakdown of  
38 continuum theories at the nano- and microscales, material models, normal contact, friction and other  
39 phenomena, as well as interdisciplinary case studies in biotribology are addressed in §3, and  
40 conclusions are given in §4.  
41  
42  
43  
44

## 45 46 **2. Tribological modeling methods**

47 This section introduces the main tools currently used in tribological modeling, starting from analytical  
48 models and discussing continuous and discrete mechanical and multiphysical methods suitable for  
49 simulations characterized by different time- and length-scales (see Fig. 1 for a map of representative  
50 tribological models built across the scales), namely finite and boundary element methods, discrete  
51 dislocation dynamics and atomistic methods, as well as multiscale approaches.  
52  
53  
54  
55  
56  
57  
58  
59  
60  
61  
62  
63  
64  
65

# Modelling in Tribology: from Electrons to Machines

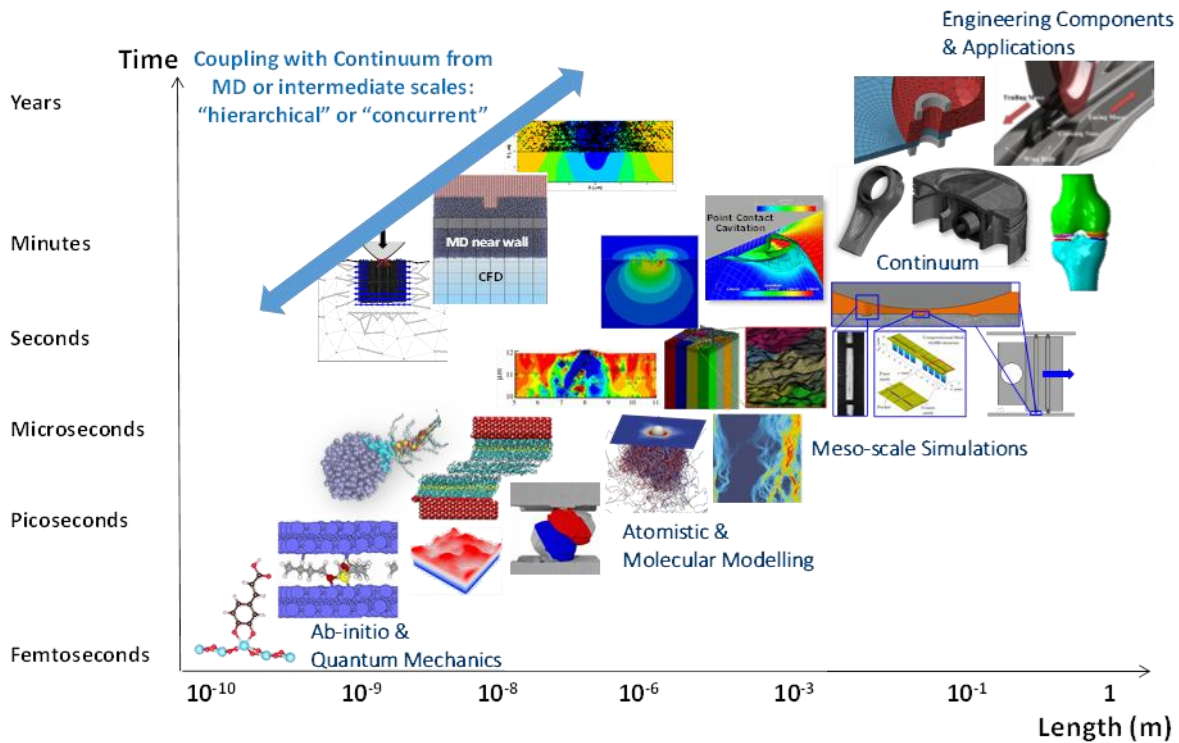


Fig. 1: A time- vs. length-scales map of models developed in tribology highlighting the intrinsic link between multiscale/physics that needs to be captured to provide predictive tools for engineering applications. Illustrations from simulations performed by the authors.

## 2.1. Analytical Methods

### 2.1.1. Contact mechanics: where we stand

A full overview of the field of contact mechanics and related developments that took place over the last century or so is out of the scope of the current contribution, as this would require a devoted review. For someone approaching this scientific area for the first time, K.L. Johnson's Contact Mechanics book [43] is still a very good starting point today. Later books and review papers, e.g. [44-48], have accounted for some of the progress made, but the field continues to expand across disciplines. The purpose of this sub-section is to briefly summarize some of the important milestones in this field and provide pointers to the readers interested in its different branches.

Starting from the mechanics of nominally smooth contact problems, the Hertzian theory, which solves the problem of two non-conformal elastic bodies being subjected to frictionless contact [49], is considered as a cornerstone of contact mechanics and tribology. Many of the analytical solutions available to practitioners and scientists have been building on Hertz; as is the case, for example, for two early models that constitute seminal advances in contact mechanics focused on the issue of adhesion: the models by Johnson-Kendall-Roberts (JKR) [50] and Derjaguin-Muller-Toporov (DMT) [51]. The JKR and DMT models, which describe the adhesive contact between compliant or hard spheres, are still very popular, while the body of literature available on this topic is immense; adhesion is discussed in detail in §3.7.

Remaining in the realm of smooth contact problems, but moving away from the Hertzian theory of elastic contacting bodies and its limitations (only accurate for small contact areas when compared to all other length scales), progress has been made in a number of other areas: these include, for example,

1 layered and coated systems, also in the presence of anisotropic and functionally graded materials [52-  
2 60], contacts in the presence of sharp edges [61-64] and conformal configurations [65]. Other  
3 examples of recent developments in the field are the use of asymptotic analyses to study the stress  
4 fields and sliding behavior associated with different contact configurations [66-69], the study of  
5 contact in the presence of anisotropic and functionally graded materials, and varying friction  
6 coefficient along the interface in sliding and partial slip conditions [70]. In the case of the normal  
7 contact of inelastic solids, significant developments have been made since Johnson's core model of  
8 elasto-plastic indentation based, for example, on the progress of instrumented nanoindentation in the  
9 last 25 years (see, e.g., [71-73]); issues of plasticity and material models are discussed further in §3.4.  
10 Some progress has also been made on tangential loading and cyclic contact with the generalized  
11 solution of contact problems characterized by time-dependent stick-slip transitions at the macroscopic  
12 scale (see, e.g. [61,74-78]).  
13  
14

15  
16 Somewhat in parallel to the above advances and studies, many developments in the study of nominally  
17 smooth contacts in the presence of lubrication have also been made; these are discussed in §2.4 and  
18 §3.8.  
19

20  
21 On dynamic effects and impact, much work was published on the rate-and-state friction (RSF) law  
22 (also discussed in §3.6.2) and Adams' instability [79-81], while impact remains a somewhat separate  
23 and large research area, with applications in different research area and applications including powder  
24 technology, manufacturing processes and ballistics [82-87]. Following the classical contributions by  
25 J.R. Barber on both static and sliding contact reviewed in Johnson's book, new refined solutions and  
26 finite element formulations have appeared on thermoelastic contact (see, e.g., recent contributions  
27 [88,89] and further discussion in §2.6).  
28  
29

30  
31 Moving on to applications strongly linked to the development of contact mechanics methodologies,  
32 various advances have been made in *e.g.* the understanding of fretting fatigue thanks to the  
33 development of various techniques, which have been used to study individually or simultaneously  
34 various aspects of this complex problem, such as stress gradients, fatigue, surface damage and wear  
35 [90-95]. Progress has also been made in the study of rolling contact of elastic and inelastic  
36 (shakedown, ratchetting, etc.) bodies and rolling contact fatigue (see, e.g., [96-103]). Calendering, *i.e.*  
37 the elastic-plastic rolling of strips have also seen some developments [104].  
38  
39

40  
41 On the topic of contact mechanics of rough surfaces, the seminal work by Greenwood and Williamson  
42 (GW) [7] forms the basis for a number of multi-asperity models (discussed critically in §2.1.2).  
43 Among many subsequent analytical models, some were developed based on the analysis of two or  
44 more scales, adding for example the periodic microgeometry of multi-layered elastic or viscoelastic  
45 half spaces to study normal contact and friction in the presence of coatings [105,106] or adhesion and  
46 lubrication [107,108]. Interestingly, one of the most popular theories after the GW is that of Majumdar  
47 and Bhushan [109], where Korcak's law was used to define a power law distribution of contact spots,  
48 a "bearing area" result very much in contrast with the present understanding of the contact area being  
49 formed by "resolution-dependent" contact spot sizes. This view of "magnification-dependent" solution  
50 is not too different from the original Archard model [110] of spheres sitting on top of spheres, or work  
51 on fractal description based on a Weierstrass series within the elasticity assumption to obtain the result  
52 that the contact area decreases without limit as the resolution (or magnification) is increased [111].  
53  
54  
55

56  
57 The alternative to the solutions proposed in the methodologies to study rough contacts reviewed above  
58 is Persson's theory [8], which has become the basis of another class of models, in which the stress  
59 probability distribution is considered as a function of the surface resolution under examination. The  
60  
61  
62



1 tribology community still uses both the GW and Persson approaches to model rough contact based on  
2 considerations of accuracy and simplicity which may well reflect the corresponding physics and  
3 engineering perspectives. The GW and Persson models are introduced in more detail next; a  
4 comparison between them in the context of the recent contact-mechanics challenge is given in §3.5,  
5 while the topic of roughness itself is described extensively in §3.2.  
6

### 7 **2.1.2. Multi-asperity models and Persson's theory: an introduction**

8 The nature and various representations of surface roughness, discussed in more detail in §3.2, have  
9 been central to the prediction of tribological quantities ranging from the true area of contact to the  
10 normal, friction and adhesion forces, as well as phenomena such as electrical conductance and  
11 percolation. Starting from the simplest problem definition of normal contact between two rough  
12 surfaces in the absence of other phenomena, two seminal works have formed the backbone of research  
13 in the field: the Greenwood-Williamson (GW) model [7] and Persson's theory [8]. These are  
14 introduced below, while the results of a recent contact-mechanics challenge are summarized in §3.5,  
15 extending beyond predictions of the true contact area and into more detailed metrics of normal contact.  
16  
17  
18

19 Greenwood and Williamson conducted a pioneering study targeted towards predicting the link  
20 between the approach of nominally flat but rough surfaces (quantified as the distance between their  
21 mean planes) and the resulting force and true contact area [7]. The GW and subsequent multi-asperity  
22 models are based on the following assumptions: 1) the effective rough surface (a superposition of two  
23 rough profiles or surfaces) can be represented by an ensemble of asperities (surface summits),  
24 characterized by the vertical coordinate of the tip and its curvature(s); 2) these characteristics are  
25 known in the statistical sense, for example, via the probability density of the asperities' vertical  
26 position; 3) the relation between penetration, force and the contact area follows the Hertzian theory of  
27 contact; 4) the asperities of the effective rough surfaces coming into contact are separated in the plane  
28 by distances at which their mutual influence can be neglected. In the original GW, all asperities are  
29 approximated as parabolic ones with the same curvature radius, and an arbitrary height distribution is  
30 assumed, contrary to numerous references in the literature erroneously stating that the GW model is  
31 based on Gaussian distribution of asperity heights: both Gaussian and exponential tails are considered  
32 in the original paper.  
33  
34  
35  
36  
37

38 Subsequent progress in statistical multi-asperity models was triggered by the seminal paper of Nayak  
39 [112], which was in turn inspired by the works of Longuet-Higgins who was the first to apply the  
40 random process model for analysis of random surfaces in the ocean [113,114]. Based on the same  
41 assumption, i.e. that a rough surface can be represented as a two-dimensional isotropic Gaussian  
42 process, Nayak obtained the relation between the spectral moments of the surface and the distribution  
43 of asperities, their density, curvature, ellipticity, etc. He also introduced a central quantity for  
44 roughness description, a dimensionless combination of the zeroth, second and fourth momenta,  
45 subsequently referred to as the *Nayak parameter* that characterizes spectral breadth. Based on Nayak's  
46 statistical results, Bush, Gibson and Thomas (BGT) [115] obtained a new approximation for the  
47 dependence of the force density and contact area fraction taking into account, among other of Nayak's  
48 results, the ellipticity of asperity tips. Much later, Greenwood [116] demonstrated that, according to  
49 Nayak's theory, the ellipticity of asperities is rather mild, and thus an approximate Hertzian equation  
50 for the elliptic contact can be employed, which makes use of the geometric mean value of two  
51 principal asperity curvatures. This "simplified elliptic model" yields relatively simple equations for  
52 force and area dependence as functions of the approach (or separation). Among other interesting  
53 results, Greenwood demonstrated that according to the random process model, the probability of  
54 finding a spherical asperity is strictly zero.  
55  
56  
57  
58  
59  
60  
61  
62  
63  
64  
65

1 Multi-asperity models predict asymptotic linearity between the contact area and the load with a factor  
2 containing a proportionality coefficient  $\kappa$  and, in the denominator, a product of the effective elastic  
3 modulus and the root mean squared roughness gradient (or equivalently, a square root of the doubled  
4 second spectral moment). However, it is important to remark here that this proportionality holds only  
5 for vanishingly small contact area intervals, which depend on the Nayak parameter: the higher this  
6 parameter is, the smaller the region of validity [116-118]. In this light, the proportionality predicted  
7 between the load and the area remains a mathematical abstraction and cannot be used directly in  
8 engineering practice. However, the usage of multi-asperity models is not restricted to vanishingly  
9 small areas, but can also be used for higher loads at which the area evolves nonlinearly with the load  
10 and strongly depends again on the Nayak parameter [115,118]: the higher the Nayak parameter, the  
11 smaller the contact area. Comparison of multi-asperity models with full numerical simulations of  
12 rough contact (free of the multiple assumptions of multi-asperity models) demonstrated that, indeed,  
13 the Nayak parameter plays an important role in contact area evolution, but its effect in multi-asperity  
14 models is strongly exaggerated [119].  
15  
16  
17

18 Further improvements in multi-asperity models attempted to incorporate elastic interaction between  
19 asperities, based on the following motivation: if one asperity comes into contact and produces a force,  
20 then the vertical position of all surrounding asperities needs to be changed by, approximately, a value  
21 proportional to this force and inversely proportional to the distance to its point of application (for the  
22 precise formulations refer to [43]). This can be done in a statistical framework by assuming zero-order  
23 interaction, i.e. the vertical positions of all asperities are decreased by a value proportional to the  
24 product of a nominal pressure and the contact area [120-122]. A further improvement in terms of  
25 elastic interaction relied on the rejection of a purely statistical model and the resorting to deterministic  
26 models instead, taking into account the in-plane positions of all asperities. In this deterministic  
27 framework, not only elastic interactions can be accurately accounted for [117,123], but so can the  
28 merging of contact areas related to distinct close asperities [124].  
29  
30  
31  
32

33 In 2001, B.N.J. Persson suggested another analytical model for predicting the contact area and other  
34 related quantities [8] that relies on completely different considerations and, therefore, does not suffer  
35 from the multiple assumptions inherent in multi-asperity models (even though it introduces its own).  
36 Persson's theory is based on the following consideration: let us assume contact between two flat  
37 surfaces squeezed together by a nominal pressure  $p_0$  such that the probability density of interfacial  
38 pressure is simply a Dirac delta-function centered at  $p_0$ . When new modes are progressively injected  
39 into the spectrum of contacting surfaces, the corresponding pressure distribution function spreads out  
40 as a Gaussian distribution. If the full contact is preserved, the link between the statistical  
41 characteristics of the height distribution and interfacial pressure distribution can be easily established:  
42 the variance of the contact pressure is proportional to the product of the variance of the surface  
43 gradient and squared effective elastic modulus. Based on these considerations, a diffusion-type  
44 equation was formulated for the contact pressure distribution (acting as the concentration quantity),  
45 with the pressure variance acting as the time and the local pressure acting as the space coordinates  
46 [8,125,126] considering, up to this point, only full contact. Since Gaussian support is infinite, tensile  
47 stresses will occur in the contact interface for an arbitrary finite external pressure. To get rid of these  
48 and extend the theory to partial contact, Persson introduced a boundary condition stating that the  
49 probability density of zero pressure vanishes during contact. This statement can be confusing since, as  
50 soon as partial contact is established, all non-contact zones do not experience any contact pressure,  
51 thus resulting in Dirac-delta function distributions at zero pressure scaled by a factor of the non-  
52 contact area fraction. Alternatively, this boundary condition can be stated in a limit-form: probability  
53 density tends to zero as pressure tends to zero. Indeed, this boundary condition seems very reasonable  
54  
55  
56  
57  
58  
59  
60  
61  
62  
63  
64  
65

1 if one thinks about the fact that, for Hertzian contact, the pressure drops to zero at the contact edges  
2 with an infinite slope, thus resulting in the linear growth of probability density near zero pressure. The  
3 main remaining assumption of Persson's theory is the validity of the diffusion equation for partial  
4 contact accounting for the fact that it was derived for full contact.

5  
6 Apart from other quantities of interest, Persson's theory predicts that the contact area evolves as an  
7 error function, from zero to full contact, which is reached for infinite nominal pressure. Since the  
8 Taylor expansion of the error function in the vicinity of zero contains only odd powers, the contact  
9 area can be approximated with a high degree of confidence by a linear function of nominal pressure  
10 with a factor given by a proportionality coefficient divided by the product of a root mean squared  
11 roughness gradient and the effective elastic modulus. The sole difference between this prediction and  
12 those of multi-asperity models is the proportionality factor  $\kappa$ , which is approximately 1.60 in Persson's  
13 theory and approximately 2.51 in multi-asperity models. The second crucial difference is that, contrary  
14 to multi-asperity models, Persson's linearity is valid for realistic area/pressure intervals. Finally, the  
15 third difference is that the sole roughness parameter needed for Persson's theory is the root mean  
16 squared roughness gradient so that, contrary to multi-asperity models, this theory has no dependence  
17 on the Nayak parameter.

18  
19 Numerous comparisons between complete numerical simulations, multi-asperity models and Persson's  
20 theory can be found in the literature [117-119,125-139]. The rough conclusion of all these studies with  
21 respect to the contact area evolution can be formulated as follows: Persson's model nicely predicts the  
22 qualitative growth of the contact area with increasing nominal pressure up to full contact. For  
23 moderate loads, the true contact area evolves slightly nonlinearly and is below the asymptotic  
24 prediction of multi-asperity models and above the prediction of Persson's theory. Meanwhile, an  
25 improvement in Persson's theory was introduced to take into account partial contacts in a more  
26 rigorous way [140], yielding results that are much closer to numerical solutions. Very recent findings  
27 demonstrate that the contact area growth is dependent not only on the root mean squared gradient but  
28 also weakly on the Nayak parameter [119] which is absent in Persson's theory, but is inherent to multi-  
29 asperity models that, however, strongly overestimate its effect.

## 30 **2.2. Finite and Boundary Element Methods**

31 Two major families of methods can be distinguished in continuum mechanics: the Finite Element  
32 Method (FEM) [141] and the Boundary Element Method (BEM) [142]. Both are based on a variational  
33 principle, the virtual work principle for the FEM and the minimization of the complementary work for  
34 the BEM. In the FEM, an explicit relation between the strain (and possibly strain rate and its history)  
35 and the stress can be prescribed, either within infinitesimal or finite strain formulations, enabling this  
36 method to consider arbitrary constitutive material models starting from simple linear elasticity up to  
37 complex crystal plasticity. The BEM uses in its formulation a fundamental solution for the normal and  
38 tangential point forces, which enables linking surface tractions with surface displacements.  
39 Equivalently, to formulate a spectral version of the BEM, a fundamental solution linking pressure and  
40 vertical displacement for a combination of harmonics in two orthogonal directions should be used  
41 [143,144]. Such solutions exist for a limited number of cases and mainly under the assumption that the  
42 solid can be locally considered as a flat half-space. These limitations imply a more restrictive field of  
43 application for the BEM compared to the FEM, which is a versatile numerical method. It is worth  
44 mentioning that, in general, contact problems are nonlinear even if frictionless and non-adhesive  
45 contact is considered between linearly elastic solids. This is because the contact area is a priori  
46 unknown, apart from simple cases such as the rigid flat stamp problem or the case of full contact. In  
47 analogy, a full stick frictional condition (infinite friction) makes the frictional problem much easier to  
48 handle than a problem with a finite friction. The detailed description of numerical methods within the



1 FEM formulation can be found in the literature, e.g., [145-147], as can be a comparative analysis of  
2 BEM formulations with application to rough contact mechanics [148]. There are also many instances  
3 in which FEM and BEM can be coupled into FEM-BEM solvers for the solution of three-dimensional  
4 contact problems [149] or can be combined to achieve different levels of refinement in the solution to  
5 the problem under investigation (see, e.g., [150]).  
6

7 The FE approach to tribological problems involves discretization of the volumes of contacting bodies  
8 and an appropriate treatment of their contact interaction. The arbitrariness of material models as well  
9 as the geometries of contacting solids and their heterogeneity that can be reached in the treatment of  
10 contact interfaces make this method a multipurpose engineering tool. However, this is all at the cost of  
11 high computational complexity as compared to the BEM, which has less versatility but much more  
12 efficiency in the treatment of interfacial problems, since it requires solving the problem only for  
13 surface degrees of freedom and does not require any discretization in the volume. On the other hand,  
14 the BEM results in dense systems of linear algebraic equations, contrary to the FEM, which renders  
15 sparse systems of equations. Thus, the BEM has to rely on iterative solvers, whereas the FEM can  
16 successfully use either iterative or direct solvers based on the sparse matrix storage.  
17  
18  
19

20  
21 When interested in near-surface stress fields, which are crucial in the reliable analysis of surface  
22 deterioration (e.g., fretting fatigue and wear) and microscopic contact at the roughness scale, imprecise  
23 integration and/or discretization may result in huge errors in local fields and, thus, in realistic  
24 estimations. To properly capture the stress field in the vicinity of a contact zone, and especially near its  
25 edges (which, in most problems, is unknown), requires a very dense spatial discretization. The  
26 accuracy of the integration technique is especially crucial when a conformal mesh cannot be ensured  
27 on the contacting parts (e.g., large-deformation or large-sliding contact systems) and if two deformable  
28 solids of comparable stiffness are brought into contact, i.e., when one of the solids cannot be  
29 considered as rigid. In addition, the path-dependence of frictional problems requires that the load  
30 increment should be chosen properly, as the temporal discretization plays a crucial role even in quasi-  
31 static problems: as an example, for the shear tractions in normal Hertzian cylindrical contact with  
32 friction in the interface, the self-similar character of the solution, as argued by Spence [151], can be  
33 obtained with one hundred load steps with the displacement increment proportional to the time  
34 squared, but not within one single load step.  
35  
36  
37  
38

39  
40 In tribology, due to its computational cost, application of the FEM is justified if the problem at hand  
41 cannot be solved within the assumptions of the BEM, namely the existence of a fundamental solution  
42 and the local flatness of the surface (infinitesimally small slope). A broad family of systems falls  
43 within this context: large-deformation, large-sliding contact of soft bodies, which can be observed in  
44 various biological systems (oral food processing, contact of skin, etc.), but also in engineering  
45 applications (contact of tires, polymeric seals and many others) or contacts involving strongly  
46 nonlinear material behavior which is hard to represent within the BEM framework such as indentation  
47 involving strong finite-strain plastic deformations or fracture in the interface.  
48  
49

50  
51 Concerning the applications to microcontacts and microtribology, both FE and BE methods are used  
52 extensively. At the scale of roughness, the macroscopic shape of the contacting solids can be usually  
53 neglected and, since the roughness slope is in general rather small, the problem satisfies the main  
54 assumption of the BEM, which can be successfully used for its solution. The evolution of the true  
55 contact area, interface permeability, electric and thermal contact resistance can all be resolved in the  
56 framework of the BEM for linear material laws. Regarding material nonlinearities, elasto-plastic [152-  
57 154] and viscoelastic [155,156] material behavior can be incorporated in the BEM framework by  
58 assuming that deformations and slopes remain small, otherwise an FEM would be needed [157,158]. It  
59  
60  
61  
62  
63  
64  
65

1 should remarked that most contact systems involving elasto-plastic materials operate mainly in the  
2 elastic regimes both at the micro- and macroscales; hence, depending on the level of stress and the  
3 type of loading, considering plastic deformation may be important during the first loading cycles but  
4 may not be needed in subsequent ones. Furthermore, severe plasticity is associated with wear and must  
5 therefore be incorporated in the simulations, but how can one explicitly model wear numerically (e.g.  
6 using both BEM and FEM)? The issue of wear is partly discussed in §3.9.1.  
7

8 The BEM framework can consider homogeneous nonlinear material behavior, but can also account for  
9 heterogeneous inclusions in the bulk, e.g., [159], which is often critical for microscale analyses in  
10 which the material's microstructure might play an important role. This, for example, is the case in  
11 contact problems involving functionally graded interfaces [160], metallic polycrystalline [161] or  
12 monocrystalline [162] microstructures, whose accurate treatment requires the FEM. Concerning  
13 multiphysical (multi-field) problems, both methods are comparable at the scale of roughness, with the  
14 same limitations and advantages: simple but fast BEM versus slow FEM but with capabilities to  
15 account for arbitrary complexity. Examples of applications include: lubrication problems [163-165],  
16 electro-elastic contact modeling [166,167], thermo-mechanical coupling [168], and many others.  
17 Using BEM-type formulations has also been used to treat elasto-dynamic frictional problems  
18 [169,170], whereas complex geometries and boundary conditions would still require usage of FEM or  
19 equivalent formulations [171,172].  
20  
21  
22  
23

24 In summary, both the FE and BE methods are well developed and able to solve most micro-  
25 tribological problems involving both material nonlinearities and multiphysical couplings with the  
26 FEM being more versatile and more easily accessible for a general researcher and engineer (numerous  
27 commercial and open software are available) but computationally costly, and the BEM being less  
28 available and versatile, but still capable of solving most problems under reasonable assumptions and  
29 for very moderate computational costs. The main challenge here for the researchers and engineers  
30 would be to promote both methods within the homologue communities and to enable them to use one  
31 or the other based on the needs of the target application.  
32  
33  
34

### 35 **2.3. Crystal plasticity and Discrete Dislocation Dynamics**

36 Crystal plasticity is a well-established constitutive framework for the modeling of elasto-plastic  
37 deformations of metal crystals [173-176]. The essential feature of crystal plasticity is that plastic  
38 deformation is assumed to result from plastic slip on specified crystallographic slip systems. An  
39 individual slip system is active when the shear stress acting on it (called the resolved shear stress)  
40 exceeds the corresponding critical resolved shear stress, the latter being governed by an evolution  
41 (hardening) law that is expressed in terms of slip rates for all active slip systems. By considering the  
42 crystallographic features of plastic deformation, crystal plasticity provides a physics-based continuum  
43 description of single crystals as well as of individual grains in polycrystalline aggregates [177,178].  
44  
45  
46  
47

48 Once combined with a suitable scale transition scheme (mean-field homogenization, Representative  
49 Volume Element (RVE)-based computational homogenization, etc.), crystal plasticity has proven to be  
50 highly successful in predicting the effective elasto-plastic behavior of polycrystalline aggregates, e.g.,  
51 [179-181]. A notable example is the visco-plastic self-consistent (VPSC) model [182], which is widely  
52 used for predicting hardening and texture evolution in plastic forming processes. The crystal plasticity  
53 framework has also been extended to include, in a simplified manner, other deformation mechanisms,  
54 such as deformation twinning [183,184] and martensitic phase transformations [185,186].  
55  
56  
57

58 Being a continuum theory, crystal plasticity is not applicable at very small scales at which discrete  
59 events, e.g., those related to the nucleation and propagation of dislocations, become important, and  
60  
61  
62  
63  
64  
65

1 other approaches, such as discrete dislocation dynamics (see below) and molecular dynamics (see  
2 §2.4), are then more appropriate. Even at higher scales, important phenomena that accompany plastic  
3 deformation, e.g., the formation of dislocation structures, deformation banding and grain refinement,  
4 are not captured by the available crystal plasticity models, even though attempts in that direction have  
5 been made [187-190]. In general, plastic deformation is inhomogeneous at multiple scales, and crystal  
6 plasticity is not capable of describing many of the related phenomena.  
7

8 Discrete Dislocation Dynamics (DDD) is a modeling technique to study plasticity at the microscale  
9 [191-196]. In DDD, the solid is modelled as a linear elastic continuum, and the dislocations by means  
10 of their linear elastic fields, which are accurate outside of the dislocation core. Atomistic aspects are  
11 included by means of constitutive rules that govern dislocation nucleation/annihilation, glide, and  
12 interaction with obstacles and dislocations. Given that both the dislocations and the solid are described  
13 using linear elasticity, it is possible to solve boundary value problems relying on the principle of  
14 superposition. The solution to the boundary value problem is given at each time increment and at  
15 every material point as the sum of the dislocation fields and their image fields. The image fields can be  
16 calculated using finite elements, although, for contact problems, where rough surfaces need to be  
17 described using a fine discretization, it is computationally more efficient to use other techniques, such  
18 as, for instance, Green's Function Molecular Dynamics (GFMD) [197].  
19  
20  
21  
22

23 Important recent advances in this area include, for example, the development of a formulation that  
24 incorporates elastodynamic effects in the description of the interactions between dislocations. The  
25 resulting methodology, Dynamic Discrete Dislocation Plasticity (D3P; see, e.g., [198], allows the  
26 treatment problems characterized by high strain rate deformation such as shock waves [199] and could  
27 be used to perform concurrent coupling (see §2.6) with atomistic simulations in order to avoid issues  
28 with the transition between the atomistic-continuum boundaries. Furthermore, concurrent  
29 methodologies (also see §2.6) to directly couple crystal plasticity and DDD have been also developed  
30 [200,201] to take advantage of the fact that the DDD formulation is only required in very small  
31 regions in the presence of stress concentrations, such as cracks and indentation of asperity-to-asperity  
32 interactions.  
33  
34  
35  
36

#### 37 **2.4. Modelling Methods for Lubrication, Solid/Fluid Interactions and Particle Dynamics**

38 The computational methods introduced in the previous two sections mainly cover formulations and  
39 methodologies adopted to model dry contact problems and focus on detailed descriptions of solid  
40 deformations and stresses. However, other techniques must be adopted when modelling lubrication  
41 and solid/fluid interactions in the presence of a fluid film interposed between contacting bodies.  
42 Hydrodynamic Lubrication (HL) and Elasto-Hydrodynamic Lubrication (EHL) are lubrication regimes  
43 where a thin lubricant film is formed between two surfaces in relative motion. HL takes place in  
44 conformal contacts, when low pressures are established between the two surfaces, while EHL takes  
45 place when pressures are significant enough to cause considerable elastic deformation of the surfaces.  
46 EHL usually occurs in non-conformal contacts and many machine elements, including rolling bearings  
47 and gears, rely on EHL in their operation. Although existence of a fluid film sufficient to separate two  
48 surfaces under hydrodynamic conditions, such as in a journal bearing, has been known since the work  
49 of Tower in 1883 [202], it was not until 1949 that Grubin predicted that a thin fluid film can also  
50 separate surfaces in high pressure, non-conformal contacts [203]. Formation of such a film is possible  
51 due to high pressure having two beneficial effects: firstly, it increases lubricant viscosity in the contact  
52 inlet and, secondly, it elastically deforms and flattens the contacting surfaces, hence the term elasto-  
53 hydrodynamic lubrication.  
54  
55  
56  
57  
58  
59  
60  
61  
62  
63  
64  
65

1 Classical solutions of HL and EHL contact problems use the Reynolds' equation [204] to describe the  
2 behavior of the lubricant, while elastic deformation is traditionally calculated using Hertz theory of  
3 elastic contact, although nowadays BEM or FEM solvers are also routinely used. Reynolds's equation  
4 is a simplification of full Navier-Stokes equations, derived by assuming a Newtonian lubricant with  
5 constant density and constant pressure and viscosity across the film thickness. Cameron et al. [205]  
6 developed the first Reynolds-based computerized numerical solutions for hydrodynamic lubrication  
7 and in 1959 Dowson and Higginson [206] produced the first full numerical solution for EHL.  
8 Subsequently, Dowson and co-workers, also proposed regression equations for prediction of the EHL  
9 film thickness based on their numerical solutions and a number of other improvements including the  
10 consideration of material properties and thermal effects (e.g., [207-209]). In the last fifty years, many  
11 numerical approaches [210-214] have been developed to address the solution of this set of equations:  
12 nowadays, it is possible to account for a variety of non-Newtonian effects, ranging from piezo-  
13 viscosity to shear thinning. The majority of these approaches uses a Finite Difference (FD) scheme,  
14 although the use of the FEM and Finite Volume (FV) methodologies has recently been proposed  
15 especially to overcome some of the limitations of FD when dealing with complex domains in the  
16 presence of micro-textured surfaces and cavitation using mass-conserving algorithms [215-217], but  
17 also to extend a Reynolds-type solver to full Computational Fluid Dynamics (CFD) studies looking at  
18 the fluid flow outside the contact, overcoming the limitations of the Reynolds' assumptions in specific  
19 extreme contact conditions [218-221]. The development of fully-coupled Solid/Fluid Interactions  
20 (SFI) solvers [222] constitutes the new frontier of this particular area of research, with the promise that  
21 advances in computational power may lead to a more comprehensive study of the multiphysics  
22 phenomena governing three-dimensional contact problems considering full field deformations, thermal  
23 and multi-field effect, and the complex rheologies of the fluids and the solids under investigation.  
24 Hybrid techniques (e.g., the element-based finite volume method – EbFVM [223,224]) have also been  
25 recently developed to combine the flexibility of finite elements in terms of studying complex domains  
26 and using unstructured meshes and the use of finite volumes to accurately solve the fluid-dynamic  
27 problem at hand.

34  
35 Another important area of interest, often to industrial applications, is the solution of problems  
36 involving particle interactions and multi-body contacts, as many industrial and natural processes  
37 involve granular systems. Diverse phenomena such as avalanches, fluidized beds and asthma inhalers  
38 all depend on assemblies of particles. The understanding of such systems is therefore of interest to a  
39 number of scientific disciplines, as well as industry. Due to their complexity, it is often very difficult  
40 to study such systems, in which large numbers of particles interact, and macroscopic behavior depends  
41 both on the physical properties of individual particles, and the interactions between them. The Discrete  
42 Element Method (DEM) is ideally placed to tackle these contact configurations, as it allows the  
43 description of the physical state of a system using a large number of discrete elements (this approach  
44 shares many similarities with atomistic simulations (see §2.5) where atoms are replaced by particles  
45 that interact via constitutive equations rather than interaction potentials); however, depending on the  
46 problem under investigation, the DEM requires constitutive laws to describe individual interactions,  
47 which often are obtained by adopting hierarchical multi-scale approaches (see §2.6). Noticeable  
48 examples are studies of particle-particle interactions to derive elastic, viscoelastic and plastic  
49 constitutive laws that capture the right kinematics during particle collisions [225-228] and the  
50 integration of the effect of adhesion [229,230], particle shape [231,232] and roughness [233,234] into  
51 DEM codes. Recently this method has been also used to study wear involving complex fragmentation,  
52 but also problems affected by complex rheological and/or multi-physics behavior [235,236].  
53  
54  
55  
56  
57  
58  
59  
60  
61  
62  
63  
64  
65

## 2.5. Atomistic methods

1 Molecular Dynamics (MD) was first developed to study the interaction of hard spheres [237] and, in  
2 the following decades, has been expanded into methods and tools suitable for investigations in a  
3 number of physical, chemical and mechanical phenomena both for diagnostic [238-243] and predictive  
4 purposes [244-253]. Classical MD essentially calculates the kinematics of atoms (or representative  
5 “particles”) by solving their Newtonian (or Langevin) equations of motion based on potentials that  
6 describe the interactions between them. This tool was applied to the study of tribological interfaces  
7 especially in the high speed regime, which lends itself to the length and timescales of MD [254-257].  
8 Other examples of studies include: elementary phenomena such as the mechanical mixing between  
9 two surfaces in contact [258]; different wear regimes [259], plastic deformation [260,261]; the  
10 tribology of Diamond-Like Carbon (DLC) coatings [262]; the frictional behavior of self-assembled  
11 layers formed from additives [263,264]; the rheology of lubricant films in contact in the EHL regime  
12 [265,266]; and other tribological phenomena including friction, adhesion, and wear [267].

17 The classical MD framework can provide a description of the dynamics at atomistic level, but without  
18 explicitly modelling individual interactions in terms of surface reactivity, bond formation and  
19 evolution of electronic structures, which can be dealt with using first principles or *ab initio* MD  
20 techniques (examples of this include Car-Parrinello MD [268] and Tight-Binding Quantum Chemical  
21 MD (TB-QCMD) [269] and will be discussed in more detail at the end of this sub-section); hence, the  
22 key ingredient of any classical MD simulation is the interaction potential (also referred to as the Force  
23 Field, FF). Even though the availability of suitable interaction potentials is still a limiting factor for the  
24 study of complex systems, several families of FFs have been presented in the literature (along with  
25 their explicit parameterization), each of them designed to capture the essential features of a different  
26 type of material. The simpler functional forms of FF are represented by pairwise interactions that  
27 generally account for an attractive (describing London dispersion forces) and a repulsive term  
28 (originating from core-core repulsion). Probably the most popular examples are the Lennard-Jones  
29 (LJ) [270] and Morse potentials [271]. The number of (free) empirical parameters is kept at a  
30 minimum (for each atomic species, this number is two and three for the LJ and Morse potentials,  
31 respectively), as is the computational cost of simulations based on these FFs. Given their extreme  
32 simplicity, the LJ and Morse potentials are not able to realistically describe the behavior of many  
33 materials (for example, the LJ potential can accurately model noble gases only). Nevertheless, the  
34 usage of the LJ potential has produced fundamental results over the years, as evinced, for example, in  
35 the prediction of the breakdown of continuum contact mechanics at the nanoscale [272,273], discussed  
36 in more detail in §3.3, and in Non-Equilibrium MD (NEMD) simulations to shed light on the phase  
37 behavior of fluids in confinement [274-276].

45 Metallic systems are more often (and more accurately) described by the family of the Embedded Atom  
46 Method (EAM) potentials [277]. These potentials are slightly more computationally expensive than  
47 their pairwise counterparts, but are also significantly more flexible since they have many more free  
48 parameters. EAM potentials comprise a pairwise repulsive term modeling the core-core interaction and  
49 a cohesive contribution representing the energy that an ion core experiences when it is “embedded” in  
50 the electron density originating from neighboring atoms. Examples of their application in tribology are  
51 studies of the frictional behavior of an indenter tip against different metallic surfaces [278-281], or the  
52 interfacial friction characteristics of different metal pairs [282]. For carbon-based (e.g., diamond,  
53 graphite/graphene, diamond-like coatings, nanotubes) and other covalent systems, a series of FFs has  
54 been developed, all based on the bond order concept originally formulated by Pauling [283]. Examples  
55 include the Finnis-Sinclair [284], Tersoff [285] and Brenner [286] potentials, as well as more recent  
56 derivations such as the Adaptive Intermolecular Reactive Empirical Bond Order (AIREBO) [287] and  
57



1 ReaxFF [288] FFs. These all share the common assumption that it is possible to properly model the  
2 strength of a chemical bond on the basis of the bonding environment, thus considering the number of  
3 bonds and, if necessary, bond lengths and bending angles. Such kinds of potentials have been  
4 successfully used to investigate the tribological properties of different systems, including the  
5 interaction between diamond samples [289-291], the frictional behavior of corrugated nano-structured  
6 surfaces [292], the wear mechanisms of tungsten-carbon systems [293], friction and adhesion  
7 properties of carbon nanotubes and polymers [294,295], and tribochemical reactions on silicon/ silicon  
8 oxide interfaces [296,297].  
9

10 Classical MD –especially when calculating and tracking the kinematics of all atoms (all-atom MD) as  
11 opposed to aggregates of these (united-atom or coarse-grained MD)– require significant computational  
12 resources, meaning that the method is usually reserved for systems of relatively small sizes, even with  
13 today’s increased capabilities. In what is essentially a boundary element method, Green’s Function  
14 MD (GFMD) [298] integrates out “all internal (harmonic) modes of an elastic body, [...] leading to  
15 effective interactions of those atoms whose degrees of freedom couple to an external force.” In this  
16 manner, “the full elastic response of semi-infinite solids is incorporated so that only the surface atoms  
17 have to be considered in molecular dynamics simulations” [299]. GFMD is being used extensively in  
18 the study of tribological systems, including in the recent contact-mechanics challenge summarized in  
19 §3.5.  
20  
21  
22  
23

24 Another class of potentials used in tribology are non-reactive FFs (see, e.g. [300-303]). This class of  
25 potentials is often employed to model intramolecular interactions in organic molecules and contains  
26 several two-, three- and four-body terms (usually including LJ, electrostatics, bond stretching, angle  
27 bending and torsional parts). As already mentioned, despite the simplicity and relatively low  
28 computational cost of such non-reactive FFs, a fixed topology has to be provided as an input for an  
29 MD simulation, thus preventing the possibility of investigating tribochemical reactions or events that  
30 require the breaking/formation of chemical bonds in general. Instead, when modeling tribochemistry,  
31 MD techniques [303-305] or quantum calculations (using Density Functional Theory, DFT) [306] are  
32 used to study atom motion during friction or chemical reactivity, respectively. To combine both types  
33 of information, reactive force-field MD [307], ab initio MD techniques [268] or tight-binding coupled  
34 with MD [308] techniques have also been used to extract in situ information of interfacial material  
35 behavior. A deeper insight of the local electronic and geometric characteristics is required to capture  
36 subtleties that a molecular mechanical description cannot represent. Indeed, quantum mechanical  
37 approaches have been used toward this aim, e.g., [309], focusing on the theoretical modeling of a  
38 specific stoichiometry and chemical composition. Tribochemistry is discussed in more detail in §3.9.2.  
39  
40  
41  
42  
43  
44

## 45 **2.6. Multiscale modeling: concurrent and hierarchical schemes**

46 By multiscale modeling, one refers to a technique in which two (or more) different models related to  
47 different scales (or different matter descriptions) interact, i.e. exchange data, in a way that enhances  
48 the information that can be obtained about the modelled phenomenon. Contact between rough surfaces  
49 with geometrical features present on multiple scales, starting from the shape of contacting solids down  
50 to the atomic fluctuating nature of the “surface” at the nanoscale, is an example of a spatially  
51 multiscale problem. Earthquakes, on the other hand, constitute the most characteristic example of a  
52 temporally multiscale problem, in which the stresses building up in the earth’s crust for many years  
53 are released within seconds inside the fault zone, giving rise to seismic waves. In general, spatially  
54 multiscale problems are much more complicated to model than temporally multiscale ones, as time is  
55 only a one-dimensional quantity. Consider, for example, a multiscale contact problem between rough  
56 surfaces: this can be solved using either a classical model (FEM, BEM and so on, as discussed in  
57 §2.2), e.g., as in [117], or a multiscale model, e.g., as in [310]. In such a multiscale model of rough  
58  
59  
60  
61  
62  
63  
64  
65

1 contact, the upper scale model (e.g., treated with the FEM) determines the state (for example, the  
2 contact pressure) for the microscale (e.g., treated with the BEM), whereas the microscale provides the  
3 upper state with some properties of the contact interface such as, for example, the contact stiffness,  
4 contact area, friction, etc.

5  
6 Having been generalized by many authors, the problem of multiscale rough contact inspired numerous  
7 theoretical and computational studies aimed at understanding the role of roughness at different scales  
8 of observation; see, e.g., [111,310-313] among many others. Recently, the topic has gained renewed  
9 interest with the increased potential of MD in studying nanoscale contact problems [259,272,314,315]  
10 that unveil interesting mechanisms of contact interactions occurring at the nanoscale. While the advent  
11 of MD opened new challenges due to the still limited time and size scales of the simulations that can  
12 be performed with the aid of supercomputers, it has also revealed new opportunities for the use of  
13 various multiscale approaches.  
14  
15

16  
17 An important question in multiscale modeling is the following: *how to identify which scales and*  
18 *mechanisms are relevant for understanding the phenomena to be modelled?* A simple recipe would be  
19 to start with a simpler model, based on a single scale and uncoupled physical processes, and then  
20 adaptively introduce additional scales to permit coupled multiscale-multiphysics considerations,  
21 whenever and wherever these are needed, until the simplest possible model is obtained. Scale, in this  
22 context, does not only refer to the spatial and temporal dimensions, but also to the different  
23 computational models relevant to different scales. Inevitably, some multiscale coupling also implies  
24 multiphysical coupling as, for example, in the case of coupling mechanical FEM with classical MD in  
25 which thermal oscillations are inherent to the model [316]. However, this simple recipe can be often  
26 ineffective as it depends on the ability of the “user” to add the right details at the right scale and may  
27 lead to the neglect of important information flow across the scales.  
28  
29  
30

31  
32 In tribological models, key processes are usually localized in a thin interface layer, but have important  
33 implications or can even fully control the macroscopic behavior of the system. In this light, the  
34 interfacial laws of friction, wear, heat and electrical transfer, as well as other relevant phenomena can  
35 be obtained with microscale models for use in macroscale ones. In terms of accuracy, one can  
36 determine two levels in this hierarchical approach: 1) the microscale model is assumed to not affect  
37 the macroscale state, in which case the microscale data can be obtained by simply post-processing the  
38 macroscale results; 2) the microscale model affects the macroscale state and, thus, the constitutive  
39 interface model has to be directly included in the latter scale. For most applications in which scale  
40 separation between the micro- and the macroscales exists, a hierarchical multiscale model is  
41 acceptable and the relevant question would be: *when would a finer and truly multiscale model –i.e.,*  
42 *one which requires stronger scale coupling– be needed?* Normally, a finer model is required when no  
43 scale separation exists, as is normally the case for surface roughness. Such models, dealing with  
44 concurrent multiscale coupling are in general much more complex and can hardly be used to obtain  
45 statistically meaningful results; see, e.g., [200,316-318]. At the same time, finer models can be used  
46 for rare-event simulations and are of high importance in understanding the physics of certain  
47 phenomena happening in contact interfaces such as dislocation-free surface interaction in contact  
48 interfaces, ballistic heat diffusion through small contact spots, partial slip conditions in lubrication at  
49 the molecular level, and so on. Most such phenomena can be studied at a single relevant scale and  
50 integrated at a bigger scale in a hierarchical manner.  
51  
52  
53  
54  
55  
56

57  
58 In the case of plastic deformations occurring, for instance, during sliding motion between two metallic  
59 surfaces, many dislocations are nucleated at the surfaces and under maintained load may travel long  
60 distances. In an MD simulation, the small size of the domain will artificially trap them and create  
61  
62  
63  
64  
65

1 artificial hardening, which should occur in very thin coatings. In order to address this issue, advanced  
2 concurrent coupling strategies are being developed where dislocations can be passed to a continuum  
3 representation [319,320]. In three dimensions, dislocations are line networks, so that a dislocation may  
4 cross the coupling interface. Such hybrid dislocations should behave as single dislocation structure,  
5 which requires the use of reciprocal boundary conditions and may significantly increase the  
6 complexity of coupling strategies.  
7

8 Another important aspect to consider is the possibility to perform concurrent coupled simulations  
9 where atomistic and molecular details need to be captured near the wall in lubricated contacts when  
10 the fluid film is larger than the Root Mean Square (RMS) composite surface roughness; this is  
11 particularly useful, for example, when slip at the wall or atomistic details of the surface topography  
12 must be explicitly modelled. In this case, MD-continuum coupling strategies involve the transfer of  
13 information between MD and CFD, and particular care must be taken when the two descriptions  
14 merge [321,322]; a number of schemes exist to achieve this [323-325].  
15  
16

17 Finally, comparison with experimental data is of crucial importance for all types of models, and  
18 multiscale ones are not an exception. Difficulties here arise from the fact that it is not always possible  
19 to reproduce the relevant scales for the application/model in the lab. For example, the friction of rocks  
20 (as well as their fracture) is a very scale-dependent phenomenon [326] that is intimately linked to the  
21 probability of presence of critical defects in a given volume. The related key question in this example  
22 would be: *what are the features of real earthquakes, which can be reproduced in the lab?* Also, *can*  
23 *multiscale models tuned at the lab scale, e.g. [327], be used at earthquake scales?* Further research on  
24 scale separation in contact interactions is required to guide the choice of the most appropriate  
25 computational method preserving the accuracy of the description of a given physical problem while  
26 considering the effect of inherent uncertainties.  
27  
28  
29  
30  
31

### 32 **3. Research themes in tribology**

33 The problem of normal contact between rough surfaces has been studied extensively –for example, the  
34 reader is referred to a recent paper on a contact-mechanics challenge whose results are summarized in  
35 §3.5– and can be considered to be well understood, but almost all other issues in tribology remain  
36 open for future research. While different theories, techniques and models used to investigate these  
37 issues were reviewed in §2, this section introduces active topics for modeling research in tribology. As  
38 a foreword, let us emphasize that, since the global forces acting on an interface are integral quantities  
39 along the interface (for example, the friction force is the integral of the shear stress over the contact  
40 area), various models can predict rather similar forces using different assumptions. Comparisons of  
41 models to experiments are therefore necessary, not only in terms of global forces but also in terms of  
42 local measurements, for instance, of temperature, strains or the real area of contact. Multiple  
43 successful examples of such comparisons can be found in the literature [328-338]. Local  
44 measurements become increasingly accessible due to the miniaturization of local probes and the  
45 development of full-field evaluation techniques like Digital Image Correlation (DIC) [339] or infrared  
46 imaging [340]. Imaging techniques are especially interesting for performing local measurements at a  
47 contact interface in a non-invasive way, but the choice of possible materials is limited as they must be  
48 transparent to the radiation used (e.g., visible or infrared light). In this context, wherever relevant, we  
49 will also present experimental results that are amenable to direct comparison with models.  
50  
51  
52  
53  
54  
55  
56

#### 57 **3.1. Multiphysical phenomena in tribology**

58 All tribological phenomena happening near interfaces between solids are determined by the atomic  
59 interactions within and between solids, as well as those between atoms of the substances present at the  
60  
61  
62  
63  
64  
65

interface. Since these interactions give rise to various physics described at the macroscale by different theories and models, the tribological interface can be considered a “paradise” of Multiphysics (coupled multiple fields; see Fig. 2). The following types of phenomena may take place in such an interface or in its immediate vicinity: mechanical (solid and fluid), thermal, electro-magnetic, metallurgical, quantum and others.

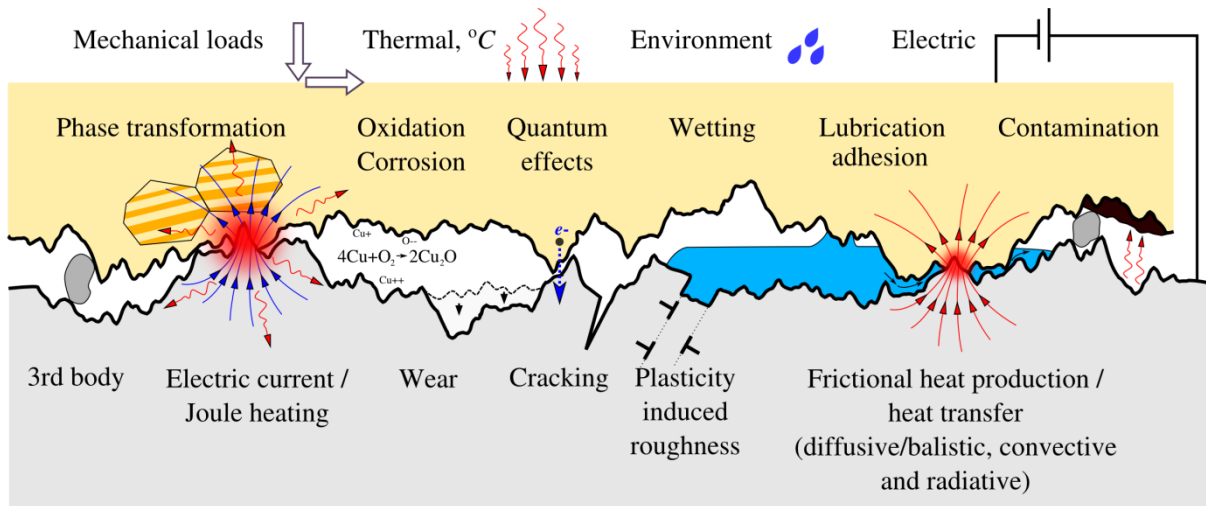


Fig. 2: A scheme representing the multiphysical nature of tribological interactions: two different solids with rough surfaces and relevant material microstructures are brought into mechanical contact and exposed to various loads: mechanical, thermal, electric, and environmental.

Mechanical phenomena can refer to the mechanical deformation of solids and their contact interaction including adhesion and friction. The process of material removal or surface deterioration (micro-cracking, abrasive and adhesive wear) can be also included within this type. Thermal phenomena are related to heat transfer from one solid to another, as well as to heat generation due to interfacial friction or due to dissipation in the bulk (viscoelasticity, viscoelastoplasticity, damage accumulation or micro-fractures): heat exchange can be either ballistic or diffusive depending on the size of contact spots [341-343], while radiative and convective heat exchange also contribute considerably to the overall heat conductance [344]. The local heating of contacting asperities up to the point of local melting, recognized in early tribological studies [345] and known as flash-heating, has important implications for friction, especially in dry contacts [346,347]. Metallurgical phenomena happening in near-interface layers span various microstructural changes that are, either, triggered by changes in temperature (e.g. because of Joule or frictional heating) or by severe deformations, and include dynamic recrystallization and various phase transformations; an example is the formation of the so-called “white layer,” a fine-grained and rather brittle martensitic layer [348].

For materials experiencing glass transition, the local rise in temperature can be critical for their mechanical performance [349]: in general, mechanical properties are strongly dependent on the temperature, thus making the thermo-mechanical problem one of the most natural and strongly coupled multiphysical problems in tribology, especially in dry contact or in the mixed lubrication regime. Because of excessive local heating, the solids can reach their melting or sublimation point and experience phase transition [345]; thus, melting, evaporation and sublimation appear to be important phenomena in dry and lubricated micromechanical interactions. More complicated physics emerge for composite and porous materials; examples of the latter are rocks experiencing chemical decomposition, water evaporation, pressurization, and so on [350,351]. A complex interaction of the aforementioned physics with a fluid present in the interface is another strongly coupled multiphysical problem, especially for EHL (see §2.4 and §3.8), sealing applications and saturated fractured media

[352-354]. In most situations, the interfacial fluid flow can be considered as a thin flow that can thus be properly described by the Reynolds equation but, in the case of the fluid viscosity depending on the pressure or temperature, a proper simplification of the Navier-Stokes equations should be performed [355].

In addition, tribofilm formation and various tribochemical phenomena taking place at tribological interfaces make them very challenging objects for multiphysical research [306,356]. At the same time, to understand and model such a complex multiphysical problem as a tribological interface, one needs to construct reliable multiphysical models and design appropriate multiphysical tools. Some recent examples of tribology-related modeling applications involving multiphysical coupling include, for example, excitable biological cells (see §3.9.5), weakly coupled modeling of creeping fluid flow through the contact interface between rough solids [357], and electro-mechanical coupling in contact problems [166]. Because of the complexity of direct experimental measurements and the inseparability of numerous multiphysical mechanisms, a big challenge is to construct reliable and precise multiphysical models having predictive power while, at the same time, being verifiable and sufficiently comprehensive.

### 3.2. Surface roughness

Real (engineering) surfaces brought into mechanical contact touch only over a number of discrete contact spots forming the real or true contact area, which, in general, is much smaller than the nominal contact area that can be computed for the case of perfectly smooth surfaces. Under increasing pressure, the true contact area grows towards the limit of the nominal one that can be reached under relatively high squeezing pressures. The integral true contact area, as well as the localization and morphology of the clusters of true contact, affect numerous tribological mechanisms and thus present a topic of intensive engineering and scientific research. In particular, the following quantities are dependent on the true contact area: 1) the stress state near the contact interface, which is proportional to the applied stress and inversely proportional to the true contact area; 2) friction, adhesion and adhesive wear; 3) the transport of electric charge and/or heat through the contact interfaces; and, finally, 4) the fluid flow through the contact interface in sealing problems. Apart from the phenomena affected by the contact area, roughness is responsible for the additional interface stiffness of contact interfaces, which can be related to heat/electrical conductivity [358]. To understand the effect of roughness on all aforementioned phenomena, accurate mechanical models are needed.

One of the fundamental issues in the modeling of contact between rough surfaces is the realistic representation of roughness. As the roughness of real engineering surfaces spans multiple length scales –whether measured experimentally or created using numerical methods, for example, via simulations of sandblasting and shot peening [359], or through surface randomization algorithms [119,133,360,361]–, the question is essentially *which length scales are relevant to a specific tribological system* or, alternatively, *to what extent should one implement accurate roughness representations in a tribological model?* The wealth of parameters used in roughness characterization –amplitude ( $S_a$ ,  $S_q$ ,  $S_{sk}$ ,  $S_{ku}$ ), spatial ( $S_{al}$ ,  $S_{tr}$ ,  $S_{td}$ ) and hybrid parameters ( $S_{dq}$ ,  $S_{dr}$ ), or Abbott-Firestone (bearing area) curve-based parameters ( $S_k$ ,  $S_{pk}$ ,  $S_{vk}$ , material ratios, and volume parameters for 3D measurements)– demonstrate the complexity of reaching a universal description of surface roughness; see, e.g. [362,363]. Indeed, most models use only a small subset of those parameters, the ones deemed necessary to describe a specific function.

Representations based on concepts of self-affinity were apparently introduced to tribology much more recently, although Archard first introduced a concept of fractals already in 1957 [110] with his model of spheres upon larger spheres upon larger spheres applied to contact and friction. A key point is what



1 was recognized into tribology with Whitehouse and Archard [364]: they first introduced the  
2 topography's Autocorrelation Function (ACF), and noted that the Fourier transform of the ACF, i.e.  
3 the Power Spectrum Density (PSD), of their topographies was a power law at large wavevectors, as  
4 Sayles and Thomas [365] would later confirm for a number of surfaces. One implication of their work  
5 was that between one-third and one-quarter of all the sample points of their topography would be a  
6 peak, regardless of the sampling interval they chose, while the mean peak curvature depended strongly  
7 on the sampling interval. The tribology community still debates on the effect of the upper wavevector  
8 truncation in the PSD, which significantly affects contact area, rubber friction dissipation, and many  
9 other physical properties. On the contrary, the fact that the lower wavevector determines the RMS  
10 amplitude for non-stationary roughness has been neglected in later literature, since the time of highly  
11 influential works on stationary roughness by Longuet-Higgins [114] and later by Nayak [112] on  
12 whose basis most multi-asperity models are constructed (see §2.1.2).  
13  
14  
15

16 A very interesting finding of Whitehouse and Archard came when they measured the profile of a  
17 rough surface along the same track, before and after a single passage of a lubricated slider. They found  
18 that, while the main scale roughness was still present, all the fine scale roughness had been removed  
19 [364], a finding which also tends to be neglected in the literature. Keeping in mind the limited  
20 metrology of the time, *one could ask to what extent we should measure or worry about the initial*  
21 *roughness when irreversible deformations might remove it?* On the other hand it is known that, if a  
22 metallic sample is heated after mechanical polishing, the initial surface roughness might reappear on  
23 its surface [366].  
24  
25  
26

27 Much emphasis in modeling is placed today on nominally flat stationary self-affine fractals, while  
28 very little work was performed on the macroscopic “shape” of surfaces –particularly in the presence of  
29 adhesion–, where the basic contact problem of a rough sphere remains incompletely understood. One  
30 exception is a rather special case of roughness for the sphere (axisymmetric waviness) which can be  
31 solved analytically [367]. Otherwise, numerical calculations are necessary and in this case it may be of  
32 little interest to argue a priori on models describing shape and roughness assuming they consist of very  
33 separate scales. Summarizing, *most of the real practical problems remain unanswered*: what is the real  
34 contact area? How can it be estimated quantitatively from “scale/magnification-dependent” quantities?  
35 Which mechanisms (plasticity, failure processes, adhesion at small scales) does one need to  
36 incorporate to converge to a well-defined value?  
37  
38  
39  
40

41 Following the introduction of fractal roughness, numerical models began to utilize the PSD to fully  
42 define surface roughness. However, one has to keep in mind that the PSD does not represent the full  
43 information about topography: different realizations of surfaces in real space are possible for the same  
44 PSD, depending on the phase associated to each spectral component [368]. While the effect of  
45 deviation from Gaussianity has limited effect on some quantities, it can be crucial for others. For  
46 example, even small deviations from the ideal Gaussian random roughness case seem to lead to a  
47 dramatic increase in adhesion for rough surfaces due to a finite number of asperities or a finite tail  
48 (unlike the infinite nominal Gaussian tail) in the asperities' height distribution [369-373]. Furthermore,  
49 as modern fractal parameters do not include such traditional ones as skewness, there might be an  
50 advantage in using traditional characterizations, perhaps to augment fractal ones for non-Gaussian  
51 surfaces, e.g. [374].  
52  
53  
54  
55

56 The perceived universality of the PSD in fully describing surface roughness was demonstrated by  
57 Persson who showed that a 1D line scan, a 2D Atomic Force Microscopy (AFM) scan and a 2D  
58 Scanning Tunnel Microscopy (STM) scan all lie on the same PSD plot for a grinded steel surface with  
59 the fractal dimension being  $D_f = 2.15 \pm 0.15$  for many engineering surfaces [359]. At the same time,  
60  
61  
62  
63  
64  
65

1 however, and in the absence of random phases, a profile PSD with a slope of  $-2$  (as in the work of  
2 Whitehouse and Archard) does not necessarily represent a rough surface, but can also be a square  
3 wave (that has all phases equal to zero), while a slope of  $-3$  may well correspond to semi-circles  
4 nestling together. Also, having a Gaussian distribution of heights does not automatically suggest  
5 uncorrelated spectra. Higher order autocorrelation functions may be needed but the topic of non-  
6 Gaussian fractal surfaces is not very developed at present. It is worth mentioning here that, in many  
7 practical applications, the surfaces in contact are actually non-Gaussian: road surfaces, worn-out or  
8 polished surfaces, blasted surfaces, etc. The class of anisotropic rough surfaces, also very frequent in  
9 engineering, is also relatively unrepresented in modern modeling.

12 On the critical issue of the definition of the low- and high-frequency cutoff values of the roughness  
13 PSD, some macroscopic quantities, such as stiffness, electrical and thermal conductance, are well  
14 known to depend principally on the RMS amplitude of roughness, i.e. on the lower frequency contents  
15 of the PSD, as demonstrated by Barber [358]. Other quantities, like the real contact area or the RMS  
16 slope of the topography depend on the higher frequency part of the PSD. This suggests that attempts to  
17 measure the real contact area with indirect methods, e.g., measuring conductance, have the intrinsic  
18 difficulty of measuring two quantities which depend very differently on the PSD content. The reader  
19 should keep in mind that the high-frequency cutoff may very well be related to the atomistic nature of  
20 the contact [375], which is usually challenging to measure and which goes beyond the continuum  
21 description of matter.

26 The metrology of surface roughness measurements plays a crucial role in our understanding of  
27 roughness as well. Abbott and Firestone measured surface roughness by using a pen-recorder to draw  
28 an amplified version of the motion of a “stylus” (a broken razor blade) over a surface [376]. Since  
29 then, a multitude of techniques have been developed or adapted for measuring roughness: contact and  
30 optical profilometry, stripe projection scanning, Scanning Probe Microscopy (SPM), Transmission  
31 Electron Microscopy (TEM), etc. The scope here is not to give an extensive overview of those various  
32 methods, which the reader can find for instance in [364,377,378]. *The main message to be conveyed*  
33 *here is that these techniques, whether contacting or non-contacting, present a number of limitations*  
34 *and artefacts that should be carefully taken into account when interpreting the data* (see e.g. [379] for  
35 white light interferometry and [380,381] for scanning force microscopy). Knowledge of those artefacts  
36 is particularly important when using contact mechanics or lubrication models based on topographical  
37 features [382]. It is well known, for example, that the stylus tip geometry filters the measured signal,  
38 while high contact stresses at the stylus tip can lead to significant deformations [383]. Post-processing  
39 is also critical in extracting roughness information from raw data with a number of aspects –shape  
40 removal (tilt), the restoration of missing data (“perforated” surface data) using built-in triangulation or  
41 grid-fit routines, and the filter type and cut-off length (Gaussian versus Robust Gaussian Regressive  
42 Filter, RGRF)– affecting the end result. Furthermore, artefacts may occur due to diffraction effects  
43 around sharp edges caused by calibration grid height steps. In certain cases, results differ across  
44 measurement methods: comparisons of contacting and non-contacting measurement techniques show  
45 large differences in predicted bearing curves, for example, with confocal microscopy typically  
46 yielding higher roughness values than atomic force microscopy [384].

### 54 **3.3. Scale effects and the breakdown of continuum theories**

55 Contact between two bodies –perceived as continua– is well-defined and occurs when the distance  
56 between them is zero; however, the same reasoning cannot be applied to the atomistic scale. Luan and  
57 Robbins studied the contact between a flat surface and nanoscale indenters of different structures  
58 (spherical crystalline, amorphous and stepped crystalline) and showed that the details of the atomic  
59 structure matter in the contact pressure distribution in adhesive versus non-adhesive contact conditions

1 [272,273]. Subsequent work by other research groups showed that the accurate calculation of the  
2 contact area at a given length scale could yield reliable results [138,240,385,386], but this requires  
3 careful post-processing and interpretation of atomistic results with appropriate definitions of criteria  
4 for contacting atoms and the “area of contact for an atom.” For the latter, one method of calculation  
5 involves the assumption that the real contact area is the sum of the contact areas of each atom  
6 determined to be in contact [240,387]. *But is the concept of contact area really meaningful for*  
7 *atomistic models?* Similarly to the notion of contact itself, the contact area is a well-defined quantity  
8 only at low magnifications, i.e. at scales where the discrete nature of atoms is not relevant. Perhaps  
9 extracting the pressure distribution over the interface by looking at the distribution of forces [272,273]  
10 may be more meaningful than attempting to measure the real contact area with indirect methods;  
11 furthermore, the contact area is difficult to measure experimentally [335] since transparent materials  
12 need to be used to image the interface, while no information can be obtained at scales below the pixel  
13 size, which may yield errors in the real area of contact of the order of 10% error (new results by Sahli  
14 et al., currently under review).  
15  
16  
17

18 The concept of contacting distance is similarly ill-defined at the atomic scale. To begin with, the  
19 thermal fluctuations of atoms play a role in the estimated contact area; this can be accounted for in  
20 atomistic simulations, for example, by averaging contacting atoms over time [314]. Even with  
21 averaging, the distance between atoms at which contact “occurs” is also not straightforward to  
22 calculate. Researchers have used various methods in atomistic simulations using idealized materials  
23 and introducing, for instance, potential energy- or distance-based cutoffs for specific crystal or  
24 amorphous material structures [387], but the situation is far from clear when real materials with  
25 multiple elements or alloys, inhomogeneities, impurities, and so on, are considered. Even in the ideal  
26 case where a Lennard-Jones-type potential can be used to define repulsion and adhesion between two  
27 particles (or atoms) [388], *contact and friction are actually described to occur at nonzero separations.*  
28  
29  
30  
31

32 Mapping roughness parameters from continuum models to discrete atomic systems is also challenging.  
33 For instance, given a continuum function of position, one can calculate the mean contact slope used,  
34 for example, in Persson’s theory (see review in §2.1.2), but how should one proceed when the surface  
35 is discrete? One possibility would be to take the step height over the terrace width to calculate a slope  
36 that would presumably match the continuum RMS slope, but is this universally true? Contact behavior  
37 in atomistic simulations is known to depend on the specific realizations of the system under study (see,  
38 e.g., [389]). Questions then arise as to which extent real local differences in atomistic structures might  
39 affect the macroscopic picture. They seem to be relevant already at the microscale for percolation  
40 problems, while statistical fluctuations seem to be important in cyclic loading (hysteresis). It appears  
41 that *robust sampling strategies are required to model representative rough surfaces at the various*  
42 *scales as well as a proper way to map quantities from one scale to another, both for crystalline and*  
43 *amorphous surfaces.*  
44  
45  
46  
47

48 The breakdown of continuum at the atomistic scale can also be observed in other phenomena. When  
49 referring to Density Functional Theory (DFT), for example, the work function of transition metals  
50 (TM) becomes non-scalable when particle clusters decrease in size, and the continuum model by  
51 Smalley [390] breaks down. The transition between the scalable and non-scalable regimes is at around  
52 100 atoms in the case of gold. An anti-correlation is found between the binding energy and the vertical  
53 detachment energy, which may have important implications in relation to catalysis: e.g., while bulk  
54 gold is inert, small gold clusters are reactive [391]. *The question that arises is whether rough metal*  
55 *surfaces are more reactive than atomically smooth surfaces and, also, whether amorphous surfaces*  
56 *are more reactive than crystalline surfaces,* given that they contain more imperfections. To tackle  
57  
58  
59  
60  
61  
62  
63  
64  
65

1 these questions there is a need for accurate tight-binding and/or empirical models at the atomistic  
2 scale.

3 In the case of fluid lubricants, the breakdown of continuum is related to an increase in viscosity and a  
4 transition towards a solid-like state, accompanied by stick-slip behavior. The increased viscosity is  
5 non-scalable: when the lubricant film thickness decreases down to a few nanometers, i.e. the size of  
6 the lubricant molecules, there is a deviation from typical bulk behavior as was observed in Surface  
7 Force Apparatus (SFA) studies [392-394]; this transition from ultra-thin lubrication to dry friction  
8 under high pressure and shear has been studied using MD [395]. The presence of nanoscale roughness  
9 frustrates the ordering of the fluid molecules, leading to high friction states. Experimentally measured  
10 viscosities were reported, for example, for perfluoropolyethylene (PFPE) molecularly thin films  
11 deposited on the atomically rough substrates used in hard disk drives [396,397] and used in subsequent  
12 analytical models to predict the tribological behavior at the head-disk interface [398]. In the case of  
13 SFA-type experiments, analytical expressions for the normal (e.g., Kapitza's solution [399]) and shear  
14 forces acting on a spherical probe sliding on a substrate with a fluid film [400] should only hold up to  
15 the point where the film can be viewed as a continuum; however, these are routinely used to extract the  
16 complex viscosity from amplitude and phase information of the probe vibrations even in cases when  
17 very few lubricant molecules exist at the interface [401]. After all, how many lubricant molecules can  
18 be said to constitute a continuum?  
19  
20  
21  
22  
23

24 Additional scale effects related to material models and plasticity are discussed in the next section.

### 25 **3.4. Material models and plasticity**

26 Crystal plasticity is the relevant constitutive framework when modeling rough surface contact and  
27 whenever the size of contact spots is comparable to the grain size in a polycrystalline material. This, of  
28 course, includes single crystals. It may seem surprising that only very few tribology-related  
29 applications of crystal plasticity can be found in the literature, apparently limited to the analysis of  
30 asperity flattening [402,403] and indentation hardness [162,404,405]. Although plasticity of crystals  
31 exhibits strong anisotropy (captured by crystal plasticity), the elasto-plastic normal compliance of a  
32 rough crystal surface is expected to only weakly depend on crystal orientation as demonstrated by  
33 instrumented spherical indentation and crystal-plasticity simulations, e.g., [406,407]. At the same time,  
34 plastic anisotropy manifests itself in complex, orientation-dependent pile-up and sink-in patterns  
35 [162,407,408]. The related effects may influence the evolution of real contact area in rough contacts,  
36 but seem not to have been studied yet.  
37  
38  
39  
40  
41  
42

43 Nano-indentation tests have revealed another important effect, namely the increase of hardness with  
44 decreasing indentation depth, which is referred to as the indentation size effect [409,410]. Several  
45 gradient crystal plasticity models have been developed with the aim to describe the related size effects,  
46 e.g., [411-414], accompanied by much more scarce three-dimensional crystal-plasticity simulations of  
47 the indentation size effect [415,416]. The related effects may also impact the elasto-plastic contact of  
48 rough surfaces. This has been illustrated using a conventional strain gradient plasticity model [417],  
49 but the corresponding gradient crystal plasticity studies have not been reported so far.  
50  
51  
52

53 An important cause of the indentation size-effect in metals is that the dislocations, which are the  
54 carriers of plastic deformation, are discrete. Continuum models, including crystal plasticity are based  
55 on the assumption that plasticity can always occur at any location, as long as a critical strength is  
56 exceeded; however, in reality, dislocation availability is limited at the small scale. Upon contact, even  
57 a very high local pressure might not induce sufficient dislocation nucleation to sustain plastic  
58 deformation. Thus, continuum plasticity models for contact and friction are expected to break down at  
59  
60  
61  
62  
63  
64  
65

1 the (sub)micron scale, since they miss a length scale capable of capturing size-dependence. Neglecting  
2 the size-dependence of plasticity would lead to the prediction of an earlier onset of plastic deformation  
3 and underestimate the amount of work hardening during plastic deformation. This would have  
4 consequences in the estimation of the evolution of the contact area. Size-dependent plasticity can,  
5 however, be captured by DDD simulations (see §2.3) [196,418], while the latter can be coupled to MD  
6 simulations to accurately capture the nucleation of dislocation loops [419].  
7

8 Contact between bodies with simple geometry has been studied using two-dimensional dislocation  
9 dynamics, where edge dislocations glide on three sets of slip systems, e.g., [420]. Contact results in  
10 highly fragmented contact areas due to the exit of dislocations from free surfaces. This leads to a  
11 serrated contact area and a peaky contact pressure profile, with high localized pressure, very different  
12 from what a continuum model would predict. A comparison between contact pressure profiles  
13 obtained using dislocation dynamics and crystal plasticity is presented in [421]. Komvopoulos et al.  
14 [422] used two-dimensional DDD to model the indentation of a flat crystal by means of a rigid rough  
15 surface with multiscale roughness. Surface asperities were treated as a collection of Hertzian contacts  
16 and dislocations could glide only on a single crystallographic slip system. An interesting outcome of  
17 this study is that, as the load increases, asperity interactions emerge at different length scales, and so  
18 does interaction between plastic zones. The onset of static friction for a flat contact was presented by  
19 Deshpande et al. [423], whose work points to the competition between plastic deformation –dominant  
20 for larger contact areas– and loss of adhesion –dominant when the contact is so small that plasticity is  
21 limited. There is wide room for additional friction studies in the framework of discrete dislocation  
22 plasticity.  
23  
24  
25  
26  
27

28 A way to incorporate microscale size-dependent plasticity into contact models could be to fit the  
29 dislocation dynamics results for the deformation of a non-local plasticity theory, such as strain  
30 gradient plasticity or even include such effects in a statistical model. The advantage of statistical  
31 models, like the one recently developed by Song et al. [424], is their extremely low computational  
32 cost, which would make them attractive for use by the industry. However, a statistical approach based  
33 on the GW model, for example, would suffer from the same limiting assumptions discussed earlier  
34 (see §2.1.2) and may not be directly applicable to realistic representations of roughness (see §3.2).  
35  
36  
37

38 Plasticity is not only limited to dislocations, as it can also appear in the form of grain boundary sliding  
39 [425-427] when high strain rates are involved. In this case, even the material crystallographic structure  
40 can change. During dry sliding, grain coarsening [261] as well as grain refinement and amorphization  
41 have been observed [428]. As an example, Stoyanov et al. [293] show that tungsten carbide (WC) in  
42 frictional contact with tungsten (W) causes the crystalline WC structure to turn into amorphous WC  
43 with a dispersion of nano-diamonds. Some interfacial phenomena in metal sliding are related to near-  
44 surface austenization induced by frictional heat and subsequent formation of fine-grained martensite  
45 known as a white layer [429-431].  
46  
47  
48

49 Material-related scale effects are also observed theoretically in simulations of sliding of a circular disk  
50 on the atomic surface of a large substrate [432]. Two regimes can be distinguished in the static friction  
51 normalized to the shear strength: one corresponds to the elastic limit and the other to the rigid limit.  
52 The transition takes place when the radius of the disc exceeds the length of the core radius of  
53 interfacial dislocations. Looking at material constitutive laws, a breakdown of isotropic plasticity is  
54 observed in the ploughing of an unconstrained micro- or nano-crystalline surface, where the material  
55 bulges until it folds. Folds similar to those observed experimentally can also be found in MD  
56 simulations [433]. The effect is caused by dislocation plasticity being active on specific slip directions  
57 in the various crystals. While this cannot be captured by isotropic plasticity or visco-plastic  
58  
59  
60  
61  
62  
63  
64  
65



regularization, a crystal plasticity model that includes a hardening law which can capture localized plasticity should be able to account for this behavior.

### 3.5. Normal contact between rough surfaces: the contact-mechanics challenge

One of the few tribological problems that is relatively well understood is normal contact between rough surfaces. A comparison of various modeling approaches in their ability to properly solve a well-defined normal contact problem has been tackled in the recent contact-mechanics challenge [434]. A surface height spectrum was generated [359] featuring a roll-off and power-law decay region, as was a realization of this randomly rough surface in real space. The following approximations were made: small surface slopes, linear elasticity, short-range adhesion (based on the value of the local Tabor parameter  $\mu_T = 3$ , which was close to the JKR limit; see §3.7), periodic boundary conditions, and a hard-wall contact constraint. The problem setup results in insignificant adhesive hysteresis up to moderate contact pressures. This information was made available to researchers who were asked to compute integral quantities, spatial and statistical distributions for purposes of comparison. Specific metrics used in the subsequent analysis included the gap and stress along a reference line; stress and contact patch histograms; and relative contact area and mean gap values. Submitted solution methods could be categorized into brute-force computing, where errors could come from the discretization, and models mapping onto simpler equations using uncontrolled approximations. More specifically, results utilized exact (boundary-value) methods, Persson theory without adhesion, multi-asperity models that assume local constitutive relations without interaction between contact patches (“bearing models”), as well as all-atom MD simulations, where the surface size was scaled down by a factor of 100, and experiments, where the surface size was scaled up by a factor of 1000. The reference solution was calculated using GFMD (see §2 for a review of computational methods and models).

Good agreement with the reference solution was found for both experiments and all-atom MD; when comparing the gap across the reference line, the effect of removing the small-slope approximation gave excellent agreement for all-atom MD. Expectedly, multi-asperity models were found to overestimate the gap, while exact methods agreed almost exactly at the greatest magnification; however, results of the stress across the reference line (local zoom-in) showed great scatter. Stress distribution histograms were almost Gaussian at compressive contacts, featuring a high adhesive peak at zero pressures and a rapid decay to tensile tractions. Multi-asperity models were found to overestimate the stress while, in the presence of adhesion, when small patches become unlikely, these models produced very similar trends for the patch-size distribution. All solutions showed reasonable agreement for the contact area as a function of load, as well as for the mean gap as a function of load with the exception (for the latter) of all-atom MD, where inherently accounting for plasticity yields deviating results for larger pressures.

In summary, very close agreement was observed between all systematic approaches with differences becoming visible when quantities required high resolution. At the same time, these approaches showed good agreement with experiments and all-atom MD, suggesting that common approximations might be less problematic than believed. Reasonable agreement was found between the reference solution and the non-adhesive Persson’s theory on all reported properties, while multi-asperity methods agreed with each other but deviated from the reference solution (it is worth mentioning that more recent asperity models accounting, for example, for asperity interaction were not compared in this study). It could therefore be argued that the suitability of modeling methods and tools can be determined based on the properties one would need to extract: for example, *predicting contact area versus load or mean gap versus load seems to be consistent across methods* and, arguably, *the most suitable model would be the simplest one*. On the other hand, extracting local quantities at higher resolution would require numerical methods able to achieve sufficient discretization. It should be noted that, as soon as the

1 contact is not only compressed but is also sheared, the contact area has been measured to evolve  
2 significantly [435], a situation that has not yet received sufficient attention in the modeling literature.

### 3 **3.6. Friction**

4 Although normal contact between rough surfaces can serve as a reference situation in many  
5 tribological systems, it is not a priori sufficient to address issues related to moving surfaces. Lateral  
6 motion does involve fundamentally new phenomena, related, for example, to frictional heating, wear,  
7 third body and shear-rate-induced dissipation (through fluid lubrication or bulk viscoelasticity). Those  
8 effects need to be understood in order to assess the origin of friction and quantify it in various  
9 tribological systems. The breadth of the field of friction is too large to attempt an extensive summary  
10 here. The reader is referred to reference books for an overview of the field, e.g. [46,436]. This section  
11 will only address a few recent advances made in the understanding of friction, from its onset and  
12 transition from static to kinetic values, to rubber friction, related to viscous bulk dissipation, two topics  
13 which were intensively discussed during the Lorentz workshop.  
14  
15  
16  
17

#### 18 **3.6.1. Friction laws**

19 As soon as any motion occurs at the interface, a transition from full stick to full slip takes place (see,  
20 e.g., [437]) and models need to incorporate a friction law. The most classical and widely known  
21 friction law is the one of Amontons-Coulomb (AC) [438], which states that no sliding occurs as long  
22 as the ratio of the shear force  $Q$  to the normal load  $P$  remains below a certain threshold defined as the  
23 static friction coefficient,  $\mu_s$ . Maintaining a constant sliding speed requires the application of a kinetic  
24 friction force,  $F_k = \mu_k P$ , with  $\mu_k$  usually being smaller than  $\mu_s$ . Note that, in the modern interpretation  
25 of the AC friction law, the friction coefficients are constants for given materials in contact. Coulomb,  
26 actually, had already found that  $\mu_s$  increases logarithmically with the contact time, and  $\mu_s$  depends  
27 logarithmically on the sliding velocity [438,439]. Today, laws incorporating those dependencies are  
28 denoted as rate-and-state friction laws, as further described below. The AC law, which has been  
29 defined here from the global forces acting on the interface, is commonly used locally along extended  
30 interfaces. In those cases, the friction coefficients are to be compared to the local ratio of shear to  
31 normal stress  $q(x)/p(x)$ . Practically, a fundamental question arises about the value to be used for the  
32 local friction coefficients: *should one use the values of the corresponding global coefficients or should*  
33 *these be different at the local contacts?*  
34  
35  
36  
37  
38  
39

40 Whereas the global and local kinetic friction coefficients are expected to be equal (in the quasi-static  
41 case), the situation is very different for static friction coefficients. It has been shown experimentally  
42 that the static friction coefficient depends on the stress distribution at the interface prior to the onset of  
43 sliding [440], and that  $q(x)/p(x)$  can exceed the macroscopic friction coefficient by a factor of two  
44 [441]; these results have been reproduced in models of heterogeneous frictional interfaces [442,443].  
45 The fundamental reason behind this behavior is that *the global and local static friction coefficients are*  
46 *equal only if all points at the interface reach their slipping threshold at the very same instant.* This  
47 situation corresponds, for instance, to an ideally homogeneous interface submitted to homogeneous  
48 loading. In practice, this never happens: when slip at the interface becomes unstable, a large portion of  
49 the interface is loaded below its threshold, so that the total tangential load born by the interface is  
50 smaller than its theoretical maximum value. The consequence is that, in general, the global static  
51 friction coefficient is smaller than its local counterpart [444,445], and it is thus challenging to infer a  
52 local static friction coefficient from macroscopic measurements. Numerical methods (e.g. ab initio  
53 MD; see §2.5) could be used to study the relative motion of few adjacent atomic layers, where  
54 frictional behavior is dictated by the local electronic and structural features of the material. If the bulk  
55 atomic layers contain no structural irregularities (dislocations, layer truncations, etc.), friction could be  
56  
57  
58  
59  
60  
61  
62  
63  
64  
65

1 considered an intrinsic property [446-448]; however, such assumptions illustrate the inherent  
2 limitations of idealized numerical solutions in capturing complex phenomena.

3 Although practically useful and rather easy to implement in models, AC's friction law cannot capture  
4 a series of effects repeatedly observed in rough contacts (see, e.g., [449] or [450] for reviews). First,  
5 the static friction coefficient,  $\mu_s$ , slowly increases with the time the interface spends at rest. This effect  
6 is interpreted as an increase of the area of real contact over time through asperity creep, an effect  
7 denoted as *geometrical aging*. Depending on the material, creep can be of viscoplastic [331] or  
8 viscoelastic in nature [451]. Another cause for the increase of  $\mu_s$  is the strengthening of the contact  
9 with time, presumably due to relaxation of the glass-like material forming the very interface, an effect  
10 denoted as *structural aging*. Secondly, the kinetic sliding friction coefficient in steady sliding is  
11 velocity-dependent, typically with a logarithmic velocity-weakening. This effect is partly due to an  
12 intrinsic velocity-dependence of the interface's shear strength, and partly to the time-dependence of  
13 the real area of contact: slower sliding gives more time to the micro-contacts to grow in size before  
14 they break and are replaced by fresh, smaller micro-contacts. Those effects are taken into account in  
15 rate-and-state friction laws, and apply to various fields related to friction, in particular earthquake and  
16 landslide science.

17  
18  
19  
20  
21  
22 Despite its many successes, the rate-and-state friction law must also be used with caution. The  
23 logarithmic velocity-weakening is based on observations at low slip-velocity, smaller than about  
24  $100 \mu\text{m/s}$ . At higher slip rates, a velocity strengthening regime due to viscous effects is also  
25 expected, and is indeed generally observed beyond some crossover velocity [452]. At even higher  
26 velocities, in the range typical to unstable slip up to a few  $\text{m/s}$ , sliding is accompanied by significant  
27 temperature rise, possibly by several hundred degrees. Such heating can induce transient phase  
28 changes in the vicinity of the contact interface [441]. In these conditions, friction may not be  
29 controlled only by a critical length scale (the average micro-contact size) but also by time scales  
30 [441,445]. Heat can also favor chemical reactions, in particular in tectonic faults with fluids and high  
31 pressure. Such reactions tend to self-lubricate the interface, with low friction resistance at the highest  
32 slipping rates [453]. Such systems remain challenging to model, due to the strong multiphysics  
33 coupling required to capture the most salient controlling phenomena.

### 3.6.2. The relevance of space and time scales on the onset of sliding

34  
35  
36  
37  
38  
39 Apart from identifying and understanding new and specific mechanisms occurring at or close to the  
40 contact interface, tribological models can be used as quantitative tools to reproduce and interpret  
41 experimental observations: this is especially true for friction. Since most contact and friction  
42 measurements are made at the system-size level (e.g., total normal and friction forces), models  
43 predicting system-size quantities could be denoted as "macroscale models", irrespective of the actual  
44 length scale considered. As a provocative example, *a model of atomic force microscopy experiments is*  
45 *a macroscale model if its aim is to predict the total friction force that the tip experiences*. But what are  
46 the properties of models actually enabling such quantitative comparisons?

47  
48  
49  
50  
51 A frictional interface can be modelled using a homogeneously loaded contact between elastic half-  
52 spaces only in very specific instances; instead, most real contacts have complex geometries, boundary  
53 conditions, and loading configurations leading to unavoidable pressure and shear stress heterogeneities  
54 along the contact interface. Since friction laws need to couple both normal and shear stresses to predict  
55 where and when slip will occur, the stress distribution along the interface needs to be accurately  
56 modelled. Although a large portion of friction-related works deals with static or quasi-static situations,  
57 most realistic contacts also experience transient phenomena: either the loading is unsteady (oscillating  
58 contacts, impacts) or the interfacial response is itself transient (instabilities). This is why, in order to  
59  
60  
61

offer improved quantitative predictions of the tribological behavior of an interface, macroscale models need to account for the elasto-dynamics of the bodies in contact: *the incorporation of temporal phenomena, together with realistic boundary conditions, into frictional models is essential.*

As a practical example, one can consider how macroscale models were progressively improved to reproduce some aspects of the experimental results reported by the group of Fineberg about the onset of sliding of extended interfaces [441,454-458]. Their main observation is that the transition from static to kinetic friction is mediated by the dynamic propagation of micro-slip fronts along the interface: ahead of the front, the interface is still in its stuck state, while it is already slipping behind it. Macroscopic sliding only occurs when the front has spanned the whole interface [454]. In this context, not all fronts lead to macroscopic sliding. Precursors to sliding are sometimes observed, which correspond to fronts spanning only a fraction of the contact interface. These precursors manifest themselves at macroscale as a series of dents in the loading curve, indicating partial load relaxation [455]. The first models for the length of precursors were one-dimensional [442,459-463]. Although the ad-hoc introduction of an initial shear stress field was improving the results [461], none of these models could be compared quantitatively with Fineberg's experiments, in which the height of the slider was not negligible. Only with two-dimensional models based on spring-block or FEM representations of the elasto-dynamics of the slider [464-466] could the predictions quantitatively match the observations. While the aforementioned models were based on the AC description of the frictional interactions at the interface with static and kinetic friction coefficients, a recent fracture-based description appears to provide equally good predictions of the precursor length [332,333], strengthening the idea of an equivalence between the friction and fracture descriptions of the onset of sliding, often used in earthquake science [467]. In particular, the fracture-like stress field around the tip of micro-slip fronts, measured through an array of miniature strain gauges was captured by analytical [457] and FEM models [458].

Although a velocity-independent AC friction law is sufficient to predict the precursor length and the fact that front speed depends on the local pressure to shear stress ratio [456], such a law fails to explain the unexpectedly large range of front speeds observed [464,468]. While the fastest fronts, propagating at about the speed of sound in the contacting materials, were expected from standard shear fracture theory, abnormally slow fronts –slower by orders of magnitude–, were observed but remained unexplained, while a single front could alternate between both types in a single event [454]. It should be noted that slow fronts here are distinct from quasi-static fronts like those involved in the onset of sliding of sphere-on-plane contacts, the propagation speed of which is proportional to the external driving velocity [43,469,470]. Dynamic slow fronts have been obtained theoretically within a one-dimensional model of the interface using an improved rate-and-state friction law featuring a velocity-weakening-then-strengthening behavior. In this model, the slow front speed is related to the velocity at which the steady-state friction coefficient is minimum [471,472], which is supported by observations of slow rock friction [473].

Unfortunately, such an approach does not explain the possible transition from fast to slow front regimes observed within a single event; this was achieved using a multi-scale model [445,474] in which a 2D model [464] is complemented by a micro-junction based description of the interface [475] in which the loading/breaking/reformation cycle of each junction is controlled by a time scale. This time scale is inspired by the one identified experimentally in [441], which was observed to control the transition from fast slip to slow slip when the interface starts to slide, and was argued to correspond to the cooling time of the interface after the rapid heat deposition as the micro-junctions break upon front passage. Such heating is presumably responsible for local melting of the interface, a phenomenon which is also clearly involved in seismology where rock melts and reforms leaving fault veins. The

1 main implication of this time scale is that, after a slip phase, the interface does not re-stick perfectly,  
2 but transiently allows for some further, slow slipping. Thus, slow fronts are fronts that would arrest in  
3 the absence of this slow slip mechanism, but can continue to propagate, much more slowly, due to the  
4 slow slipping occurring in the broken part of the interface. It was also found that the selection of the  
5 front type (fast or slow) is not only dependent on the shear to normal stress ratio, but also on the local  
6 disorder in shear forces sustained by the micro-junctions [445]. As a result, local static friction is  
7 history-dependent, with potentially a factor of two in the variation of the coefficient of static friction  
8 due to the rupture history of the interface [475]. All these results suggest that *friction features*  
9 *multiscale aspects both in the spatial and time domains, that must be accounted for in models.*

### 11 **3.6.3. Rubber friction: Some open issues from mesoscale experiments on elastomers**

12 Rubber friction has received much attention in the literature, both because of its practical relevance,  
13 for instance to tire/road contact, and because of the particular way energy is dissipated through  
14 friction. The seminal work of Grosch [476] has shown that the temperature and sliding velocity-  
15 dependence of the friction coefficient closely follows that of the viscoelastic moduli of the rubber. His  
16 results suggest that both the surface and bulk dissipation during rubber friction are of viscoelastic  
17 origin. As for the bulk, each spatial frequency present in the surface roughness is expected, through  
18 the sliding velocity, to correspond to a temporal frequency for the excitation of the viscoelastic  
19 material. Persson's 2001 multiscale theory of contact [8] was aimed at clarifying the relationship  
20 between the continuum of frequencies within the roughness and the dissipation caused by them. For a  
21 review of this issue, the reader is referred to the following review paper [477]. In the rest of the  
22 section, the focus is mainly on the recent use of elastomers to gain insights into specific frictional  
23 phenomena.  
24

25 It has already been argued that new insights into friction can be reached by comparing model  
26 predictions to experimental measurements made not only at the system-sized scale (macroscopic  
27 loads) but also at local scales (ideally full field evaluations). In several aspects, elastomers are good  
28 model materials with which to perform such comparisons. Due to their low elastic modulus, the  
29 amplitude of the interfacial displacements under tribological solicitations is typically large enough to  
30 be easily monitored optically, using contact imaging techniques (see e.g., [478,479] for tire rubber). In  
31 particular, polydimethylsiloxane (PDMS) is increasingly used for in situ measurements of  
32 displacement fields (see e.g., [469,470,480-482]). PDMS has the further advantages to have a low loss  
33 modulus, and to fracture at extremely high strains, well beyond those associated with frictional  
34 solicitations. Thus, its behavior can be compared to elastic models, sometimes incorporating nonlinear  
35 elasticity at high strains [334].  
36

37 Access to local displacement and stress at such rubber interfaces enabled the identification of some  
38 phenomena that are not yet satisfactorily incorporated into friction models. As a first example, rough  
39 interfaces have finite normal and shear stiffness due to the compliance of each individual micro-  
40 contact. Although those stiffness values affect the behavior of contact interfaces (see e.g., [483] for the  
41 role of the normal stiffness [470] and that of tangential stiffness on rough sphere-on-plane contacts),  
42 most models consider, for the sake of simplicity, perfectly smooth interfaces. Such models could be  
43 improved by including the effect of roughness through effective boundary conditions on smooth  
44 interfaces (as done, for example, in [484,485]). As a second example, the contact mechanics and  
45 frictional properties of elastomer contacts are found to be affected by the value of a pre-stretching  
46 applied to the rubber (see, e.g., [486,487]), due to a stretching-induced anisotropy of the interface.  
47 Keeping in mind that any contact loading leads to a non-vanishing field of in-plane tensile strain, in  
48 particular near the contact edges, *stretching effects are expected to be involved in virtually all*  
49 *tribological situations.* Improved friction models should aim at incorporating those effects.  
50  
51  
52  
53  
54  
55  
56  
57  
58  
59  
60  
61  
62  
63  
64  
65

#### 3.6.4. Dry friction between patterned surfaces

1 In many practical applications, the emergent frictional behavior is not only determined by microscopic  
2 degrees of freedom or surface roughness, but also by other mesoscopic or macroscopic length scales  
3 characterizing the material surfaces. The hierarchical structure of the gecko paw is one of the most  
4 cited examples to illustrate the role of a complex contact structure, and many research efforts have  
5 been devoted to understanding the origin of its properties of adhesion and friction [13,488-490]  
6 (biotribology is further discussed in §3.9.3-5). In general, many biological materials are characterized  
7 by a non-uniform complex surface structure, e.g., insect legs [491], lotus leaves [492,493], nacre  
8 [494], as well as animal [495-497] and human skin [498-500], which are intrinsically multiscale and  
9 multiphysics systems, and therefore difficult to model in a single framework. The exceptional  
10 mechanical properties of these systems have attracted a lot of interest, and led to attempts to reproduce  
11 their behaviors artificially with specific geometric features of the surfaces. The main focus of research  
12 in bio-inspired materials is to design new materials by mimicking nature, aiming to manipulate the  
13 mechanical properties of a system through a complex organization of microscopic components rather  
14 than introducing new chemical and physical features [31,501-505]. Understanding and optimizing  
15 friction in these bio-inspired complex surfaces is an open challenge.  
16  
17  
18  
19  
20

21 Recently, experimental results have been obtained for the friction of specific textured surfaces, e.g.  
22 honeycomb structures [506,507], periodic regular grooves both in dry and wet conditions [38,508-  
23 511], as well as pillars and dimples [512-515]. MD simulations (see §2.5) have been adopted to  
24 investigate the effect of patterning in the presence of lubricants [516], but the theoretical and  
25 numerical modeling of dry friction in these systems shares the difficulties inherent to that of the  
26 friction of rough surfaces: how to take into account within a unified framework concurrent length  
27 scales spanning orders of magnitude and involving many physical mechanisms. For this reason, much  
28 work remains to be done on this topic. Some results have been obtained by means of a simplified  
29 approach based on numerical simulations of the spring-block model [517], aiming to investigate the  
30 qualitative frictional behavior of patterned surfaces [518-520]. In order to study the role of specific  
31 surface structures, it is not necessary to include into a model the details of all microscopic interactions,  
32 since they can be taken into account with an effective description at the mesoscale, where the system  
33 is discretized into elementary components whose interactions are described in terms of forces within  
34 the framework of classical mechanics. Thus, surface structures are introduced by means of the  
35 arrangement of elementary components, and the effects on the macroscopic friction coefficient are  
36 deduced from the numerical solution of the overall equations of motion of the system. With this  
37 procedure, some versions of the spring-block model have been successfully used to model and  
38 understand specific aspects of the transition between static to dynamic friction [445,459-  
39 461,464,468,474,521,522], which have been compared with experimental results [454-457].  
40  
41  
42  
43  
44  
45  
46

47 Thus, despite the approximations and apparent simplicity of the model, the spring-block approach can  
48 provide a qualitative understanding of relevant phenomena with computationally inexpensive  
49 numerical simulations. The results of these studies show how static friction can be tuned and  
50 optimized by means of a specific arrangement of surface structures. In particular, it has been  
51 demonstrated that the static friction coefficient is reduced by means of large surface grooves [518] and  
52 that a hierarchical organization of grooves with different length scales can be used to tune it to a  
53 desired value [519]. Also, it has been proved that a remarkable reduction of the global static friction of  
54 a surface can be obtained by means of a hierarchical organization of regions with different local static  
55 friction coefficients [520]. A natural development based on this research is to improve the spring-  
56 block model by relaxing some of its approximations, for example, by simulating more realistic two- or  
57  
58  
59  
60  
61  
62  
63  
64  
65

three-dimensional surfaces; furthermore, variations of the surface roughness after the onset of sliding or other long-term effects during the dynamic phase can be incorporated.

### 3.7. Adhesion

Research on adhesion in the field of contact mechanics saw significant progress only in the 1970s. Any review of the literature on adhesive contacts will start with the two analytical models developed in this period, the JKR model [50] and the DMT model [51]. These models considered adhesive contact between a smooth sphere and a flat body, but with different approaches and making significantly different assumptions. They were shown to apply equally well to different contact conditions by Tabor [523] who identified a characteristic parameter, now known as the Tabor parameter, which can be systematically used to identify whether short-range or long-range adhesion dominates the contact interactions; in particular, the JKR model captures mainly short-range interactions, representative only for contacts with a large value for the Tabor parameter ( $\gg 1$ , soft solids, small curvature, large adhesion), while the DMT model is valid for contacts with a small value ( $\ll 0.1$ , rigid solids, large curvature, weak adhesion) [524]. Muller et al. [525] attempted to bridge the two models by removing the assumption that the Hertz profile is not affected by adhesion and developing a self-consistent analysis of adhesive contact between a sphere and a flat. Similar analyses to a higher level of accuracy were later performed by Greenwood [526].

Whilst the latter analyses by Muller et al. and Greenwood seem to provide the solution to contact mechanics of smooth adhesive contacts, their complexity and numerical basis hindered exploitation until more recently, when alternative models were developed. Maugis applied a Dugdale-type analysis (from fracture mechanics to contact mechanics) to the problem [527], replacing the true adhesive forces with a constant adhesive force acting between the surfaces at all points separated less than a critical distance. Greenwood and Johnson used a “double-Hertz” analysis to similarly simplify the solution and provide results suitable for analytical manipulation [528]. These methods, while offering a step forward in analytical capabilities, are a downgrade in terms of accuracy from the Muller and Greenwood analyses, which were relevant for the development of newer deterministic formulations. More recently, finite element models for adhesive contact problems have also been developed, where the contact description obtained using the Lennard-Jones potential is incorporated into the framework of nonlinear continuum mechanics, e.g. [529] and [530], also in the presence of plasticity [531] and within the context of multi-scale simulations, e.g., [273,532]. Alternative approaches have also been developed based on the BEM, which incorporates adhesion through energy minimization; see, e.g., [533,534].

Most of the models discussed above were developed for or applied to smooth surface contact, nominally between a sphere and a flat. A common justification for neglecting adhesive forces is the existence of surface roughness and, starting from this point, an early and significant analysis was carried out by Fuller and Tabor [535], who showed that the adhesive influence could be described by an “adhesion parameter,” which is, in effect, a ratio of the adhesive force of “lower” asperities to the elastic push of “higher” asperities. The theory was found to show reasonable agreement when fitted to experimental results. Fuller and Tabor had used the JKR model on an asperity level; Maugis repeated the analysis using the DMT model and found that an additional load would be caused by adhesive forces around each asperity [536]. Further advancements were made through the inclusion of an elastic–plastic representation of the asperities based on the DMT model, e.g., [537]. Other attempts have been recently made to incorporate the effect of thin films [538], and to extend the validity of the maps proposed by Johnson and Greenwood [539] to account for the strength limit [540].



1 Looking at other non-deterministic models of multi-asperity contacts, in some of the early  
2 contributions, Persson and Tosatti considered adhesion through a fractal representation of surface  
3 roughness and showed that adhesion dropped significantly at higher fractal dimensions [541]. They  
4 suggested that the simpler analysis of Fuller and Tabor and their adhesion parameter adequately  
5 described the full detachment stage of a particle. More recently, Persson and Scaraggi [542] used  
6 Persson's theory and a power spectrum representation of the contact roughness to introduce a Tabor  
7 number that depends on the length scale or magnification, and which gives information about the  
8 nature of the adhesion at different length scales. They proposed the analytical study of the two limiting  
9 cases (JKR –see also Persson [543]– and DMT) for randomly rough surfaces using the Persson contact  
10 mechanics theory (see §2.1.2); it was shown that adhesion problems that are “JKR-like” for large  
11 length scales and “DMT-like” for short length scales can be approximately treated using the theory  
12 with different levels of approximations, which depend on how quickly the behavior transitions  
13 between the two limits across the scales. While these rough surface models (or asperity models) are  
14 limited to a stochastic description of the surfaces and thus cannot provide a complete contact  
15 mechanics solution for all surfaces, they may constitute a good approximation and provide a useful  
16 design tool, especially when numerical simulations may struggle or fail to produce fast and reliable  
17 results. *Extensions to include hysteretic effects would be a very useful addition to the literature.*

22 Deterministic adhesion models of contact in the presence of roughness are expected to provide an  
23 accurate representation of the response of real bodies in contact. MD simulations of contacts (see §2.5)  
24 can potentially provide an extremely accurate deterministic description of adhesive forces in a contact  
25 (see, e.g., [273,544,545]); however, the limitation in terms of the number of atoms and system sizes  
26 that can be included in MD simulations reduces the applicability of this method to large-scale contacts.  
27 Given the advent of new and improved numerical methodologies and increased computational power,  
28 there has been a recent resurgence in the development of contact mechanics models able to address  
29 contact between surfaces of arbitrary shape and roughness, of small and large scale, and capable of  
30 providing accurate information for contact forces, surface displacements and hysteretic effects (where  
31 present) throughout the contact. Many of these methodologies can be seen as BE methods (discussed  
32 in §2.2) relying on different discretizations and numerical techniques to solve the contact problem  
33 using “brute force” [434], and include GFMD [136,546], FFT-based (e.g., [547,548]), and Multi-Level  
34 Multi-Integration (MLMI)-based techniques [549]. These methods have been shown to capture the  
35 response of rough contact surfaces in the presence of adhesion in a number of configurations and can  
36 be used successfully to predict the scales and regimes at which roughness will play a significant role in  
37 adhesive contacts, as well as computing hysteretic losses. These models can also be applied all the  
38 way down to the nanoscale as long as the surface interactions are well captured and can be  
39 approximated using simple Lennard-Jones potential interactions [549].

46 An open question is *whether or not adhesion depends on the topography's RMS amplitude*, an issue  
47 that sees contradicting findings and opinions in the recent literature: while asperity theories predicted a  
48 strong influence of RMS amplitude, Pastewka and Robbins [546] formulated a criterion for  
49 “stickiness” by numerical observation of the slope of the (repulsive) area-load, which appears to be  
50 independent of the RMS amplitude. Discussion about this issue is currently still active [369,370,550].  
51 Furthermore, future perspectives also include the need to integrate realistic adhesive interactions,  
52 which describe the surface behavior accounting for chemical interactions and bonding energies that go  
53 beyond Van Der Waals forces, into multiscale roughness simulations via MD-continuum coupling  
54 strategies, which in principle allow for chemo-mechanical interactions to be more accurately captured.

### 3.8. Lubrication and viscoelasticity

Everyday experience shows that interposing a fluid between two contacting bodies dramatically drops the friction force. Lubrication has, then, a paramount importance in engineering and applied science research since it is clearly related to an improved energy efficiency, to a better durability of components and systems, and, ultimately, to economic savings. Theoretical investigations take their origin in the pioneering studies made by Reynolds in the 19th century [204]: Reynolds equations enable the analysis, in terms of velocity and pressure distribution, of a flow in the lubrication channel. In the last fifty years, a lot of approaches, mainly numerical [210], have been developed to address the solution of this set of equations: nowadays, it is even possible to account for a variety of non-Newtonian effects, ranging from piezo-viscosity to shear thinning. For a more comprehensive overview the reader is also referred to Hamrock's classical book [212], while modeling approaches are discussed in §2.4.

In recent years, textured surfaces for the optimization of hydrodynamically lubricated contacts have been developed (see, e.g., [551], also inspired by nature [552]). The main effect of the presence of dimples, pockets or asperities is an increase in the load-carrying capacity of the bearing and eventually a reduction in the coefficient of friction. The main challenge in modeling the hydrodynamic lubrication between textured surfaces remains the description of the cavitation, for which many models have been proposed (e.g., finite difference algorithms [553,554] based on the well-accepted JFO boundary conditions [555,556]. In addition, multiphase CFD simulations have been used to model cavitation but, given the complexity of the problem and the coupling with the appropriate turbulence models, it is still a challenging task [557]. *Multiscale approaches should be developed in order to capture both the macroscopic tribological characteristics of a lubricated contact and the micro-hydrodynamics, with the related phenomena of roughness-induced cavitation and turbulence.*

Furthermore, in order to completely assess the problem, the solution of the lubricant fluid dynamics has to be coupled with the analysis of the contacting solids' mechanics: in the so-called EHL regime (also see §2.4), the fluid pressure is high enough to entail an elastic deformation of the lubricated bodies. Consequently, the pressure field has to satisfy, at the same time, the Reynolds equations and the elasticity constitutive relations. The intricacy of the problem surges when the roughness of the contacting solids is accounted for. Indeed, the mathematical form of the problem does not change, but the number of elements required to find a numerical solution and, in particular, to explicitly resolve the effects of rough contact cannot be handled with the computational resources currently available. Consequently, a deterministic approach which accounts for the contact interactions at all relevant roughness scales is unfeasible; instead, various homogenization methods have been developed to overcome these limitations. The most commonly used approach solves the Reynolds equation as if the surfaces were smooth and uses "flow factors" as statistically corrective terms for the surface roughness [558]. This approach was pioneered by Patir and Cheng in [559], and then further developed by Elrod [560] and Tripp [561] to account for anisotropic effects. Furthermore, recent investigations have shown that more accurate estimations may be performed by employing, instead of scalar coefficients, flow factor tensors, which are functions of the surface roughness and, specifically, of the anisotropy roughness tensor [562].

When contact or environmental conditions do not permit fluid film lubrication, e.g., when extreme temperatures and/or pressures are present, as in aerospace applications [563], solid lubricants are generally employed. It should be noted that, in the literature, a distinction is made between powder and granular lubricants, on the basis of the particle characteristics and the load-carrying capacity generation mechanisms [564]. Many analytical models of solid lubrication have been developed over the years, starting from analogies with fluid mechanics and the conservation laws for mass,

1 momentum and energy [565,566]. The kinetic theory of gases, instead, has been the basis for the  
2 development of the granular kinetic lubrication theory [567,568]. Both continuum and discrete models  
3 are available for the description of solid lubrication or, more in general, of third body friction [569].  
4 Continuum modeling approaches are based on rheological laws describing the third body, originally  
5 introduced by Heshmat [570]. Discrete simulations, instead, allow the precise computation of particle  
6 dynamics and taking into account individual particle-particle and particle-wall interactions [571].  
7 Solid lubrication is intrinsically a multiscale and multiphysics problem. Therefore, an effective  
8 modeling approach should be able to include the microscopic physical (e.g., surface roughness),  
9 chemical (e.g., tribo-corrosion [572]) and thermal interactions, and to link them to the frictional  
10 characteristics of the tribo-contact. Hence, discrete approaches and particle-based methods seem more  
11 promising, despite necessitating further efforts to make the micro-to-macro correlation.  
12  
13

14 The lubrication problem becomes even more complicated when it involves the wide class of soft  
15 materials. Given its practical interest –related to the continuously increasing demand for new polymers  
16 [573,574], soft tissues [575], biomedical implants [576], biomimetic solutions [546,577] and smart  
17 materials [578]–, soft matter lubrication is a field which is currently attracting a variety of research  
18 contributions. The main challenge in these investigations is in dealing with the lubricated bodies’  
19 rheology, which is usually not perfectly elastic, and, on the contrary, is marked by nonlinear time-  
20 dependent stress-strain constitutive laws. Indeed, hyper-elasticity has been embedded in a number of  
21 models (see e.g. [165]) and was shown to be responsible for significant quantitative deviations from  
22 the classical EHL theory. However, such a step has not been sufficient to explain a variety of  
23 experimental observations involving soft materials. These include, for example, film thickness maps  
24 and contact patches whose shapes and values show, depending on the flow speed, a marked shrinkage  
25 at the flow outlet, thus looking very different from conventional Hertzian-like contact configurations  
26 [579]. Another surprising experimental finding linked to the interplay between solids and fluids in soft  
27 contact problems can be found in [580], where it is shown that the rupture of the fluid film occurs at  
28 the flow inlet in lubricated interfaces in the presence of strongly viscoelastic solids: this is very hard to  
29 explain in the absence of strong time-independent deformations, and is unexpected in classical  
30 lubrication. For these reasons, recently, new models for two-dimensional [581] and full three-  
31 dimensional interfaces [582] have been developed to account for the viscoelasticity of lubricated  
32 solids. Specifically, in the latter case, when considering a viscoelastic rheology, it is possible to  
33 appreciate a dramatic deviation from classical EHL theory, both in terms of fluid pressure and film  
34 thickness. Indeed, the film thickness has a marked shrinkage at the fluid outlet, so that the absolute  
35 minimum of the film thickness can move from the flow outlet to the inlet and the pressure distribution  
36 is peaked accordingly. All this has paramount importance when focusing on the friction developed in  
37 tribo-systems involving viscoelastic soft materials. Indeed, the *viscoelastic material hysteresis has to*  
38 *be added to the fluid viscous losses*, a trend which is far from the classical EHL friction-speed  
39 dependence and is consistent with very recent experimental observations [583].  
40  
41  
42  
43  
44  
45  
46  
47  
48

49 Beyond lubrication, the contact mechanics and tribology of soft matter itself can be studied via the  
50 BEM, which is significantly more cost-effective in modeling rough surfaces than FEM (see §2.2). In  
51 general, viscoelasticity causes shrinkage of the contact area for increasing speed [155]. For example,  
52 the contact behavior of a rigid sphere in reciprocating sliding contact with a viscoelastic half-space  
53 ranges from the steady-state viscoelastic solution, with traction forces always opposing the direction of  
54 the sliding rigid punch, to a multi-peaked pressure distribution with tangential forces in the direction  
55 of the sliding rigid punch. This behavior is controlled by the size of the contact, the frequency and  
56 amplitude of the reciprocating motion, and the relaxation time of the viscoelastic body [584]. *The*  
57  
58  
59  
60  
61  
62  
63  
64  
65

development of comprehensive tools is necessary to simultaneously manage surface roughness, lubricant rheology and the geometry of the contacting bodies.

### 3.9. Other tribological phenomena and applications

#### 3.9.1. Wear

Despite three centuries of scientific investigations on wear mechanisms [585], which led to the emergence of a myriad of empirical models (amongst which the ubiquitous Archard's wear law [586]), wear remains one of the least understood areas of mechanics [587]. Wear processes emerge from a rich variety of complex physical and chemical mechanisms at disparate time and length scales. Due to the vastness of the literature, this brief and incomplete overview is limited to dry adhesive sliding wear focusing only on a few recent works in the literature. A fairly complete synthesis of the existing empirical models can be found in [588].

Starting in the eighties with the advancement of AFM, tribology has taken a turn towards identifying molecular mechanisms behind friction [589], bringing about the era of nanotribology. This has naturally lead to uncovering three fundamental asperity-level mechanisms behind wear: atom-by-atom attrition [590-592], gradual smoothening by plastic deformation [593-596] and fracture-induced third body formation [428,597,598].

Beside theoretical studies [599-602], numerical modeling of wear processes has appealed to many as it opens the possibility to zoom in on an otherwise buried contact interface; however, numerical modeling comes with its share of difficulties. This is due, on one hand, to the challenge of the length scales of wear processes (engineering wear debris are often orders of magnitude larger than the scale of molecular processes that lead to them) and, on the other hand, to the diversity of underlying mechanisms (including plasticity, third body interactions, formation and propagation of cracks, chemistry). For instance, third bodies can have a significant effect on the frictional properties of the tribo-contact [603], sometimes even reducing the coefficient of friction [604].

Wear modeling approaches can be decomposed into continuum and discrete types. Continuum models, which include the popular finite element (FE) approach (see §2.2), have the advantage of being comparatively computationally affordable, while it is also fairly easy to introduce material parameters within macroscopic constitutive laws [605-611]. Correspondingly, DDD (see §2.3) has been recently used as a mesoscale approach to investigate plasticity upon asperity collision [421,612,613]. Both approaches are commonly used to study the onset of wear only, as they suffer in performance and require adaptive meshing when intense deformation due to shearing occurs. In general, when debris are formed, it is best to use a discrete description of matter. The most prominent discrete modeling technique to model wear is classical MD (see §2.4). This is a very useful approach in particular because it is relevant in scale to a large body of experimental work in nanotribology [250,269,614-621]. The quality of the results is very much influenced by the care put into the choice of atomistic potentials [259,622,623]. Naturally, classical MD are limited to sizes below microns, which are relevant to nanotribology but not to a vast category of engineering wear scenarios, i.e. with debris sizes of the order of or above micrometers. At a scale above, an interesting approach is the DEM (see §2.4) [571,624,625]. In this method, numerical points aim to represent an ensemble of particles, or a grain, and the physical sizes of the model can be much larger. Of course, this is at the expense of material modeling accuracy, and the artificial length scale introduced when specifying a distance between particles can influence the wear mechanisms, and has to be carefully chosen.

A recent intermediate approach aims at coarse-graining simple atomistic potentials. In particular, a recently-developed coarse-grained atomistic potential [259] (i.e. discrete particles are meant to

1 represent an ensemble of atoms) permits one to capture the formation of a steady-state debris particle  
2 generated during an adhesive wear process. Steady state implies here that the debris reaches a size that  
3 becomes eventually independent of time, and, in fact, that can be predicted at the asperity level [626],  
4 following a local Archard's law [586] (i.e. the debris size is dictated by the junction size) and a local  
5 Reye's law [627] (i.e. the debris volume scales with frictional work). Numerical evidence shows that  
6 there exists a critical length scale for junction size, above which surface asperities lead to "fracture"  
7 and thus produce wear debris particles, while smaller junctions exhibit "plastic" deformation [259].  
8 This concept might be applied to *contact wear maps to analyze which micro contacts lead to debris*,  
9 and using probabilistic arguments to *deduce wear coefficients from first principles*, which to-date  
10 remain fully empirical parameters.  
11  
12

13 Due to the complex multiscale and multiphysics nature of wear processes, there is need of more  
14 systematic and multidisciplinary research to *better understand the origins of wear at different scales*.  
15 The recent advances summarized above give new hope at revisiting empirical engineering wear  
16 models and promoting physics-based mechanistic wear models at both the single and multiple-asperity  
17 levels.  
18  
19

### 20 **3.9.2. Tribochemistry**

21 The control of friction and wear in a tribological contact is known to be related to several parameters  
22 such as the nature of the rubbing surfaces (roughness, physico-chemical composition, mechanical  
23 properties), contact conditions (pressure, shear stress), temperature, environment, etc. In particular  
24 cases, chemical reactions occurring during sliding will strongly influence the tribological behavior of  
25 the interface through the generation of new compounds. These phenomena are studied in the field of  
26 tribochemistry and are often observed in boundary lubricated contacts [436]: a characteristic example  
27 is molybdenum dialkyldithiocarbamate (MoDTC) which is a well-known friction modifier additive  
28 used in engine oil that is able to significantly reduce friction through the generation of molybdenum  
29 disulfide ( $\text{MoS}_2$ ) lamellar flakes in the contact [628,629]. The classical approach to study such  
30 phenomena is to characterize surfaces by identifying new compounds after tribological tests (post-  
31 mortem characterization). The thickness of the tribofilms usually ranges from few to several hundreds  
32 of nanometers. Surface-sensitive tools are so needed to physico-chemically characterize surfaces over  
33 a depth of a few nanometers. The analyzed area should also be as small as possible in order to spatially  
34 resolve nanoscale features. Recently, more and more in-situ experimental tools, coupling friction  
35 testing and in-situ characterization, have been used to gain access into interfacial material  
36 modifications during rubbing [630-634]. Alternatively, tribochemistry is studied with MD and  
37 quantum calculation tools, as discussed in §2.5.  
38  
39  
40  
41  
42  
43  
44

45 The activation of tribochemical reactions cannot be described with a universal mechanism but depends  
46 on conditions at the interface. During severe contact, for example, a "new" (nascent) surface is  
47 revealed, which reacts differently with the additives or the chemical environment from the initial one  
48 [635]. In the presence of insulating materials –mostly under dry conditions–, studies suggest that  
49 electrons and particles are emitted during sliding that could influence tribochemical reactions  
50 [636,637]. In general, the interface is at thermodynamical equilibrium when the temperature stays  
51 constant in the contact, either, at very low sliding speeds when no significant increase of temperature  
52 is found, or at high sliding speeds when the melting point of the contacting material has been reached.  
53 In all other cases, the interface is not at thermodynamical equilibrium and its behavior becomes  
54 significantly more complex [638]: For instance, under high-speed contact, the increase of temperature  
55 could be important with the thermal energy pushing through the energy barriers of chemical reactions.  
56 In such a case, the tribochemical reaction mainly occurs because of thermal energy generated in the  
57 contact. Furthermore, in some cases, normal and shear stresses applied on the "interfacial material"  
58  
59  
60  
61  
62  
63  
64  
65

could promote a tribochemical reaction [631,639,640]. In this case, tribochemical reactions are promoted by the mechanical energy, which helps decrease the energy barriers of the chemical reaction pathway. Relevant models about these topics have been reviewed by Spikes and Tysoe [641].

### 3.9.3. Contact scale issues in experimental biotribology

Nanotribological experimental approaches have been employed for contact mechanics and friction studies of biological tissues. Concerning the synovial joint system, for example, the use of AFM has given new insight on the frictional properties of cartilage tissues [642-644] –including in the study of synovial joints [645]–, allowed for the detection of different elasticity (stiffness) on the proximal versus distal areas [646,647] and the identification of more compliant characteristics of the pericellular matrix than territorial/ interterritorial matrices of cartilage [648]. The distinction between healthy areas and enzymatically defected areas of cartilage is possible exclusively with very sharp (nanometer-sized) AFM probes [649], which led to the development of AFM-based arthroscopy [650].

A common observation is that the excellent lubricating capabilities of cartilage tissues, reported by many macroscale experimental studies [651], were not found at the small scale, not even on experiments performed on thin films prepared with the individual constituents of cartilage [652-655]. In studies with sharp AFM tips the very small contact area achieved by the AFM probe on the cartilage surface is likely to inhibit the activation of interstitial fluid pressurization. This may indicate an intrinsic hurdle or, alternatively, a fundamental challenge in the usage of AFM for nanotribological studies of cartilage. When it comes to the frictional properties of cartilage tissues and model thin films for small scale contact, computational modeling studies have been relatively scarce to date. Multiscale and multiphysical tribological models are necessary to fill this gap.

### 3.9.4. Skin tribology

The skin controls many types of exchanges between our inner and outside worlds which take the form of mechanical, thermal, biological, chemical and electromagnetic processes [656]. These processes concurrently operate as parts of a very dynamic system featuring highly non-linear feedback mechanisms [500,657,658] where mechanics is pivotal. As mounting evidence suggests, skin microstructure can play a critical role in how macroscopic deformations are modulated at the microscopic level [659]. These structural mechanisms are also at the heart of skin tribology by constituting and conditioning mechanical load transmission [499,500,660,661].

It is widely accepted that skin friction is made of deformation-induced and adhesion components [499,662-665] but, up to now [500], adhesion-induced friction has been deemed to be the dominant contributor to macroscopic friction. Applying a computational homogenization procedure to a 2D anatomically-based finite element multilayer model of the skin, Leyva-Mendivil et al. [500] recently showed that deformation-induced friction can be significant when the skin surface is subjected to the action of a single rigid indenter of sub-millimeter size. It was shown that the macroscopic coefficient of friction between the skin and a rigid slider moving across its surface is noticeably higher than the local coefficient of friction applied as an input parameter to the finite element analyses [500]. Similar observations were reported in a 3D computational contact homogenization study [666]: geometrical effects alone can have a significant impact on the macroscopic frictional response of elastic contacts. These results support the idea that accounting for the microstructure of biological tissues and the heterogeneous nature of their mechanical properties could be critical in determining their biotribological properties.

To date, despite many experimental and modeling studies investigating shear stress at the surface of the skin in relation to skin injuries and pressure ulcers [667-669], very little effort has been devoted to



1 develop methodologies to gain a more quantitative and mechanistic understanding of how shear  
2 stresses are induced at the level of skin micro-relief asperities, and how they propagate from the skin  
3 surface to the deeper layers where they are likely to mechanically stress living cells [38].

4 Ultimately, excessive stress or strain can lead to cell damage and death, which, at a meso/macrosopic  
5 level translates into tissue damage and loss of biological structural integrity. If one considers that, non-  
6 withstanding the strong sensitivity of the skin to fluctuations in environmental conditions, (finite  
7 strain) mechanics is typically coupled to biochemistry and other physical processes such as thermal  
8 transfer, it is clear that the formulation of any type of sufficiently descriptive contact theory of the skin  
9 is going to require substantial integrative efforts. Due to the fibrous nature of their cytoskeleton, cells  
10 also feature strongly anisotropic properties, which, combined with their extreme deformability, calls  
11 for new contact theories of biological soft matter. This presents numerous challenges at a theoretical,  
12 computational and experimental level but also provides outstanding opportunities to establish an  
13 ambitious research roadmap to push further the boundaries of our current knowledge and capabilities,  
14 in biotribology and biological soft matter in general, and in skin tribology in particular.

### 19 **3.9.5. Cardiac dynamics: multiphysical biotribology**

20 In the last few years, new perspectives for contact mechanics research in biotribology are emerging as  
21 far as the problem of contact interactions between biological cells is concerned; see, for example, a  
22 wide overview in [670-674]. In cardiac dynamics, myocytes, which are the fundamental cells  
23 composing the cardiac tissue, interact in a very complex way across their boundaries, transferring  
24 physiological quantities, electric current, and also mechanical tractions [675]. Moreover, as an  
25 additional source of complexity, their boundaries evolve in time, as a result of growth, remodeling and  
26 aging effects [676]. From the mathematical point of view, the complex myocyte dynamics and its  
27 electrophysiological behavior can be described by a set of reaction-diffusion partial differential  
28 equations for the diffusive membrane voltage and for the local electrophysiological gating fields  
29 [677,678]. The nonlinear coupling between electrophysiology and the hyperelastic material response  
30 induced by the excitation-contraction mechanisms is typically modelled via the multiplicative  
31 decomposition of the deformation gradient into elastic and anelastic parts; see, for example, [679-681]  
32 for more details on theoretical and computational aspects related to this modeling strategy.  
33 Specifically, the anelastic active deformation gradient can be provided by the subcellular  
34 calcium/voltage dynamics, while the elastic deformation gradient is computed as customary [679].

35  
36  
37  
38  
39  
40  
41 Complementing these continuum mechanics formulations with suitable interface constitutive relations  
42 to address the problem of myocyte-myocyte interaction is an open problem, with preliminary attempts  
43 to solve having already been proposed in [675,682]. Mechanical interactions should account for  
44 adhesion and contact tractions dependent on the local cell-cell separation, to reproduce the  
45 experimental evidence. Finally, as a further model improvement, the roughness of cell-cell interfaces  
46 should be accounted for, leading to a distribution of partially insulated conductive spots rather than a  
47 fully conductive interface. In this regard, the fundamental discoveries in the field of electric and  
48 thermal contact problems in the presence of roughness are expected to be applicable and extendable  
49 also to myocyte contacts. As proposed by Paggi and Gizzi [682], the myocyte interface can be  
50 modelled as an imperfect zero-thickness boundary layer, whose response can be governed by  
51 nonlinear constitutive relations generalizing the popular cohesive zone models used in fracture  
52 mechanics for pure mechanical interactions. The mechanical field has to be coupled with other fields,  
53 such as the electric one, to be transferred across the interface. Notably, the results established by  
54 Barber [358,683] are expected to play an important role regarding the relation between electric current  
55 and voltage.

### 3.9.6. Industrial case studies: Steel forming processes, wafer lithography and roller bearings

Controlling tribological properties in steel-making processes is necessary to improve quality and increase the production rate. Undesirable phenomena include temperature-dependent adhesive wear, flaking and galling. The industry currently uses tribological models that are based on continuum theories and incorporate limited microscale aspects and simplified roughness representations, or phenomenological models that strongly rely on experience: e.g., the friction coefficient is varied within a known range to predict process parameters. Philips Drachten, for example, currently uses a micromechanics-based numerical model to predict friction coefficients that vary with local pressure, strain and temperature [684]. Such models calculate the load-carrying capacity of lubricant-filled cavities, where the Young's modulus and flow stress are modelled as temperature-dependent. There is a need for numerical models that satisfy certain criteria: they should use computationally-efficient simulation strategies, be usable in automated control systems to allow in-line adjustment of process settings based on (meta)data, and they should be robust across various processes and demonstrable results at both ends of the dimensional range. Hence, there is need for simple (perhaps, even, analytical) but comprehensive predictive models of friction as well as system-level simulations that can incorporate tribological aspects into the modeling of multi-stage deformation processes.

While unanswered questions remain and improved models are needed in the "classical" manufacturing world, tribological issues persist also for semiconductor companies such as ASML that use fast extreme ultraviolet (EUV) lithography on large tens-of-micrometers-thick wafers to manufacture integrated circuits with positioning accuracies of the order of nanometers. Physics and chemistry questions are relevant for such processes, focusing on EUV source, scanner, metrology and process attributes. Current positioning methods involve electrostatic forces used to fix the wafers onto burls on the substrate; improving and optimizing positioning accuracy requires multiphysics modeling across scales since wafer-support forces lead to wafer distortions and, in turn, to overlay and height (out of focus) errors. Adhesion and friction play an important role in wafer support as does the contact and clamping history: the order in which contact with individual burls is established is different every time. Furthermore, positioning is a dynamical contact phenomenon that, at such small scales, results in accelerations of about 50g. One major advance for the industry would be to realize switchable friction without wear.

A final example of an industrial case study is the understanding of friction in roller bearing. Having this as the ultimate goal, researchers at SKF performed, in collaboration with the tribology group at Imperial College, non-equilibrium molecular dynamics simulations of stearic acid adsorbed on iron surfaces with nanoscale roughness [685]. The stearic acid films were found to be able to maintain separation of asperities on opposing surfaces due to strong adsorption of the head groups, thereby decreasing the friction coefficients and Derjaguin offsets. These effects were negligibly affected by an increase in surface roughness. To tackle larger size and time scales, multiscale methods are likely candidates for future research. Of particular interest are the quasi-continuum method [686], and the CPL library (<http://cpl-library.org/>) [687], a recently developed communication and topology management system for coupling continuum fluid dynamics to molecular dynamics. Other possible avenues for further research are accelerated molecular dynamics techniques.

## 4. Conclusions

One of the main outcomes of the Lorentz workshop on "Micro/Nanoscale Models for Tribology" was the realization that, despite the modeling community's ability to address elastic problems of great complexity at various scales, significant effort is still required to account for effects like plasticity, adhesion, friction, wear, lubrication and surface chemistry in tribological models. Although many

1 systems do involve two or more of those phenomena at various scales, multiscale and multiphysics  
2 models are still scarce and challenging to use by non-specialists. Breakthroughs are thus expected  
3 from the future development of versatile and efficient multiscale/physics tools dedicated to tribology.  
4 On the other hand, tribologists still need to identify key elementary processes specific to rough  
5 contacts under shear, and associated, for example, to crack nucleation and propagation, chemical  
6 reactions, or fluid-solid interactions. In order to keep a clear physical understanding of the outcome of  
7 complex models, those processes will preferably be first studied on their own, before introducing the  
8 related behavior laws in more comprehensive tools. Only by pursuing simultaneously both research  
9 avenues will the tribology community have a chance to (i) advance on the fundamental understanding  
10 of frictional interfaces and (ii) propose simple but comprehensive models useful to optimize and  
11 control industrial processes.  
12  
13

14 As a good way of improving existing models and testing new ones, one agreement that was reached  
15 among the participants of the workshop was the need for more exercises like the contact-mechanics  
16 challenge described in §3.5. This is not a trivial task<sup>1</sup>, and no general consensus was reached about  
17 what could be the most important challenge to launch. However, the need to propose tribology  
18 challenges for quantities that can be also experimentally measured in parallel was clearly expressed. In  
19 such a way, challenges would not be mainly academic exercises of computing capabilities, but may  
20 help set up realistic problems which can have reasonable experimental counterparts. In this context,  
21 quantitative comparison with experiments will naturally lead to considering effects not taken into  
22 account in the contact-mechanics challenge, such as plasticity, long-range adhesion, large  
23 deformations and friction. Those effects could first be assessed separately and then simultaneously  
24 with an extensive range of parameters and not just one precise choice. The development of  
25 deterministic ways of preparing surfaces (e.g. 3D printing, or micro-milling) opens the way for  
26 experimental assessment of the role of various roughness scales on tribological properties, by adding  
27 more and more scales in the surface topography.  
28  
29  
30  
31  
32

33 Considering the contrast between the convergence of interests among the workshop participants and  
34 the diversity of cultures and modeling traditions in their respective communities of origin, a need for  
35 collaborative platforms for tribologists has emerged. A shared platform, organized via a dedicated  
36 website, could include the following sections: (i) open source software provided by research groups,  
37 useful also for dissemination purposes; (ii) a collection of contact problem results, reporting, for each  
38 case study, the surface topography used as an input for the simulation/experiment, the material  
39 parameters and the constitutive model, and a description of the assumptions of the computational  
40 model used to obtain the contact response; (iii) a list of simulation and testing facilities of research  
41 groups working on contact mechanics, with links to their websites and laboratories, organized  
42 according to the major problems of industrial interest. This collaborative platform is envisaged to have  
43 an important impact on the community to foster novel round robin campaigns like the challenges  
44 mentioned in the previous paragraph, provide material useful for benchmark tests, increase the  
45 awareness of companies in the applicability of tribology and contact mechanics research to solve  
46 problems of industrial interest and ultimately accelerate tribological research in the interdisciplinary  
47 manner necessary to lead to breakthroughs in the field.  
48  
49  
50  
51  
52

## 53 **Acknowledgements**

54 This review is the result of a Lorentz Center workshop on “Micro/Nanoscale Models for Tribology”  
55 held in Leiden between 30 January and 3 February 2017. The workshop was co-organized by M.  
56 Ciavarella, A. Fasolino, L. Nicola, J. Scheibert, A.I. Vakis and V.A. Yastrebov and sponsored by the  
57 Lorentz Center, the Royal Netherlands Academy of Arts and Sciences (KNAW), the Materials  
58 Innovation Institute (M2i), the Groningen University Fund (GUF) and the company Nanovea.  
59  
60  
61  
62  
63  
64  
65

Participants came from engineering, materials science, applied physics and chemistry backgrounds with a 9:1 ratio of academia to industry and 85% being (predominantly) modelers and theoreticians versus 15% being (predominantly) experimentalists (for more information, please visit the conference-specific website at <https://tribomodels2017.sciencesconf.org/>). Interactive discussions were held over a broad range of topics relevant to tribology with emphasis on modeling, facilitated via 7 keynote lectures and 16 round-table discussion sessions. We acknowledge the input of the participants in the writing of this manuscript, both by supplying useful comments and suggestions as well as providing up-to-date and pertinent references.

G.C. and F.B. are supported by H2020 FET Proactive “Neurofibres” grant No. 732344. R.G. is supported by Bonfiglioli Riduttori SpA. N.M.P. is supported by the European Commission H2020 under the Graphene Flagship Core 1 No. 696656 (WP14 “Polymer Nanocomposites”) and FET Proactive “Neurofibres” grant No. 732344.

N.M.P. is supported by the European Commission H2020 under the Graphene Flagship Core 1 No. 696656 (WP14 “Polymer composites”) and FET Proactive “Neurofibres” grant No. 732344.

A. C. is supported by the Czech Science Foundation, project 17-24164Y.

P.N. acknowledges the support of the Czech Science Foundation through the project 16-11516Y.

D.D. acknowledges the support of the Engineering and Physical Sciences Research Council (EPSRC) under the Established Career Fellowship grant EP/N025954/1.

## References

- [1] Jost HP. Lubrication: Tribology; Education and Research; Report on the Present Position and Industry's Needs (submitted to the Department of Education and Science by the Lubrication Engineering and Research) Working Group. : HM Stationery Office, 1966.
- [2] Tzanakis I, Hadfield M, Thomas B, Noya S, Henshaw I, Austen S. Future perspectives on sustainable tribology. *Renewable and Sustainable Energy Reviews* 2012;16:4126-40.
- [3] Donnet C, Erdemir A. Solid lubricant coatings: recent developments and future trends. *Tribology Letters* 2004;17:389-97.
- [4] Spikes H. Sixty years of EHL. *Lubr Sci* 2006;18:265-91.
- [5] Neville A, Morina A, Haque T, Voong M. Compatibility between tribological surfaces and lubricant additives—how friction and wear reduction can be controlled by surface/lube synergies. *Tribol Int* 2007;40:1680-95.
- [6] Holmberg K, Andersson P, Erdemir A. Global energy consumption due to friction in passenger cars. *Tribol Int* 2012;47:221-34.
- [7] Greenwood J, Williamson J. Contact of Nominally Flat Surfaces. *Proc R Soc A* 1966;295:300-19.
- [8] Persson BNJ. Theory of rubber friction and contact mechanics. *J Chem Phys* 2001;115:3840-61.
- [9] Carpick RW, Salmeron M. Scratching the surface: fundamental investigations of tribology with atomic force microscopy. *Chem Rev* 1997;97:1163-94.
- [10] Persson B, Albohr O, Tartaglino U, Volokitin A, Tosatti E. On the nature of surface roughness with application to contact mechanics, sealing, rubber friction and adhesion. *Journal of Physics: Condensed Matter* 2004;17:R1.
- [11] Morales-Espejel GE. Surface roughness effects in elastohydrodynamic lubrication: A review with contributions. *Proc Inst Mech Eng Part J* 2014;228:1217-42.
- [12] Kim SH, Asay DB, Dugger MT. Nanotribology and MEMS. *Nano today* 2007;2:22-9.
- [13] Bhushan B. Nanotribology and nanomechanics of MEMS/NEMS and BioMEMS/BioNEMS materials and devices. *Microelectronic Engineering* 2007;84:387-412.
- [14] Canchi SV, Bogy DB. Thermal fly-height control slider instability and dynamics at touchdown: Explanations using nonlinear systems theory. *J Tribol* 2011;133:021902.

- 1 [15] Vakis AI, Hadjicostis CN, Polycarpou AA. Three-DOF dynamic model with lubricant contact for  
2 thermal fly-height control nanotechnology. *J Phys D* 2012;45:135402.
- 3 [16] Cann P, Wimmer M. Welcome to the first issue of *Biotribology*. *Biotribology* 2015:1.
- 4 [17] van Kuilenburg J, Masen MA, van der Heide E. A review of fingerpad contact mechanics and  
5 friction and how this affects tactile perception. *Proc Inst Mech Eng Part J* 2015;229:243-58.
- 6 [18] Ma S, Scaraggi M, Wang D, Wang X, Liang Y, Liu W et al. Nanoporous Substrate- Infiltrated  
7 Hydrogels: a Bioinspired Regenerable Surface for High Load Bearing and Tunable Friction.  
8 *Advanced Functional Materials* 2015;25:7366-74.
- 9 [19] Rashid H. The effect of surface roughness on ceramics used in dentistry: A review of literature.  
10 *Eur J Dent* 2014;8:571-9.
- 11 [20] Martin J, Donnet C, Le Mogne T, Epicier T. Superlubricity of molybdenum disulphide. *Physical*  
12 *Review B* 1993;48:10583.
- 13 [21] Dienwiebel M, Verhoeven GS, Pradeep N, Frenken JW, Heimberg JA, Zandbergen HW.  
14 Superlubricity of graphite. *Phys Rev Lett* 2004;92:126101.
- 15 [22] Hirano M, Shinjo K. Superlubricity and frictional anisotropy. *Wear* 1993;168:121-5.
- 16 [23] Urbakh M. Friction: Towards macroscale superlubricity. *Nature nanotechnology* 2013;8:893-4.
- 17 [24] Berman D, Deshmukh SA, Sankaranarayanan SK, Erdemir A, Sumant AV. Friction. Macroscale  
18 superlubricity enabled by graphene nanoscroll formation. *Science* 2015;348:1118-22.
- 19 [25] Carbone G, Pierro E, Gorb SN. Origin of the superior adhesive performance of mushroom-shaped  
20 microstructured surfaces. *Soft Matter* 2011;7:5545-52.
- 21 [26] Afferrante L, Carbone G, Demelio G, Pugno N. Adhesion of elastic thin films: double peeling of  
22 tapes versus axisymmetric peeling of membranes. *Tribology Letters* 2013;52:439-47.
- 23 [27] Kim TW, Bhushan B. The adhesion model considering capillarity for gecko attachment system. *J*  
24 *R Soc Interface* 2008;5:319-27.
- 25 [28] Persson B, Gorb S. The effect of surface roughness on the adhesion of elastic plates with  
26 application to biological systems. *J Chem Phys* 2003;119:11437-44.
- 27 [29] Papangelo A, Ciavarella M. A Maugis-Dugdale cohesive solution for adhesion of a surface with a  
28 dimple. *J R Soc Interface* 2017;14:10.1098/rsif.2016.0996.
- 29 [30] Geim AK, Dubonos S, Grigorieva I, Novoselov K, Zhukov A, Shapoval SY. Microfabricated  
30 adhesive mimicking gecko foot-hair. *Nature materials* 2003;2:461.
- 31 [31] Zhou M, Pesika N, Zeng H, Tian Y, Israelachvili J. Recent advances in gecko adhesion and  
32 friction mechanisms and development of gecko-inspired dry adhesive surfaces. *Friction*  
33 2013;1:114-29.
- 34 [32] Huber G, Mantz H, Spolenak R, Mecke K, Jacobs K, Gorb SN et al. Evidence for capillarity  
35 contributions to gecko adhesion from single spatula nanomechanical measurements. *Proc Natl*  
36 *Acad Sci U S A* 2005;102:16293-6.
- 37 [33] Ma S, Scaraggi M, Lin P, Yu B, Wang D, Dini D et al. Nanohydrogel Brushes for Switchable  
38 Underwater Adhesion. *The Journal of Physical Chemistry C* 2017;121:8452-63.
- 39 [34] Kappl M, Kaveh F, Barnes WJP. Nanoscale friction and adhesion of tree frog toe pads.  
40 *Bioinspiration & biomimetics* 2016;11:035003.
- 41 [35] Gorb SN, Sinha M, Peressadko A, Daltorio KA, Quinn RD. Insects did it first: a micropatterned  
42 adhesive tape for robotic applications. *Bioinspiration & biomimetics* 2007;2:S117.
- 43 [36] Autumn K, Sitti M, Liang YA, Peattie AM, Hansen WR, Sponberg S et al. Evidence for van der  
44 Waals adhesion in gecko setae. *Proc Natl Acad Sci U S A* 2002;99:12252-6.
- 45 [37] Cho K, Koh J, Kim S, Chu W, Hong Y, Ahn S. Review of manufacturing processes for soft  
46 biomimetic robots. *International Journal of Precision Engineering and Manufacturing*  
47 2009;10:171-81.
- 48 [38] Scheibert J, Laurent S, Prevost A, Debregeas G. The role of fingerprints in the coding of tactile  
49 information probed with a biomimetic sensor. *Science* 2009;323:1503-6.
- 50 [39] Hayward V. Is there a 'plenhaptic' function? *Philos Trans R Soc Lond B Biol Sci* 2011;366:3115-  
51 22.
- 52 [40] Prescott TJ, Diamond ME, Wing AM. Active touch sensing. *Philos Trans R Soc Lond B Biol Sci*  
53 2011;366:2989-95.
- 54 [41] Klöcker A, Wiertlewski M, Théate V, Hayward V, Thonnard J. Physical factors influencing  
55 pleasant touch during tactile exploration. *Plos one* 2013;8:e79085.
- 56  
57  
58  
59  
60  
61  
62  
63  
64  
65

- 1 [42] Johnson MT, Sluis VD, Brokken D. User interface with haptic feedback. 2013;US 13/879,420.
- 2 [43] Johnson KL. Contact mechanics. Cambridge, UK: Cambridge University Press, 1985.
- 3 [44] Barber JR, Ciavarella M. Contact mechanics. *Int J Solids Structures* 2000;37:29-43.
- 4 [45] Popov V. Contact mechanics and friction: physical principles and applications. : Springer Science  
5 & Business Media, 2010.
- 6 [46] Persson B. Sliding friction: physical principles and applications. : Springer Science & Business  
7 Media, 2013.
- 8 [47] Adams G, Nosonovsky M. Contact modeling—forces. *Tribol Int* 2000;33:431-42.
- 9 [48] Tichy JA, Meyer DM. Review of solid mechanics in tribology. *Int J Solids Structures*  
10 2000;37:391-400.
- 11 [49] Hertz H. Über die berührung fester elastische Körper und über die Harte. *Verhandlungen des*  
12 *Vereins zur Beförderung des Gewerbefleisses* 1882.
- 13 [50] Johnson KL, Kendall K, Roberts AD. Surface energy and the contact of elastic solids. *Proc R Soc*  
14 *A* 1971;324:301-13.
- 15 [51] Derjaguin BV, Muller VM, Toporov YP. Effect of contact deformations on the adhesion of  
16 particles. *J Colloid Interface Sci* 1975;53:314-26.
- 17 [52] Constantinescu A, Korsunsky A, Pison O, Oueslati A. Symbolic and numerical solution of the  
18 axisymmetric indentation problem for a multilayered elastic coating. *Int J Solids Structures*  
19 2013;50:2798-807.
- 20 [53] Komvopoulos K, Gong Z-. Stress analysis of a layered elastic solid in contact with a rough  
21 surface exhibiting fractal behavior. *Int J Solids Structures* 2007;44:2109-29.
- 22 [54] Chen WW, Zhou K, Keer LM, Wang QJ. Modeling elasto-plastic indentation on layered materials  
23 using the equivalent inclusion method. *Int J Solids Structures* 2010;47:2841-54.
- 24 [55] Bagault C, Nélias D, Baietto MC, Ovaert TC. Contact analyses for anisotropic half-space coated  
25 with an anisotropic layer: Effect of the anisotropy on the pressure distribution and contact area.  
26 *Int J Solids Structures* 2013;50:743-54.
- 27 [56] Chidlow SJ, Teodorescu M. Sliding contact problems involving inhomogeneous materials  
28 comprising a coating-transition layer-substrate and a rigid punch. *Int J Solids Structures*  
29 2014;51:1931-45.
- 30 [57] Putignano C, Carbone G, Dini D. Mechanics of rough contacts in elastic and viscoelastic thin  
31 layers. *Int J Solids Structures* 2015;69–70:507-17.
- 32 [58] Stan G, Adams GG. Adhesive contact between a rigid spherical indenter and an elastic multi-  
33 layer coated substrate. *Int J Solids Structures* 2016;87:1-10.
- 34 [59] Zhang M, Zhao N, Glaws P, Hegedus P, Zhou Q, Wang Z et al. Elasto-plastic contact of materials  
35 containing double-layered inhomogeneities. *Int J Solids Structures* 2017;126–127:208-24.
- 36 [60] Reina S, Dini D, Hills D, Iida Y. A quadratic programming formulation for the solution of  
37 layered elastic contact problems: Example applications and experimental validation. *European*  
38 *Journal of Mechanics-A/Solids* 2011;30:236-47.
- 39 [61] Ciavarella M. The generalized Cattaneo partial slip plane contact problem. I-Theory. *Int J Solids*  
40 *Structures* 1998;35:2349-62.
- 41 [62] Dini D, Hills DA. A method based on asymptotics for the refined solution of almost complete  
42 partial slip contact problems. *European Journal of Mechanics - A/Solids* 2003;22:851-9.
- 43 [63] Sackfield A, Hills DA, Qiu H. Side-contact of sharp indenters, including the effects of friction.  
44 *Int J Mech Sci* 2007;49:567-76.
- 45 [64] Flicek RC, Hills DA, Dini D. Sharp edged contacts subject to fretting: A description of corner  
46 behaviour. *Int J Fatigue* 2015;71:26-34.
- 47 [65] Sundaram N, Farris T. Mechanics of advancing pin-loaded contacts with friction. *J Mech Phys*  
48 *Solids* 2010;58:1819-33.
- 49 [66] Fleury R, Hills DA, Ramesh R, Barber JR. Incomplete contacts in partial slip subject to varying  
50 normal and shear loading, and their representation by asymptotes. *J Mech Phys Solids*  
51 2017;99:178-91.
- 52 [67] Hills DA, Dini D. A new method for the quantification of nucleation of fretting fatigue cracks  
53 using asymptotic contact solutions. *Tribol Int* 2006;39:1114-22.
- 54  
55  
56  
57  
58  
59  
60  
61  
62  
63  
64  
65



- [68] Mugadu A, Hills D, Barber J, Sackfield A. The application of asymptotic solutions to characterising the process zone in almost complete frictional contacts. *Int J Solids Structures* 2004;41:385-97.
- [69] Dini D, Barber J, Churchman C, Sackfield A, Hills D. The application of asymptotic solutions to contact problems characterised by logarithmic singularities. *European Journal of Mechanics-A/Solids* 2008;27:847-58.
- [70] Ballard P. Steady sliding frictional contact problem for a 2d elastic half-space with a discontinuous friction coefficient and related stress singularities. *J Mech Phys Solids* 2016;97:225-59.
- [71] Oliver WC, Pharr GM. An improved technique for determining hardness and elastic modulus using load and displacement sensing indentation experiments. *J Mater Res* 1992;7:1564-83.
- [72] Oliver WC, Pharr GM. Measurement of hardness and elastic modulus by instrumented indentation: Advances in understanding and refinements to methodology. *J Mater Res* 2004;19:3-20.
- [73] Butt H, Cappella B, Kappl M. Force measurements with the atomic force microscope: Technique, interpretation and applications. *Surf Sci Rep* 2005;59:1-152.
- [74] Ramesh R, Hills D. Recent progress in understanding the properties of elastic contacts. *Proc Inst Mech Eng Part C* 2015;229:2117-26.
- [75] Kartal ME, Barber JR, Hills DA, Nowell D. Partial slip problem for two semi-infinite strips in contact. *Int J Eng Sci* 2011;49:203-11.
- [76] Flicek RC, Hills DA, Barber JR, Dini D. Determination of the shakedown limit for large, discrete frictional systems. *European Journal of Mechanics - A/Solids* 2015;49:242-50.
- [77] Eriten M, Polycarpou A, Bergman L. Physics-based modeling for fretting behavior of nominally flat rough surfaces. *Int J Solids Structures* 2011;48:1436-50.
- [78] Papangelo A, Ciavarella M, Barber J. Fracture mechanics implications for apparent static friction coefficient in contact problems involving slip-weakening laws. 2015;471:20150271.
- [79] Ruina A, Rice JR. Stability of steady frictional slipping. *Journal of Applied Mechanics* 1983;50:343-9.
- [80] Adams GG. Self-excited oscillations of two elastic half-spaces sliding with a constant coefficient of friction. *J appl Mech* 1995;62:867-72.
- [81] Adams GG, Muftu S. Improvements to a scale-dependent model for contact and friction. *J Phys D* 2005;38:1402-9.
- [82] Stronge WJ. *Impact mechanics*. : Cambridge university press, 2004.
- [83] Thornton C, Cummins SJ, Cleary PW. On elastic-plastic normal contact force models, with and without adhesion. *Powder Technol* 2017;315:339-46.
- [84] Yildirim B, Yang H, Gouldstone A, Müftü S. Rebound mechanics of micrometre-scale, spherical particles in high-velocity impacts. 2017;473:20160936.
- [85] Ye Y, Zeng Y. A size-dependent viscoelastic normal contact model for particle collision. *Int J Impact Eng* 2017;106:120-32.
- [86] Yu K, Elghannay HA, Tafti D. An impulse based model for spherical particle collisions with sliding and rolling. *Powder Technol* 2017;319:102-16.
- [87] Banerjee A, Chanda A, Das R. Historical origin and recent development on normal directional impact models for rigid body contact simulation: a critical review. *Archives of Computational Methods in Engineering* 2017;24:397-422.
- [88] Yi Y, Barber JR, Zagrodzki P. Eigenvalue solution of thermoelastic instability problems using Fourier reduction. *Proceedings of the Royal Society of London A: Mathematical, Physical and Engineering Sciences* 2000;456:2799-821.
- [89] Afferrante L, Ciavarella M, Decuzzi P, Demelio G. Transient analysis of frictionally excited thermoelastic instability in multi-disk clutches and brakes. *Wear* 2003;254:136-46.
- [90] Nowell D, Dini D, Hills D. Recent developments in the understanding of fretting fatigue. *Eng Fract Mech* 2006;73:207-22.
- [91] Hills DA, Nowell D. Mechanics of fretting fatigue-Oxford's contribution. *Tribol Int* 2014;76:1-5.
- [92] Araujo J, Nowell D. The effect of rapidly varying contact stress fields on fretting fatigue. *Int J Fatigue* 2002;24:763-75.

- 1 [93] Kinyon SE. Fretting fatigue: advances in basic understanding and applications. : Astm  
2 International, 2003.
- 3 [94] Ciavarella M. A 'crack-like' notch analogue for a safe-life fretting fatigue design methodology.  
4 Fatigue & Fracture of Engineering Materials & Structures 2003;26:1159-70.
- 5 [95] Hoepfner DW. Fretting fatigue case studies of engineering components. Tribol Int 2006;39:1271-  
6 6.
- 7 [96] Bower A. The influence of crack face friction and trapped fluid on surface initiated rolling contact  
8 fatigue cracks. Journal of Tribology 1988;110:704-11.
- 9 [97] Afferrante L, Ciavarella M, Demelio G. A re-examination of rolling contact fatigue experiments  
10 by Clayton and Su with suggestions for surface durability calculations. Wear 2004;256:329-34.
- 11 [98] Ponter A, Afferrante L, Ciavarella M. A note on Merwin's measurements of forward flow in  
12 rolling contact. Wear 2004;256:321-8.
- 13 [99] Franklin FJ, Widiyarta I, Kapoor A. Computer simulation of wear and rolling contact fatigue.  
14 Wear 2001;251:949-55.
- 15 [100] Kalker JJ. Three-dimensional elastic bodies in rolling contact. : Springer Science & Business  
16 Media, 2013.
- 17 [101] Sadeghi F, Jalalahmadi B, Slack TS, Raje N, Arakere NK. A review of rolling contact fatigue.  
18 Journal of tribology 2009;131:041403.
- 19 [102] Yang W, Huang Y, Zhou Q, Wang J, Jin X, Keer LM. Parametric study on stressed volume and  
20 its application to the quantification of rolling contact fatigue performance of heterogeneous  
21 material. Tribol Int 2017;107:221-32.
- 22 [103] Solano-Alvarez W, Peet MJ, Pickering EJ, Jaiswal J, Bevan A, Bhadeshia HKDH. Synchrotron  
23 and neural network analysis of the influence of composition and heat treatment on the rolling  
24 contact fatigue of hypereutectoid pearlitic steels. Materials Science and Engineering: A  
25 2017;707:259-69.
- 26 [104] Jiang Y, Xu B, Sehitoglu H. Three-dimensional elastic-plastic stress analysis of rolling contact.  
27 Journal of Tribology 2002;124:699-708.
- 28 [105] Goryacheva IG. Contact mechanics in tribology. : Springer Science & Business Media, 2013.
- 29 [106] Torskaya EV. Modeling of frictional interaction of a rough indenter and a two-layer elastic half-  
30 space. Physical Mesomechanics 2012;15:245-50.
- 31 [107] Goryacheva I, Makhovskaya Y. Adhesion effect in sliding of a periodic surface and an  
32 individual indenter upon a viscoelastic base. The Journal of Strain Analysis for Engineering  
33 Design 2016;51:286-93.
- 34 [108] Goryacheva I, Shpenev A. Modelling of a punch with a regular base relief sliding along a  
35 viscoelastic foundation with a liquid lubricant. J Appl Math Mech 2012;76:582-9.
- 36 [109] Majumdar A, Bhushan B. Fractal model of elastic-plastic contact between rough surfaces.  
37 ASME J Tribol 1991;113:1-11.
- 38 [110] Archard JF. Elastic Deformation and the Laws of Friction. Proceedings of the Royal Society of  
39 London. Series A, Mathematical and Physical Sciences 1957;243:190-205.
- 40 [111] Ciavarella M, Demelio G, Barber JR, Jang YH. Linear elastic contact of the Weierstrass profile.  
41 Proceedings of the Royal Society of London A: Mathematical, Physical and Engineering  
42 Sciences 2000;456:387-405.
- 43 [112] Nayak PR. Random Process Model of Rough Surfaces. J Lubr Technol 1971;93:398-407.
- 44 [113] Longuet-Higgins MS. The statistical analysis of a random, moving surface. Philosophical  
45 Transactions of the Royal Society of London A: Mathematical, Physical and Engineering  
46 Sciences 1957;249:321-87.
- 47 [114] Longuet-Higgins MS. Statistical properties of an isotropic random surface. Philosophical  
48 Transactions of the Royal Society of London A: Mathematical, Physical and Engineering  
49 Sciences 1957;250:157-74.
- 50 [115] Bush AW, Gibson RD, Thomas TR. The elastic contact of a rough surface. Wear 1975;35:87-  
51 111.
- 52 [116] Greenwood JA. A simplified elliptic model of rough surface contact. Wear 2006;261:191-200.
- 53 [117] Paggi M, Ciavarella M. The coefficient of proportionality  $k$  between real contact area and load,  
54 with new asperity models. Wear 2010;268:1020-9.
- 55  
56  
57  
58  
59  
60  
61  
62  
63  
64  
65

- 1 [118] Carbone G, Bottiglione F. Asperity contact theories: Do they predict linearity between contact  
2 area and load? *J Mech Phys Solids* 2008;56:2555-72.
- 3 [119] Yastrebov VA, Anciaux G, Molinari J. The role of the roughness spectral breadth in elastic  
4 contact of rough surfaces. arXiv preprint arXiv:1704.05650 2017.
- 5 [120] Ciavarella M, Greenwood JA, Paggi M. Inclusion of "interaction" in the Greenwood and  
6 Williamson contact theory. *Wear* 2008;265:729-34.
- 7 [121] Chandrasekar S, Eriten M, Polycarpou AA. An Improved Model of Asperity Interaction in  
8 Normal Contact of Rough Surfaces. *J Appl Mech* 2013;80:011025.
- 9 [122] Vakis AI. Asperity Interaction and Substrate Deformation in Statistical Summation Models of  
10 Contact Between Rough Surfaces. *J Appl Mech* 2014;81:41012.
- 11 [123] Ciavarella M, Delfine V, Demelio G. A "re-vitalized" Greenwood and Williamson model of  
12 elastic contact between fractal surfaces. *J Mech Phys Solids* 2006;54:2569-91.
- 13 [124] Putignano C, Afferrante L, Carbone G, Demelio G. The influence of the statistical properties of  
14 self-affine surfaces in elastic contacts: A numerical investigation. *J Mech Phys Solids*  
15 2012;60:973-82.
- 16 [125] Persson B, Bucher F, Chiaia B. Elastic contact between randomly rough surfaces: comparison of  
17 theory with numerical results. *Physical Review B* 2002;65:184106.
- 18 [126] Manners W, Greenwood JA. Some observations on Persson's diffusion theory of elastic contact.  
19 *Wear* 2006;261:600-10.
- 20 [127] Hyun S, Pei L, Molinari J, Robbins MO. Finite-element analysis of contact between elastic self-  
21 affine surfaces. *Physical Review E* 2004;70:026117.
- 22 [128] Zavarise G, Borri-Brunetto M, Paggi M. On the reliability of microscopical contact models.  
23 *Wear* 2004;257:229-45.
- 24 [129] Hyun S, Robbins MO. Elastic contact between rough surfaces: Effect of roughness at large and  
25 small wavelengths. *Tribol Int* 2007;40:1413-22.
- 26 [130] Campaná C, Müser MH. Contact mechanics of real vs. randomly rough surfaces: A Green's  
27 function molecular dynamics study. *EPL (Europhysics Letters)* 2007;77:38005.
- 28 [131] Campañá C, Müser MH, Robbins MO. Elastic contact between self-affine surfaces: comparison  
29 of numerical stress and contact correlation functions with analytic predictions. *J Phys : Cond*  
30 *Matter* 2008;20:354013.
- 31 [132] Almqvist A, Campañá C, Prodanov N, Persson BNJ. Interfacial separation between elastic solids  
32 with randomly rough surfaces: Comparison between theory and numerical techniques. *J Mech*  
33 *Phys Solids* 2011;59:2355-69.
- 34 [133] Putignano C, Afferrante L, Carbone G, Demelio G. A new efficient numerical method for  
35 contact mechanics of rough surfaces. *Int J Solids Structures* 2012;49:338-43.
- 36 [134] Pastewka L, Prodanov N, Lorenz B, Müser MH, Robbins MO, Persson BN. Finite-size scaling  
37 in the interfacial stiffness of rough elastic contacts. *Physical Review E* 2013;87:062809.
- 38 [135] Dapp WB, Prodanov N, Müser MH. Systematic analysis of Persson's contact mechanics theory  
39 of randomly rough elastic surfaces. *Journal of Physics: Condensed Matter* 2014;26:355002.
- 40 [136] Prodanov N, Dapp WB, Müser MH. On the Contact Area and Mean Gap of Rough, Elastic  
41 Contacts: Dimensional Analysis, Numerical Corrections, and Reference Data. *Tribol Lett*  
42 2014;53:433-48.
- 43 [137] Yastrebov VA, Anciaux G, Molinari J. From infinitesimal to full contact between rough  
44 surfaces: Evolution of the contact area. *Int J Solids Structures* 2015;52:83-102.
- 45 [138] Solhjoo S, Vakis AI. Continuum mechanics at the atomic scale: Insights into non-adhesive  
46 contacts using molecular dynamics simulations. *J Appl Phys* 2016;120:215102.
- 47 [139] Papangelo A, Hoffmann N, Ciavarella M. Load-separation curves for the contact of self-affine  
48 rough surfaces. *Scientific Reports* 2017.
- 49 [140] Yang C, Persson B. Contact mechanics: contact area and interfacial separation from small  
50 contact to full contact. *Journal of Physics: Condensed Matter* 2008;20:215214.
- 51 [141] Zienkiewicz OC, Taylor RL. The finite element method: solid mechanics. : Butterworth-  
52 Heinemann, 2000.
- 53 [142] Banerjee PK, Butterfield R. Boundary element methods in engineering science. : McGraw-Hill  
54 London, 1981.
- 55  
56  
57  
58  
59  
60  
61  
62  
63  
64  
65

- 1 [143] Johnson KL, Greenwood JA, Higginson JG. The contact of elastic regular wavy surfaces. *Int J*  
2 *Mech Sci* 1985;27:383-96.
- 3 [144] Stanley HM, Kato T. An FFT-Based Method for Rough Surface Contact. *Journal of Tribology*  
4 1997;119:481-5.
- 5 [145] Laursen TA. *Computational Contact and Impact Mechanics: Fundamentals of Modelling*  
6 *Interfacial Phenomena in Nonlinear Finite Element Analysis.* : Springer, Berlin, 2002.
- 7 [146] Wriggers P. *Computational contact mechanics.* : Springer, 2006.
- 8 [147] Yastrebov VA. *Numerical methods in contact mechanics.* : John Wiley & Sons, 2013.
- 9 [148] Bemporad A, Paggi M. Optimization algorithms for the solution of the frictionless normal  
10 contact between rough surfaces. *Int J Solids Structures* 2015;69–70:94-105.
- 11 [149] Rodríguez-Tembleque L, Abascal R. A 3D FEM–BEM rolling contact formulation for  
12 unstructured meshes. *Int J Solids Structures* 2010;47:330-53.
- 13 [150] Zografos A, Dini D, Olver AV. Fretting fatigue and wear in bolted connections: A multi-level  
14 formulation for the computation of local contact stresses. *Tribol Int* 2009;42:1663-75.
- 15 [151] Spence D. The Hertz contact problem with finite friction. *Journal of elasticity* 1975;5:297-319.
- 16 [152] Jacq C, Nélias D, Lormand G, Girodin D. Development of a three-dimensional semi-analytical  
17 elastic-plastic contact code. 2002.
- 18 [153] Sahlin F, Larsson R, Almqvist A, Lugt PM, Marklund P. A mixed lubrication model  
19 incorporating measured surface topography. Part 1: Theory of flow factors. *Proc Inst Mech Eng*  
20 *Part J* 2010;224:335-51.
- 21 [154] Sahlin F, Larsson R, Marklund P, Almqvist A, Lugt PM. A mixed lubrication model  
22 incorporating measured surface topography. Part 2: Roughness treatment, model validation, and  
23 simulation. *Proc Inst Mech Eng Part J* 2010;224:353-65.
- 24 [155] Carbone G, Putignano C. A novel methodology to predict sliding and rolling friction of  
25 viscoelastic materials: theory and experiments. *J Mech Phys Solids* 2013;61:1822-34.
- 26 [156] Bugnicourt R, Sainsot P, Lesaffre N, Lubrecht A. Transient frictionless contact of a rough rigid  
27 surface on a viscoelastic half-space. *Tribol Int* 2017.
- 28 [157] Yastrebov VA, Durand J, Proudhon H, Cailletaud G. Rough surface contact analysis by means  
29 of the Finite Element Method and of a new reduced model. *Comptes Rendus Mécanique*  
30 2011;339:473-90.
- 31 [158] Scaraggi M, Comingio D, Al-Qudsi A, De Lorenzis L. The influence of geometrical and  
32 rheological non-linearity on the calculation of rubber friction. *Tribol Int* 2016;101:402-13.
- 33 [159] Leroux J, Fulleringer B, Nelias D. Contact analysis in presence of spherical inhomogeneities  
34 within a half-space. *Int J Solids Structures* 2010;47:3034-49.
- 35 [160] Paggi M, Zavarise G. Contact mechanics of microscopically rough surfaces with graded  
36 elasticity. *European Journal of Mechanics-A/Solids* 2011;30:696-704.
- 37 [161] Dick T, Cailletaud G. Fretting modelling with a crystal plasticity model of Ti6Al4V.  
38 *Computational Materials Science* 2006;38:113-25.
- 39 [162] Casals O, Forest S. Finite element crystal plasticity analysis of spherical indentation in bulk  
40 single crystals and coatings. *Computational Materials Science* 2009;45:774-82.
- 41 [163] Yang B, Laursen TA. A mortar-finite element approach to lubricated contact problems. *Comput*  
42 *Methods Appl Mech Eng* 2009;198:3656-69.
- 43 [164] Nanbu T, Ren N, Yasuda Y, Zhu D, Wang QJ. Micro-textures in concentrated conformal-  
44 contact lubrication: effects of texture bottom shape and surface relative motion. *Tribology*  
45 *Letters* 2008;29:241-52.
- 46 [165] Stupkiewicz S, Lengiewicz J, Sadowski P, Kucharski S. Finite deformation effects in soft  
47 elastohydrodynamic lubrication problems. *Tribol Int* 2016;93:511-22.
- 48 [166] Rodríguez-Tembleque L, Sáez A, Buroni FC, Aliabadi FM. Quasistatic electro-elastic contact  
49 modeling using the boundary element method. 2016;681:185-96.
- 50 [167] Yastrebov VA, Cailletaud G, Proudhon H, Mballa FSM, Noël S, Testé P et al. Three-level multi-  
51 scale modeling of electrical contacts sensitivity study and experimental validation. 2015:414-22.
- 52 [168] Zhu D, Hu Y. A computer program package for the prediction of EHL and mixed lubrication  
53 characteristics, friction, subsurface stresses and flash temperatures based on measured 3-D  
54 surface roughness. *Tribol Trans* 2001;44:383-90.
- 55  
56  
57  
58  
59  
60  
61  
62  
63  
64  
65

- 1 [169] Geubelle PH, Rice JR. A spectral method for three-dimensional elastodynamic fracture  
2 problems. *J Mech Phys Solids* 1995;43:1791-824.
- 3 [170] Ranjith K. Spectral formulation of the elastodynamic boundary integral equations for bi-material  
4 interfaces. *Int J Solids Structures* 2015;59:29-36.
- 5 [171] Kammer DS, Yastrebov VA, Spijker P, Molinari J. On the propagation of slip fronts at frictional  
6 interfaces. *Tribology Letters* 2012;48:27-32.
- 7 [172] Yastrebov VA. Sliding without slipping under Coulomb friction: opening waves and inversion  
8 of frictional force. *Tribology Letters* 2016;62:1-8.
- 9 [173] Hill R. Generalized constitutive relations for incremental deformation of metal crystals by  
10 multislip. *J Mech Phys Solids* 1966;14:95-102.
- 11 [174] Rice JR. Inelastic constitutive relations for solids: an internal-variable theory and its application  
12 to metal plasticity. *J Mech Phys Solids* 1971;19:433-55.
- 13 [175] Hill R, Rice J. Constitutive analysis of elastic-plastic crystals at arbitrary strain. *J Mech Phys  
14 Solids* 1972;20:401-13.
- 15 [176] Asaro RJ. Micromechanics of crystals and polycrystals. *Adv Appl Mech* 1983;23:1-115.
- 16 [177] Barbe F, Decker L, Jeulin D, Cailletaud G. Intergranular and intragranular behavior of  
17 polycrystalline aggregates. Part 1: FE model. *Int J Plast* 2001;17:513-36.
- 18 [178] Barbe F, Forest S, Cailletaud G. Intergranular and intragranular behavior of polycrystalline  
19 aggregates. Part 2: Results. *Int J Plast* 2001;17:537-63.
- 20 [179] Berveiller M, Zaoui A. An extension of the self-consistent scheme to plastically-flowing  
21 polycrystals. *J Mech Phys Solids* 1978;26:325-44.
- 22 [180] Miehe C, Schröder J, Schotte J. Computational homogenization analysis in finite plasticity  
23 simulation of texture development in polycrystalline materials. *Comput Methods Appl Mech  
24 Eng* 1999;171:387-418.
- 25 [181] Roters F, Eisenlohr P, Hantcherli L, Tjahjanto DD, Bieler TR, Raabe D. Overview of  
26 constitutive laws, kinematics, homogenization and multiscale methods in crystal plasticity finite-  
27 element modeling: Theory, experiments, applications. *Acta Materialia* 2010;58:1152-211.
- 28 [182] Lebensohn RA, Tomé C. A self-consistent anisotropic approach for the simulation of plastic  
29 deformation and texture development of polycrystals: application to zirconium alloys. *Acta  
30 Metallurgica et Materialia* 1993;41:2611-24.
- 31 [183] Kalidindi SR. Incorporation of deformation twinning in crystal plasticity models. *J Mech Phys  
32 Solids* 1998;46:267273-71290.
- 33 [184] Staroselsky A, Anand L. Inelastic deformation of polycrystalline face centered cubic materials  
34 by slip and twinning. *J Mech Phys Solids* 1998;46:671675-3696.
- 35 [185] Thamburaja P, Anand L. Polycrystalline shape-memory materials: effect of crystallographic  
36 texture. *J Mech Phys Solids* 2001;49:709-37.
- 37 [186] Turteltaub S, Suiker A. Transformation-induced plasticity in ferrous alloys. *J Mech Phys Solids*  
38 2005;53:1747-88.
- 39 [187] Ortiz M, Repetto E. Nonconvex energy minimization and dislocation structures in ductile single  
40 crystals. *J Mech Phys Solids* 1999;47:397-462.
- 41 [188] Tóth LS, Estrin Y, Lapovok R, Gu C. A model of grain fragmentation based on lattice curvature.  
42 *Acta Materialia* 2010;58:1782-94.
- 43 [189] Petryk H, Kurka M. The energy criterion for deformation banding in ductile single crystals. *J  
44 Mech Phys Solids* 2013;61:1854-75.
- 45 [190] Frydrych K, Kowalczyk-Gajewska K. A three-scale crystal plasticity model accounting for grain  
46 refinement in fcc metals subjected to severe plastic deformations. *Materials Science and  
47 Engineering: A* 2016;658:490-502.
- 48 [191] Van der Giessen E, Needleman A. Discrete dislocation plasticity: a simple planar model. *Modell  
49 Simul Mater Sci Eng* 1995;3:689.
- 50 [192] Devincre B, Kubin L. Mesoscopic simulations of dislocations and plasticity. *Materials Science  
51 and Engineering: A* 1997;234:8-14.
- 52 [193] Wang Z, Ghoniem N, Swaminarayan S, LeSar R. A parallel algorithm for 3D dislocation  
53 dynamics. *Journal of computational physics* 2006;219:608-21.
- 54 [194] Arsenlis A, Cai W, Tang M, Rhee M, Opperstrup T, Hommes G et al. Enabling strain hardening  
55 simulations with dislocation dynamics. *Modell Simul Mater Sci Eng* 2007;15:553.
- 56  
57  
58  
59  
60  
61  
62  
63  
64  
65

- 1 [195] Verdier M, Fivel M, Groma I. Mesoscopic scale simulation of dislocation dynamics in fcc  
2 metals: Principles and applications. *Modell Simul Mater Sci Eng* 1998;6:755.
- 3 [196] Senger J, Weygand D, Gumbsch P, Kraft O. Discrete dislocation simulations of the plasticity of  
4 micro-pillars under uniaxial loading. *Scr Mater* 2008;58:587-90.
- 5 [197] Venugopalan SP, Müser MH, Nicola L. Green's function molecular dynamics meets discrete  
6 dislocation plasticity. *Model. Simul. Mater. Sc. Eng.* 2017.
- 7 [198] Gurrutxaga-Lerma B, Balint DS, Dini D, Eakins DE, Sutton AP. A dynamic discrete dislocation  
8 plasticity method for the simulation of plastic relaxation under shock loading.  
9 2013;469:20130141.
- 10 [199] Gurrutxaga-Lerma B, Balint DS, Dini D, Eakins DE, Sutton AP. Attenuation of the dynamic  
11 yield point of shocked aluminum using elastodynamic simulations of dislocation dynamics. *Phys*  
12 *Rev Lett* 2015;114:174301.
- 13 [200] Wallin M, Curtin W, Ristinmaa M, Needleman A. Multi-scale plasticity modeling: Coupled  
14 discrete dislocation and continuum crystal plasticity. *J Mech Phys Solids* 2008;56:3167-80.
- 15 [201] Xu Y, Balint D, Dini D. A method of coupling discrete dislocation plasticity to the crystal  
16 plasticity finite element method. *Modell Simul Mater Sci Eng* 2016;24:045007.
- 17 [202] Tower B. First report on friction experiments. *Proceedings of the institution of mechanical*  
18 *engineers* 1883;34:632-59.
- 19 [203] Grubin A. Fundamentals of the hydrodynamic theory of lubrication of heavily loaded cylindrical  
20 surfaces. *Investigation of the Contact Machine Componets* 1949;2.
- 21 [204] Reynolds O. On the Theory of Lubrication and Its Application to Mr. Beauchamp Tower's  
22 Experiments, Including an Experimental Determination of the Viscosity of Olive Oil.  
23 *Proceedings of the Royal Society of London* 1886;40:191-203.
- 24 [205] Cameron A, Wood W. The full journal bearing. *Proceedings of the Institution of Mechanical*  
25 *Engineers* 1949;161:59-72.
- 26 [206] Dowson D, Higginson G. A numerical solution to the elasto-hydrodynamic problem. *Journal of*  
27 *Mechanical Engineering Science* 1959;1:6-15.
- 28 [207] Dowson D, Higginson G. The effect of material properties on the lubrication of elastic rollers.  
29 *Journal of Mechanical Engineering Science* 1960;2:188-94.
- 30 [208] Dowson D, Higginson G, Whitaker A. Elasto-hydrodynamic lubrication: a survey of isothermal  
31 solutions. *Journal of Mechanical Engineering Science* 1962;4:121-6.
- 32 [209] Dowson D, Ehret P. Past, present and future studies in elasto-hydrodynamics. *Proc Inst Mech*  
33 *Eng Part J* 1999;213:317-33.
- 34 [210] Venner CH, Lubrecht AA. *Multi-level methods in lubrication.* : Elsevier, 2000.
- 35 [211] Hooke C. A review of the paper 'A numerical solution to the elasto-hydrodynamic problem' by  
36 D. Dowson and GR Higginson. *Proc Inst Mech Eng Part C* 2009;223:49-63.
- 37 [212] Hamrock BJ, Schmid SR, Jacobson BO. *Fundamentals of fluid film lubrication.* : CRC press,  
38 2004.
- 39 [213] Conry T, Wang S, Cusano C. A Reynolds-Eyring equation for elasto-hydrodynamic lubrication  
40 in line contacts. *Journal of tribology* 1987;109:648-54.
- 41 [214] Gohar R. *Elastohydrodynamics.* : World Scientific, 2001.
- 42 [215] Giacomini M, Fowell MT, Dini D, Strozzi A. A mass-conserving complementarity formulation  
43 to study lubricant films in the presence of cavitation. *Journal of Tribology* 2010;132:041702.
- 44 [216] Bertocchi L, Dini D, Giacomini M, Fowell MT, Baldini A. Fluid film lubrication in the presence  
45 of cavitation: a mass-conserving two-dimensional formulation for compressible, piezoviscous  
46 and non-Newtonian fluids. *Tribol Int* 2013;67:61-71.
- 47 [217] Woloszynski T, Podsiadlo P, Stachowiak GW. Efficient solution to the cavitation problem in  
48 hydrodynamic lubrication. *Tribology Letters* 2015;58:18.
- 49 [218] Tucker P, Keogh P. On the dynamic thermal state in a hydrodynamic bearing with a whirling  
50 journal using CFD techniques. *Journal of Tribology* 1996;118:356-63.
- 51 [219] Almqvist T, Larsson R. The Navier–Stokes approach for thermal EHL line contact solutions.  
52 *Tribol Int* 2002;35:163-70.
- 53 [220] Hartinger M, Dumont M, Ioannides S, Gosman D, Spikes H. CFD modeling of a thermal and  
54 shear-thinning elasto-hydrodynamic line contact. *Journal of Tribology* 2008;130:041503.



- 1 [221] Bruyere V, Fillot N, Morales-Espejel GE, Vergne P. Computational fluid dynamics and full  
2 elasticity model for sliding line thermal elasto-hydrodynamic contacts. *Tribol Int* 2012;46:3-13.
- 3 [222] Hajishafiee A, Kadiric A, Ioannides S, Dini D. A coupled finite-volume CFD solver for two-  
4 dimensional elasto-hydrodynamic lubrication problems with particular application to rolling  
5 element bearings. *Tribol Int* 2017;109:258-73.
- 6 [223] Profito FJ, Giacomini M, Zachariadis DC, Dini D. A general finite volume method for the  
7 solution of the Reynolds lubrication equation with a mass-conserving cavitation model.  
8 *Tribology Letters* 2015;60:18.
- 9 [224] Profito FJ, Vlădescu S, Reddyhoff T, Dini D. Transient experimental and modelling studies of  
10 laser-textured micro-grooved surfaces with a focus on piston-ring cylinder liner contacts. *Tribol*  
11 *Int* 2017;113:125-36.
- 12 [225] Vu-Quoc L, Zhang X, Lesburg L. Normal and tangential force–displacement relations for  
13 frictional elasto-plastic contact of spheres. *Int J Solids Structures* 2001;38:6455-89.
- 14 [226] Kruggel-Emden H, Wirtz S, Scherer V. A study on tangential force laws applicable to the  
15 discrete element method (DEM) for materials with viscoelastic or plastic behavior. *Chemical*  
16 *Engineering Science* 2008;63:1523-41.
- 17 [227] Thornton C, Cummins SJ, Cleary PW. An investigation of the comparative behaviour of  
18 alternative contact force models during elastic collisions. *Powder Technol* 2011;210:189-97.
- 19 [228] Rathbone D, Marigo M, Dini D, van Wachem B. An accurate force–displacement law for the  
20 modelling of elastic–plastic contacts in discrete element simulations. *Powder Technol*  
21 2015;282:2-9.
- 22 [229] Moreno-Atanasio R, Xu B, Ghadiri M. Computer simulation of the effect of contact stiffness  
23 and adhesion on the fluidization behaviour of powders. *Chemical engineering science*  
24 2007;62:184-94.
- 25 [230] Wilson R, Dini D, van Wachem B. A numerical study exploring the effect of particle properties  
26 on the fluidization of adhesive particles. *AIChE J* 2016;62:1467-77.
- 27 [231] Wensrich C, Katterfeld A. Rolling friction as a technique for modelling particle shape in DEM.  
28 *Powder Technol* 2012;217:409-17.
- 29 [232] van Wachem B, Zastawny M, Zhao F, Mallouppas G. Modelling of gas–solid turbulent channel  
30 flow with non-spherical particles with large Stokes numbers. *Int J Multiphase Flow* 2015;68:80-  
31 92.
- 32 [233] Jensen RP, Bosscher PJ, Plesha ME, Edil TB. DEM simulation of granular media—structure  
33 interface: effects of surface roughness and particle shape. *Int J Numer Anal Methods Geomech*  
34 1999;23:531-47.
- 35 [234] Wilson R, Dini D, Van Wachem B. The influence of surface roughness and adhesion on particle  
36 rolling. *Powder Technol* 2017;312:321-33.
- 37 [235] Iordanoff I, Battentier A, Neauport J, Charles J. A discrete element model to investigate sub-  
38 surface damage due to surface polishing. *Tribol Int* 2008;41:957-64.
- 39 [236] Richard D, Iordanoff I, Renouf M, Berthier Y. Thermal study of the dry sliding contact with  
40 third body presence. *Journal of Tribology* 2008;130:031404.
- 41 [237] Alder BJ, Wainwright TE. Studies in molecular dynamics. I. General method. *J Chem Phys*  
42 1959;31:459-66.
- 43 [238] Komanduri R, Chandrasekaran N, Raff LM. MD simulation of indentation and scratching of  
44 single crystal aluminum. *Wear* 2000;240:113-43.
- 45 [239] Brukman MJ, Gao G, Nemanich RJ, Harrison JA. Temperature Dependence of Single-Asperity  
46 Diamond–Diamond Friction Elucidated Using AFM and MD Simulations. *J Phys Chem C*  
47 2008;112:9358-69.
- 48 [240] Mo Y, Turner KT, Szlufarska I. Friction laws at the nanoscale. *Nature* 2009;457:1116-9.
- 49 [241] Onodera T, Morita Y, Nagumo R, Miura R, Suzuki A, Tsuboi H et al. A Computational  
50 Chemistry Study on Friction of h-MoS<sub>2</sub>. Part II. Friction Anisotropy. *J Phys Chem B*  
51 2010;114:15832-8.
- 52 [242] Schall JD, Gao G, Harrison JA. Effects of Adhesion and Transfer Film Formation on the  
53 Tribology of Self-Mated DLC Contacts. *J Phys Chem C* 2010;114:5321-30.
- 54 [243] Zhu Y, Zhang Y, Shi Y, Lu X, Li J, Lu L. Lubrication Behavior of Water Molecules Confined in  
55 TiO<sub>2</sub> Nanoslits: A Molecular Dynamics Study. *J Chem Eng Data* 2016;61:4023-30.
- 56  
57  
58  
59  
60  
61  
62  
63  
64  
65

- 1 [244] Harrison JA, White CT, Colton RJ, Brenner DW. Molecular-dynamics simulations of atomic-  
2 scale friction of diamond surfaces. *Phys Rev B* 1992;46:9700-8.
- 3 [245] Zhang L, Tanaka H. Towards a deeper understanding of wear and friction on the atomic  
4 scale—a molecular dynamics analysis. *Wear* 1997;211:44-53.
- 5 [246] Müser MH, Wenning L, Robbins MO. Simple Microscopic Theory of Amontons's Laws for  
6 Static Friction. *Phys Rev Lett* 2001;86:1295-8.
- 7 [247] Chandross M, Webb EB, Stevens MJ, Grest GS, Garofalini SH. Systematic Study of the Effect  
8 of Disorder on Nanotribology of Self-Assembled Monolayers. *Phys Rev Lett* 2004;93:166103.
- 9 [248] Mulliah D, Kenny SD, Smith R. Modeling of stick-slip phenomena using molecular dynamics.  
10 *Phys Rev B* 2004;69:205407.
- 11 [249] Tangney P, Louie SG, Cohen ML. Dynamic Sliding Friction between Concentric Carbon  
12 Nanotubes. *Phys Rev Lett* 2004;93:065503.
- 13 [250] Ewen JP, Gattinoni C, Thakkar FM, Morgan N, Spikes HA, Dini D. Nonequilibrium Molecular  
14 Dynamics Investigation of the Reduction in Friction and Wear by Carbon Nanoparticles  
15 Between Iron Surfaces. *Tribology Letters* 2016;63:38.
- 16 [251] Nakaoka S, Yamaguchi Y, Omori T, Joly L. Molecular dynamics analysis of the friction  
17 between a water-methanol liquid mixture and a non-polar solid crystal surface. *J Chem Phys*  
18 2017;146:174702.
- 19 [252] Harrison JA, White CT, Colton RJ, Brenner DW. Investigation of the atomic-scale friction and  
20 energy dissipation in diamond using molecular dynamics. *Thin Solid Films* 1995;260:205-11.
- 21 [253] Bhattacharya B, Dinesh Kumar GR, Agarwal A, Erkoç Ş, Singh A, Chakraborti N. Analyzing  
22 Fe-Zn system using molecular dynamics, evolutionary neural nets and multi-objective genetic  
23 algorithms. *Computational Materials Science* 2009;46:821-7.
- 24 [254] Thompson PA, Grest GS, Robbins MO. Phase transitions and universal dynamics in confined  
25 films. *Phys Rev Lett* 1992;68:3448.
- 26 [255] Cieplak M, Smith ED, Robbins MO. Molecular origins of friction: the force on adsorbed layers.  
27 *Science* 1994;265:1209-12.
- 28 [256] Yan W, Komvopoulos K. Three-dimensional molecular dynamics analysis of atomic-scale  
29 indentation. *J Tribol* 1998;120.
- 30 [257] Jabbarzadeh A, Atkinson JD, Tanner RI. Effect of the wall roughness on slip and rheological  
31 properties of hexadecane in molecular dynamics simulation of Couette shear flow between two  
32 sinusoidal walls. *Phys Rev E* 2000;61:690-9.
- 33 [258] Rigney DA, Karthikeyan S. The evolution of tribomaterial during sliding: a brief introduction.  
34 *Tribology Letters* 2010;39:3-7.
- 35 [259] Aghababaei R, Warner DH, Molinari J. Critical length scale controls adhesive wear  
36 mechanisms. *Nature communications* 2016;7.
- 37 [260] Junge T, Molinari J. Plastic activity in nanoscratch molecular dynamics simulations of pure  
38 aluminium. *Int J Plast* 2014;53:90-106.
- 39 [261] Romero PA, Järvi TT, Beckmann N, Mrovec M, Moseler M. Coarse graining and localized  
40 plasticity between sliding nanocrystalline metals. *Phys Rev Lett* 2014;113:036101.
- 41 [262] Vahdat V, Ryan KE, Keating PL, Jiang Y, Adiga SP, Schall JD et al. Atomic-scale wear of  
42 amorphous hydrogenated carbon during intermittent contact: a combined study using  
43 experiment, simulation, and theory. *Acs Nano* 2014;8:7027-40.
- 44 [263] Lorenz CD, Lane JMD, Chandross M, Stevens MJ, Grest GS. Molecular dynamics simulations  
45 of water confined between matched pairs of hydrophobic and hydrophilic self-assembled  
46 monolayers. *Langmuir* 2009;25:4535-42.
- 47 [264] Doig M, Warrens CP, Camp PJ. Structure and friction of stearic acid and oleic acid films  
48 adsorbed on iron oxide surfaces in squalane. *Langmuir* 2013;30:186-95.
- 49 [265] Savio D, Fillot N, Vergne P, Hetzler H, Seemann W, Espejel GM. A Multiscale Study on the  
50 Wall Slip Effect in a Ceramic–Steel Contact With Nanometer-Thick Lubricant Film by a Nano-  
51 to-Elastohydrodynamic Lubrication Approach. *Journal of Tribology* 2015;137:031502.
- 52 [266] Martini A, Liu Y, Snurr RQ, Wang QJ. Molecular dynamics characterization of thin film  
53 viscosity for EHL simulation. *Tribol Lett* 2006;21:217-25.
- 54 [267] Vanossi A, Manini N, Urbakh M, Zapperi S, Tosatti E. Colloquium: Modeling friction: From  
55 nanoscale to mesoscale. *Reviews of Modern Physics* 2013;85:529.
- 56  
57  
58  
59  
60  
61  
62  
63  
64  
65

- 1 [268] Levita G, Righi MC. Effects of Water Intercalation and Tribochemistry on MoS<sub>2</sub> Lubricity: An  
2 Ab Initio Molecular Dynamics Investigation. *ChemPhysChem* 2017;18:1475-80.
- 3 [269] Onodera T, Martin JM, Minfray C, Dassenoy F, Miyamoto A. Antiwear Chemistry of ZDDP:  
4 Coupling Classical MD and Tight-Binding Quantum Chemical MD Methods (TB-QCMD).  
5 *Tribology Letters* 2013;50:31-9.
- 6 [270] Jones JE. On the Determination of Molecular Fields. II. From the Equation of State of a Gas.  
7 *Proc R Soc Lond A Math Phys Sci* 1924;106:463.
- 8 [271] Morse PM. Diatomic Molecules According to the Wave Mechanics. II. Vibrational Levels. *Phys*  
9 *Rev* 1929;34:57-64.
- 10 [272] Luan B, Robbins MO. The breakdown of continuum models for mechanical contacts. *Nature*  
11 2005;435:929-32.
- 12 [273] Luan B, Robbins MO. Contact of single asperities with varying adhesion: Comparing continuum  
13 mechanics to atomistic simulations. *Phys Rev E* 2006;74:026111.
- 14 [274] Heyes D, Smith E, Dini D, Spikes H, Zaki T. Pressure dependence of confined liquid behavior  
15 subjected to boundary-driven shear. *J Chem Phys* 2012;136:134705.
- 16 [275] Gattinoni C, Heyes DM, Lorenz CD, Dini D. Traction and nonequilibrium phase behavior of  
17 confined sheared liquids at high pressure. *Physical Review E* 2013;88:052406.
- 18 [276] Maćkowiak S, Heyes D, Dini D, Brańka A. Non-equilibrium phase behavior and friction of  
19 confined molecular films under shear: A non-equilibrium molecular dynamics study. *J Chem*  
20 *Phys* 2016;145:164704.
- 21 [277] Daw MS, Baskes MI. Embedded-atom method: Derivation and application to impurities,  
22 surfaces, and other defects in metals. *Phys Rev B* 1984;29:6443-53.
- 23 [278] Buldum A, Ciraci S, Batra IP. Contact, nanoindentation, and sliding friction. *Phys Rev B*  
24 1998;57:2468-76.
- 25 [279] Mulliah D, Kenny SD, McGee E, Smith R, Richter A, Wolf B. Atomistic modelling of  
26 ploughing friction in silver, iron and silicon. *Nanotechnology* 2006;17:1807.
- 27 [280] Narulkar R, Bukkapatnam S, Raff LM, Komanduri R. Graphitization as a precursor to wear of  
28 diamond in machining pure iron: A molecular dynamics investigation. *Computational Materials*  
29 *Science* 2009;45:358-66.
- 30 [281] Cao Y, Zhang J, Liang Y, Yu F, Sun T. Mechanical and tribological properties of Ni/Al  
31 multilayers-A molecular dynamics study. *Appl Surf Sci* 2010;257:847-51.
- 32 [282] Lin E, Niu L, Shi H, Duan Z. Molecular dynamics simulation of nano-scale interfacial friction  
33 characteristic for different tribopair systems. *Appl Surf Sci* 2012;258:2022-8.
- 34 [283] Pauling L. Atomic Radii and Interatomic Distances in Metals. *J Am Chem Soc* 1947;69:542-53.
- 35 [284] Finnis M, Sinclair J. A simple empirical N-body potential for transition metals. *Philos Mag A*  
36 1984;50:45-55.
- 37 [285] Tersoff J. New empirical approach for the structure and energy of covalent systems. *Physical*  
38 *Review B* 1988;37:6991.
- 39 [286] Brenner DW. Empirical potential for hydrocarbons for use in simulating the chemical vapor  
40 deposition of diamond films. *Physical Review B* 1990;42:9458.
- 41 [287] Stuart SJ, Tutein AB, Harrison JA. A reactive potential for hydrocarbons with intermolecular  
42 interactions. *J Chem Phys* 2000;112:6472-86.
- 43 [288] Van Duin AC, Dasgupta S, Lorant F, Goddard WA. ReaxFF: a reactive force field for  
44 hydrocarbons. *The Journal of Physical Chemistry A* 2001;105:9396-409.
- 45 [289] Perry MD, Harrison JA. Universal aspects of the atomic-scale friction of diamond surfaces. *J*  
46 *Phys Chem* 1995;99:9960-5.
- 47 [290] Servantie J, Gaspard P. Translational dynamics and friction in double-walled carbon nanotubes.  
48 *Physical Review B* 2006;73:125428.
- 49 [291] Gao G, Cannara RJ, Carpick RW, Harrison JA. Atomic-scale friction on diamond: a comparison  
50 of different sliding directions on (001) and (111) surfaces using MD and AFM. *Langmuir*  
51 2007;23:5394-405.
- 52 [292] Kim H, Kim D. Molecular dynamics simulation of atomic-scale frictional behavior of  
53 corrugated nano-structured surfaces. *Nanoscale* 2012;4:3937-44.
- 54  
55  
56  
57  
58  
59  
60  
61  
62  
63  
64  
65

- 1 [293] Stoyanov P, Stemmer P, Järvi TT, Merz R, Romero PA, Scherge M et al. Friction and wear  
2 mechanisms of tungsten–carbon systems: A comparison of dry and lubricated conditions. *ACS*  
3 *Applied Materials & Interfaces* 2013;5:6123-35.
- 4 [294] Sawyer W, Perry S, Phillpot S, Sinnott S. Integrating experimental and simulation length and  
5 time scales in mechanistic studies of friction. *Journal of Physics: Condensed Matter*  
6 2008;20:354012.
- 7 [295] Huang P. Atomistic simulations of shearing friction and dynamic adhesion of double-walled  
8 carbon nanotubes on Au substrates. *Composites Sci Technol* 2012;72:599-607.
- 9 [296] Wen J, Ma T, Zhang W, Psafogiannakis G, van Duin AC, Chen L et al. Atomic insight into  
10 tribochemical wear mechanism of silicon at the Si/SiO<sub>2</sub> interface in aqueous environment:  
11 Molecular dynamics simulations using ReaxFF reactive force field. *Appl Surf Sci*  
12 2016;390:216-23.
- 13 [297] Yeon J, He X, Martini A, Kim SH. Mechanochemistry at solid surfaces: Polymerization of  
14 adsorbed molecules by mechanical shear at tribological interfaces. *ACS Applied Materials &*  
15 *Interfaces* 2017;9:3142-8.
- 16 [298] Campaná C, Müser MH. Practical Green's function approach to the simulation of elastic semi-  
17 infinite solids. *Physical Review B* 2006;74:075420.
- 18 [299] Kong LT, Bartels G, Campaña C, Denniston C, Müser MH. Implementation of Green's function  
19 molecular dynamics: An extension to LAMMPS. *Comput Phys Commun* 2009;180:1004-10.
- 20 [300] Legoas SB, Giro R, Galvão DS. Molecular dynamics simulations of C<sub>60</sub> nanobearings.  
21 *Chemical Physics Letters* 2004;386:425-9.
- 22 [301] Matsushita K, Matsukawa H, Sasaki N. Atomic scale friction between clean graphite surfaces.  
23 *Solid State Commun* 2005;136:51-5.
- 24 [302] Onodera T, Morita Y, Suzuki A, Koyama M, Tsuboi H, Hatakeyama N et al. A computational  
25 chemistry study on friction of h-MoS<sub>2</sub>. Part I. Mechanism of single sheet lubrication. *The*  
26 *Journal of Physical Chemistry B* 2009;113:16526-36.
- 27 [303] Ewen JP, Gattinoni C, Morgan N, Spikes HA, Dini D. Nonequilibrium Molecular Dynamics  
28 Simulations of Organic Friction Modifiers Adsorbed on Iron Oxide Surfaces. *Langmuir*  
29 2016;32:4450-63.
- 30 [304] De Barros Bouchet MI, Matta C, Vacher B, Le-Mogne T, Martin JM, von Lantz J et al. Energy  
31 filtering transmission electron microscopy and atomistic simulations of tribo-induced  
32 hybridization change of nanocrystalline diamond coating. *Carbon* 2015;87:317-29.
- 33 [305] Loehle S, Matta C, Minfray C, Le Mogne T, Martin J, Iovine R et al. Mixed Lubrication with  
34 C18 Fatty Acids: Effect of Unsaturation. *Tribology Letters* 2014;53:319-28.
- 35 [306] De Barros-Bouchet MI, Righi MC, Philippon D, Mambingo-Doumbe S, Le-Mogne T, Martin  
36 JM et al. Tribochemistry of phosphorus additives: experiments and first-principles calculations.  
37 *RSC Adv* 2015;5:49270-9.
- 38 [307] Pastewka L, Klemenz A, Gumbsch P, Moseler M. Screened empirical bond-order potentials for  
39 Si-C. *Phys Rev B* 2013;87:205410.
- 40 [308] Loehlé S, Matta C, Minfray C, Mogne TL, Iovine R, Obara Y et al. Mixed lubrication of steel by  
41 C18 fatty acids revisited. Part I: Toward the formation of carboxylate. *Tribol Int* 2015;82, Part  
42 A:218-27.
- 43 [309] Levita G, Cavaleiro A, Molinari E, Polcar T, Righi M. Sliding properties of MoS<sub>2</sub> layers: load  
44 and interlayer orientation effects. *The Journal of Physical Chemistry C* 2014;118:13809-16.
- 45 [310] Wriggers P, Reinelt J. Multi-scale approach for frictional contact of elastomers on rough rigid  
46 surfaces. *Comput Methods Appl Mech Eng* 2009;198:1996-2008.
- 47 [311] Ciavarella M, Demelio G. Elastic multiscale contact of rough surfaces: Archard's model  
48 revisited and comparisons with modern fractal models. *RN* 2001;3:2.
- 49 [312] Borri-Brunetto M, Carpinteri A, Chiaia B. Scaling phenomena due to fractal contact in concrete  
50 and rock fractures. *Int J Fract* 1999;95:221.
- 51 [313] Zavarise G, Borri-Brunetto M, Paggi M. On the resolution dependence of micromechanical  
52 contact models. *Wear* 2007;262:42-54.
- 53 [314] Cheng S, Robbins MO. Defining Contact at the Atomic Scale. *Tribology Letters* 2010;39:329-  
54 48.

- [315] Pastewka L, Sharp TA, Robbins MO. Seamless elastic boundaries for atomistic calculations. *Physical Review B* 2012;86:075459.
- [316] Anciaux G, Ramisetti SB, Molinari J. A finite temperature bridging domain method for MD-FE coupling and application to a contact problem. *Comput Methods Appl Mech Eng* 2012;205:204-12.
- [317] Budarapu PR, Reinoso J, Paggi M. Concurrently coupled solid shell-based adaptive multiscale method for fracture. *Comput Methods Appl Mech Eng* 2017;319:338-65.
- [318] Shilkrot L, Miller RE, Curtin WA. Multiscale plasticity modeling: coupled atomistics and discrete dislocation mechanics. *J Mech Phys Solids* 2004;52:755-87.
- [319] Cho J, Molinari J, Anciaux G. Mobility law of dislocations with several character angles and temperatures in FCC aluminum. *Int J Plast* 2017;90:66-75.
- [320] Cho J, Junge T, Molinari J, Anciaux G. Toward a 3D coupled atomistic and discrete dislocation dynamics simulation: dislocation core structures and Peierls stresses with several character angles in FCC aluminum. *Advanced Modeling and Simulation in Engineering Sciences* 2015;2:12.
- [321] Smith E, Heyes D, Dini D, Zaki T. Control-volume representation of molecular dynamics. *Physical Review E* 2012;85:056705.
- [322] Smith E, Heyes D, Dini D, Zaki T. A localized momentum constraint for non-equilibrium molecular dynamics simulations. *J Chem Phys* 2015;142:074110.
- [323] Flekkøy E, Wagner G, Feder J. Hybrid model for combined particle and continuum dynamics. *EPL (Europhysics Letters)* 2000;52:271.
- [324] Nie X, Chen S, Robbins MO. A continuum and molecular dynamics hybrid method for micro- and nano-fluid flow. *J Fluid Mech* 2004;500:55-64.
- [325] Ren W. Analytical and numerical study of coupled atomistic-continuum methods for fluids. *Journal of Computational Physics* 2007;227:1353-71.
- [326] Yamashita F, Fukuyama E, Mizoguchi K, Takizawa S, Xu S, Kawakata H. Scale dependence of rock friction at high work rate. *Nature* 2015;528:254-7.
- [327] Hatano T. Scaling properties of granular rheology near the jamming transition. *Journal of the Physical Society of Japan* 2008;77:123002-.
- [328] Szolwinski MP, Harish G, Farris TN, Sakagami T. In-Situ Measurement of Near-Surface Fretting Contact Temperatures in an Aluminum Alloy. *Journal of Tribology* 1999;121:11-9.
- [329] Scheibert J, Prevost A, Frelat J, Rey P, Debrégeas G. Experimental evidence of non-Amontons behaviour at a multi-contact interface. *Europhysics Letters* 2008;83:34003.
- [330] Scheibert J, Prevost A, Debrégeas G, Katzav E, Adda-Bedia M. Stress field at a sliding frictional contact: Experiments and calculations. *J Mech Phys Solids* 2009;57:1921-33.
- [331] Dieterich JH, Kilgore BD. Direct observation of frictional contacts: New insights for state-dependent properties. *Pure Appl Geophys* 1994;143:283-302.
- [332] Bayart E, Svetlizky I, Fineberg J. Fracture mechanics determine the lengths of interface ruptures that mediate frictional motion. *Nat Phys* 2016;12:166-70.
- [333] Kammer DS, Radiguet M, Ampuero J, Molinari J. Linear Elastic Fracture Mechanics Predicts the Propagation Distance of Frictional Slip. *Tribology Letters* 2015;57:23.
- [334] Nguyen DT, Paolino P, Audry M, Chateauminois A, Frétygny C, Le Chenadec Y et al. Surface pressure and shear stress fields within a frictional contact on rubber. *The Journal of Adhesion* 2011;87:235-50.
- [335] Woo K, Thomas T. Contact of rough surfaces: a review of experimental work. *Wear* 1980;58:331-40.
- [336] Lorenz B, Persson BN. Leak rate of seals: Effective-medium theory and comparison with experiment. *The European Physical Journal E: Soft Matter and Biological Physics* 2010;31:159-67.
- [337] Putignano C, Reddyhoff T, Carbone G, Dini D. Experimental investigation of viscoelastic rolling contacts: a comparison with theory. *Tribology Letters* 2013;51:105-13.
- [338] Carbone G, Putignano C. Rough viscoelastic sliding contact: theory and experiments. *Physical Review E* 2014;89:032408.
- [339] Hild F, Roux S. Digital Image Correlation: from Displacement Measurement to Identification of Elastic Properties – a Review. *Strain* 2006;42:69-80.

- [340] Usamentiaga R, Venegas P, Guerediaga J, Vega L, Molleda J, Bulnes GF. Infrared Thermography for Temperature Measurement and Non-Destructive Testing. *Sensors* 2014;14.
- [341] Schwab K, Henriksen E, Worlock J, Roukes ML. Measurement of the quantum of thermal conductance. *Nature* 2000;404:974-7.
- [342] Chen G. Ballistic-diffusive heat-conduction equations. *Phys Rev Lett* 2001;86:2297.
- [343] Anciaux G, Molinari J. A molecular dynamics and finite elements study of nanoscale thermal contact conductance. *Int J Heat Mass Transfer* 2013;59:384-92.
- [344] Madhusudana C. Thermal contact conductance. : Springer, 1996.
- [345] Bowden FP, Tabor D. The friction and lubrication of solids. : Oxford university press, 2001.
- [346] Rice JR. Heating and weakening of faults during earthquake slip. *Journal of Geophysical Research: Solid Earth* 2006;111.
- [347] Goldsby DL, Tullis TE. Flash heating leads to low frictional strength of crustal rocks at earthquake slip rates. *Science* 2011;334:216-8.
- [348] Ramesh A, Melkote SN. Modeling of white layer formation under thermally dominant conditions in orthogonal machining of hardened AISI 52100 steel. *Int J Mach Tools Manuf* 2008;48:402-14.
- [349] Ward I, Hine P. The science and technology of hot compaction. *Polymer* 2004;45:1413-27.
- [350] Dieterich JH. Time- dependent friction in rocks. *Journal of Geophysical Research* 1972;77:3690-7.
- [351] Collettini C, Viti C, Tesi T, Mollo S. Thermal decomposition along natural carbonate faults during earthquakes. *Geology* 2013;41:927-30.
- [352] Dresel W. Lubricants and lubrication. : John Wiley & Sons, 2007.
- [353] Müller HK, Nau BS. Fluid sealing technology: principles and applications. : M. Dekker, 1998.
- [354] Power W, Durham W. Topography of natural and artificial fractures in granitic rocks: Implications for studies of rock friction and fluid migration. *Int J Rock Mech Min Sci* 1997;34:979-89.
- [355] Rajagopal K, Szeri A. On an inconsistency in the derivation of the equations of elastohydrodynamic lubrication. 2003;459:2771-86.
- [356] Zilibotti G, Corni S, Righi M. Load-induced confinement activates diamond lubrication by water. *Phys Rev Lett* 2013;111:146101.
- [357] Dapp WB, Lücke A, Persson BNJ, Müser MH. Self-Affine Elastic Contacts: Percolation and Leakage. *Phys Rev Lett* 2012;108:244301.
- [358] Barber JR. Bounds on the electrical resistance between contacting elastic rough bodies. *Proceedings of the Royal Society of London. Series A: Mathematical, Physical and Engineering Sciences* 2003;459:53.
- [359] Persson BNJ. On the Fractal Dimension of Rough Surfaces. *Tribol Lett* 2014;54:99-106.
- [360] Hu YZ, Tonder K. Simulation of 3-D random rough surface by 2-D digital filter and fourier analysis. *International Journal of Machine Tools and Manufacture* 1992;32:83-90.
- [361] Meakin P. Fractals, scaling and growth far from equilibrium. : Cambridge university press, 1998.
- [362] Suh AY, Polycarpou AA, Conry TF. Detailed surface roughness characterization of engineering surfaces undergoing tribological testing leading to scuffing. *Wear* 2003;255:556-68.
- [363] Deltombe R, Kubiak K, Bigerelle M. How to select the most relevant 3D roughness parameters of a surface. *Scanning* 2014;36:150-60.
- [364] Whitehouse DJ, Archard JF. The Properties of Random Surfaces of Significance in their Contact. *Proc R Soc Lond A Math Phys Sci* 1970;316:97.
- [365] Sayles RS, Thomas TR. Surface topography as a nonstationary random process. *Nature* 1978;271:431-4.
- [366] Bowden F, Tabor D. The influence of surface films on the friction and deformation of surfaces in Properties of Metallic Surfaces. *Institute of Metals, London* 1953:197-212.
- [367] Guduru PR. Detachment of a rigid solid from an elastic wavy surface: theory. *J Mech Phys Solids* 2007;55:445-72.
- [368] Borodich FM, Pepelyshev A, Savencu O. Statistical approaches to description of rough engineering surfaces at nano and microscales. *Tribol Int* 2016;103:197-207.

- 1 [369] Ciavarella M, Papangelo A. A modified form of Pastewka-Robbins criterion for adhesion. The  
2 Journal of Adhesion 2017.
- 3 [370] Ciavarella M. On Pastewka and Robbins' Criterion for Macroscopic Adhesion of Rough  
4 Surfaces. Journal of Tribology 2017;139:031404.
- 5 [371] Jacobs TD, Martini A. Measuring and understanding contact area at the nanoscale: a review.  
6 Appl Mech Rev 2017;69:061101.
- 7 [372] Ciavarella M, Papangelo A. Discussion of “Measuring and Understanding Contact Area at the  
8 Nanoscale: A Review” by Tevis DB Jacobs and Ashlie Martini. Appl Mech Rev 2017.
- 9 [373] Ciavarella M, Papangelo A. On the sensitivity of adhesion between rough surfaces to asperity  
10 height distribution. Physical Mesomechanics 2018;1.
- 11 [374] Rapetto MP, Almqvist A, Larsson R, Lugt PM. On the influence of surface roughness on real  
12 area of contact in normal, dry, friction free, rough contact by using a neural network. Wear  
13 2009;266:592-5.
- 14 [375] Solhjoo S, Vakis AI. Surface roughness of gold substrates at the nanoscale: an atomistic  
15 simulation study. Tribology International 2017:165-78.
- 16 [376] Abbott EJ, Firestone FA. Specifying surface quality. Mech Eng 1933;65:569-72.
- 17 [377] Jiang X, Scott PJ, Whitehouse DJ, Blunt L. Paradigm shifts in surface metrology. Part I.  
18 Historical philosophy. 2007;463:2049-70.
- 19 [378] Jiang X, Scott PJ, Whitehouse DJ, Blunt L. Paradigm shifts in surface metrology. Part II. The  
20 current shift. 2007;463:2071-99.
- 21 [379] Gao F, Leach RK, Petzing J, Coupland JM. Surface measurement errors using commercial  
22 scanning white light interferometers. Measurement Science and Technology 2007;19:015303.
- 23 [380] Schwarz U, Haefke H, Reimann P, GÜNTHERODT H. Tip artefacts in scanning force  
24 microscopy. J Microsc 1994;173:183-97.
- 25 [381] Lechenault F, Pallares G, George M, Rountree C, Bouchaud E, Ciccotti M. Effects of finite  
26 probe size on self-affine roughness measurements. Phys Rev Lett 2010;104:025502.
- 27 [382] Almqvist A, Essel EK, Persson L-, Wall P. Homogenization of the unstationary incompressible  
28 Reynolds equation. Tribol Int 2007;40:1344-50.
- 29 [383] Poon CY, Bhushan B. Comparison of surface roughness measurements by stylus profiler, AFM  
30 and non-contact optical profiler. Wear 1995;190:76-88.
- 31 [384] Spencer A, Dobryden I, Almqvist N, Almqvist A, Larsson R. The influence of AFM and VSI  
32 techniques on the accurate calculation of tribological surface roughness parameters. Tribol Int  
33 2013;57:242-50.
- 34 [385] Anciaux G, Molinari J. Contact mechanics at the nanoscale, a 3D multiscale approach. Int J  
35 Numer Methods Eng 2009;79:1041-67.
- 36 [386] Solhjoo S, Vakis AI. Single asperity nanocontacts: Comparison between molecular dynamics  
37 simulations and continuum mechanics models. Comp Mater Sci 2015;99:209-20.
- 38 [387] Solhjoo S, Vakis AI. Definition and detection of contact in atomistic simulations. Computational  
39 Materials Science 2015;109:172-82.
- 40 [388] Yu N, Polycarpou AA. Adhesive contact based on the Lennard-Jones potential: A correction to  
41 the value of the equilibrium distance as used in the potential. J Colloid Interface Sci  
42 2004;278:428-35.
- 43 [389] Pastewka L, Robbins MO. Contact area of rough spheres: Large scale simulations and simple  
44 scaling laws. Appl Phys Lett 2016;108:221601.
- 45 [390] Taylor KJ, Pettiette- Hall CL, Cheshnovsky O, Smalley RE. Ultraviolet photoelectron spectra of  
46 coinage metal clusters. J Chem Phys 1992;96:3319-29.
- 47 [391] Mills G, Gordon MS, Metiu H. Oxygen adsorption on Au clusters and a rough Au(111) surface:  
48 The role of surface flatness, electron confinement, excess electrons, and band gap. J Chem Phys  
49 2003;118:4198-205.
- 50 [392] Gee ML, McGuiggan PM, Israelachvili JN, Homola AM. Liquid to solidlike transitions of  
51 molecularly thin films under shear. J Chem Phys 1990;93:1895-906.
- 52 [393] Landman U, Luedtke WD, Gao J. Atomic-Scale Issues in Tribology: Interfacial Junctions and  
53 Nano-elastohydrodynamics. Langmuir 1996;12:4514-28.
- 54 [394] Demirel AL, Granick S. Origins of solidification when a simple molecular fluid is confined  
55 between two plates. J Chem Phys 2001;115:1498-512.
- 56  
57  
58  
59  
60  
61  
62  
63  
64  
65

- 1 [395] Savio D, Fillot N, Vergne P. A Molecular Dynamics Study of the Transition from Ultra-Thin  
2 Film Lubrication Toward Local Film Breakdown. *Tribol Lett* 2013;50:207-20.
- 3 [396] Fukuzawa K, Itoh S, Mitsuya Y. Fiber wobbling shear force measurement for nanotribology of  
4 confined lubricant molecules. *IEEE Trans Magn* 2003;39:2453-5.
- 5 [397] Itoh S, Fukuzawa K, Hamamoto Y, Hedong Z, Mitsuya Y. Fiber wobbling method for dynamic  
6 viscoelastic measurement of liquid lubricant confined in molecularly narrow gaps. *Tribol Lett*  
7 2008;30:177-89.
- 8 [398] Vakis AI, Eriten M, Polycarpou AA. Modeling Bearing and Shear Forces in Molecularly Thin  
9 Lubricants. *Tribol Lett* 2011;41:573-86.
- 10 [399] Williams J. *Engineering Tribology*. : Cambridge University Press, 2005.
- 11 [400] Goldman AJ, Cox RG, Brenner H. Slow viscous motion of a sphere parallel to a plane wall--II  
12 Couette flow. *Chem Eng Sci* 1967;22:653-60.
- 13 [401] Fukuzawa K, Hayakawa K, Matsumura N, Itoh S, Zhang H. Simultaneously Measuring Lateral  
14 and Vertical Forces with Accurate Gap Control for Clarifying Lubrication Phenomena at  
15 Nanometer Gap. *Tribol Lett* 2009;37:497-505.
- 16 [402] Nicola L, Bower AF, Kim K, Needleman A, Van Der Giessen E. Multi-asperity contact: A  
17 comparison between discrete dislocation and crystal plasticity predictions. *Philosophical*  
18 *Magazine* 2008;88:3713-29.
- 19 [403] Li H, Jiang Z, Wei D. Crystal plasticity finite modelling of 3D surface asperity flattening in  
20 uniaxial planar compression. *Tribology Letters* 2012;46:101-12.
- 21 [404] Sabnis PA, Forest S, Arakere NK, Yastrebov VA. Crystal plasticity analysis of cylindrical  
22 indentation on a Ni-base single crystal superalloy. *Int J Plast* 2013;51:200-17.
- 23 [405] Renner E, Gaillard Y, Richard F, Amiot F, Delobelle P. Sensitivity of the residual topography to  
24 single crystal plasticity parameters in Berkovich nanoindentation on FCC nickel. *Int J Plast*  
25 2016;77:118-40.
- 26 [406] Liu Y, Varghese S, Ma J, Yoshino M, Lu H, Komanduri R. Orientation effects in  
27 nanoindentation of single crystal copper. *Int J Plast* 2008;24:1990-2015.
- 28 [407] Kucharski S, Stupkiewicz S, Petryk H. Surface pile-up patterns in indentation testing of Cu  
29 single crystals. *Exp Mech* 2014;54:957-69.
- 30 [408] Wang Y, Raabe D, Klüber C, Roters F. Orientation dependence of nanoindentation pile-up  
31 patterns and of nanoindentation microtextures in copper single crystals. *Acta Materialia*  
32 2004;52:2229-38.
- 33 [409] Nix WD, Gao H. Indentation size effects in crystalline materials: a law for strain gradient  
34 plasticity. *J Mech Phys Solids* 1998;46:411-25.
- 35 [410] Pharr GM, Herbert EG, Gao Y. The indentation size effect: a critical examination of  
36 experimental observations and mechanistic interpretations. *Annual Review of Materials*  
37 *Research* 2010;40:271-92.
- 38 [411] Gurtin ME. On the plasticity of single crystals: free energy, microforces, plastic-strain gradients.  
39 *J Mech Phys Solids* 2000;48:989-1036.
- 40 [412] Evers L, Brekelmans W, Geers M. Non-local crystal plasticity model with intrinsic SSD and  
41 GND effects. *J Mech Phys Solids* 2004;52:2379-401.
- 42 [413] Han C, Gao H, Huang Y, Nix WD. Mechanism-based strain gradient crystal plasticity—I.  
43 Theory. *J Mech Phys Solids* 2005;53:1188-203.
- 44 [414] Petryk H, Stupkiewicz S. A minimal gradient-enhancement of the classical continuum theory of  
45 crystal plasticity. Part I: The hardening law. *Archives of Mechanics* 2016;68:459-85.
- 46 [415] Lee W, Chen Y. Simulation of micro-indentation hardness of FCC single crystals by  
47 mechanism-based strain gradient crystal plasticity. *Int J Plast* 2010;26:1527-40.
- 48 [416] Stupkiewicz S, Petryk H. A minimal gradient-enhancement of the classical continuum theory of  
49 crystal plasticity. Part II: Size effects. *Archives of Mechanics* 2016;68:487-513.
- 50 [417] Song H, Van der Giessen E, Liu X. Strain gradient plasticity analysis of elasto-plastic contact  
51 between rough surfaces. *J Mech Phys Solids* 2016;96:18-28.
- 52 [418] Fivel M, Robertson C, Canova G, Boulanger L. Three-dimensional modeling of indent-induced  
53 plastic zone at a mesoscale. *Acta Materialia* 1998;46:6183-94.
- 54 [419] Chang H, Fivel M, Rodney D, Verdier M. Multiscale modelling of indentation in FCC metals:  
55 From atomic to continuum. *Comptes Rendus Physique* 2010;11:285-92.
- 56  
57  
58  
59  
60  
61  
62  
63  
64  
65



- [420] Siang KNW, Nicola L. Discrete dislocation plasticity analysis of contact between deformable bodies of simple geometry. *Modell Simul Mater Sci Eng* 2016;24:045008.
- [421] Sun F, Van der Giessen E, Nicola L. Interaction between neighboring asperities during flattening: A discrete dislocation plasticity analysis. *Mech Mater* 2015;90:157-65.
- [422] Yin X, Komvopoulos K. A discrete dislocation plasticity analysis of a single-crystal semi-infinite medium indented by a rigid surface exhibiting multi-scale roughness. *Philosophical Magazine* 2012;92:2984-3005.
- [423] Deshpande V, Needleman A, Van der Giessen E. Discrete dislocation plasticity analysis of static friction. *Acta materialia* 2004;52:3135-49.
- [424] Song H, Vakis AI, Liu X, Van der Giessen E. Statistical model of rough surface contact accounting for size-dependent plasticity and asperity interaction. *Journal of the Mechanics and Physics of Solids* 2017;106:1-14.
- [425] Raj R, Ashby M. On grain boundary sliding and diffusional creep. *Metallurgical and Materials Transactions B* 1971;2:1113-27.
- [426] Van Swygenhoven H, Derlet P. Grain-boundary sliding in nanocrystalline fcc metals. *Physical Review B* 2001;64:224105.
- [427] Argibay N, Chandross M, Cheng S, Michael JR. Linking microstructural evolution and macro-scale friction behavior in metals. *J Mater Sci* 2017;52:2780-99.
- [428] Stoyanov P, Romero PA, Järvi TT, Pastewka L, Scherge M, Stemmer P et al. Experimental and numerical atomistic investigation of the third body formation process in dry tungsten/tungsten-carbide tribo couples. *Tribology Letters* 2013;50:67-80.
- [429] Bosheh S, Mativenga P. White layer formation in hard turning of H13 tool steel at high cutting speeds using CBN tooling. *Int J Mach Tools Manuf* 2006;46:225-33.
- [430] Ranganath S, Guo C, Hegde P. A finite element modeling approach to predicting white layer formation in nickel superalloys. *CIRP Annals-Manufacturing Technology* 2009;58:77-80.
- [431] Lindroos M, Ratia V, Apostol M, Valtonen K, Laukkanen A, Molnar W et al. The effect of impact conditions on the wear and deformation behavior of wear resistant steels. *Wear* 2015;328:197-205.
- [432] Sharp TA, Pastewka L, Robbins MO. Elasticity limits structural superlubricity in large contacts. *Phys Rev B* 2016;93:121402.
- [433] Beckmann N, Romero PA, Linsler D, Dienwiebel M, Stolz U, Moseler M et al. Origins of Folding Instabilities on Polycrystalline Metal Surfaces. *Phys Rev Applied* 2014;2:064004.
- [434] Müser MH, Dapp WB, Bugnicourt R, Sainsot P, Lesaffre N, Lubrecht AA et al. Meeting the Contact-Mechanics Challenge. *Tribology Letters* 2017;65:118.
- [435] Nagata K, Nakatani M, Yoshida S. A revised rate- and state- dependent friction law obtained by constraining constitutive and evolution laws separately with laboratory data. *Journal of Geophysical Research: Solid Earth* 2012;117.
- [436] Stachowiak G, Batchelor AW. *Engineering tribology*. : Butterworth-Heinemann, 2013.
- [437] Paggi M, Pohrt R, Popov VL. Partial-slip frictional response of rough surfaces. *Scientific reports* 2014;4:5178.
- [438] Coulomb CA. *Théorie des machines simples en ayant égard au frottement de leurs parties et à la roideur des cordages*. : Bachelier, 1821.
- [439] Popova E, Popov VL. The research works of Coulomb and Amontons and generalized laws of friction. *Friction* 2015;3:183-90.
- [440] Ben-David O, Fineberg J. Static Friction Coefficient Is Not a Material Constant. *Phys Rev Lett* 2011;106:254301.
- [441] Ben-David O, Rubinstein SM, Fineberg J. Slip-stick and the evolution of frictional strength. *Nature* 2010;463:76-9.
- [442] Scheibert J, Dysthe DK. Role of friction-induced torque in stick-slip motion. *EPL (Europhysics Letters)* 2010;92:54001.
- [443] Otsuki M, Matsukawa H. Systematic Breakdown of Amontons' Law of Friction for an Elastic Object Locally Obeying Amontons' Law. *Scientific Reports* 2013;3:1586.
- [444] Farkas Z, Dahmen SR, Wolf DE. Static versus dynamic friction: the role of coherence. *Journal of Statistical Mechanics: Theory and Experiment* 2005;2005:P06015.

- 1 [445] Trømborg JK, Sveinsson HA, Scheibert J, Thøgersen K, Amundsen DS, Malthe-Sørensen A.  
2 Slow slip and the transition from fast to slow fronts in the rupture of frictional interfaces.  
3 Proceedings of the National Academy of Sciences 2014;111:8764-9.
- 4 [446] Cammarata A, Polcar T. Electro-vibrational coupling effects on “intrinsic friction” in transition  
5 metal dichalcogenides. RSC Advances 2015;5:106809-18.
- 6 [447] Cammarata A, Polcar T. Tailoring Nanoscale Friction in MX<sub>2</sub> Transition Metal  
7 Dichalcogenides. Inorg Chem 2015;54:5739-44.
- 8 [448] Cammarata A, Polcar T. Layering effects on low frequency modes in n-layered MX<sub>2</sub> transition  
9 metal dichalcogenides. Physical Chemistry Chemical Physics 2016;18:4807-13.
- 10 [449] Baumberger T, Caroli C. Solid friction from stick-slip down to pinning and aging. Adv Phys  
11 2006;55:279-348.
- 12 [450] Marone C. Laboratory-derived friction laws and their application to seismic faulting. Annu Rev  
13 Earth Planet Sci 1998;26:643-96.
- 14 [451] Ronsin O, Coeyrehourcq KL. State, rate and temperature-dependent sliding friction of  
15 elastomers. 2001;457:1277-94.
- 16 [452] Bar-Sinai Y, Spatschek R, Brener EA, Bouchbinder E. On the velocity- strengthening behavior  
17 of dry friction. Journal of Geophysical Research: Solid Earth 2014;119:1738-48.
- 18 [453] Di Toro G, Han R, Hirose T, De Paola N, Nielsen S, Mizoguchi K et al. Fault lubrication during  
19 earthquakes. Nature 2011;471:494-8.
- 20 [454] Rubinstein SM, Cohen G, Fineberg J. Detachment fronts and the onset of dynamic friction.  
21 Nature 2004;430:1005-9.
- 22 [455] Rubinstein S, Cohen G, Fineberg J. Dynamics of precursors to frictional sliding. Phys Rev Lett  
23 2007;98:226103.
- 24 [456] Ben-David O, Cohen G, Fineberg J. The Dynamics of the Onset of Frictional Slip. Science  
25 2010;330:211.
- 26 [457] Svetlizky I, Fineberg J. Classical shear cracks drive the onset of dry frictional motion. Nature  
27 2014;509:205-8.
- 28 [458] Svetlizky I, Pino Muñoz D, Radiguet M, Kammer DS, Molinari J, Fineberg J. Properties of the  
29 shear stress peak radiated ahead of rapidly accelerating rupture fronts that mediate frictional slip.  
30 Proceedings of the National Academy of Sciences 2016;113:542-7.
- 31 [459] Braun O, Barel I, Urbakh M. Dynamics of transition from static to kinetic friction. Phys Rev  
32 Lett 2009;103:194301.
- 33 [460] Maegawa S, Suzuki A, Nakano K. Precursors of Global Slip in a Longitudinal Line Contact  
34 Under Non-Uniform Normal Loading. Tribology Letters 2010;38:313-23.
- 35 [461] Amundsen DS, Scheibert J, Thøgersen K, Trømborg J, Malthe-Sørensen A. 1D model of  
36 precursors to frictional stick-slip motion allowing for robust comparison with experiments.  
37 Tribology Letters 2012;45:357-69.
- 38 [462] Braun O, Scheibert J. Propagation length of self-healing slip pulses at the onset of sliding: a toy  
39 model. Tribology Letters 2014;56:553-62.
- 40 [463] Papangelo A, Stingl B, Hoffmann NP, Ciavarella M. A simple model for friction detachment at  
41 an interface of finite size mimicking Fineberg’s experiments on uneven loading. Physical  
42 Mesomechanics 2014;17:311-20.
- 43 [464] Trømborg J, Scheibert J, Amundsen DS, Thøgersen K, Malthe-Sørensen A. Transition from  
44 Static to Kinetic Friction: Insights from a 2D Model. Phys Rev Lett 2011;107:074301.
- 45 [465] Radiguet M, Kammer DS, Gillet P, Molinari J. Survival of Heterogeneous Stress Distributions  
46 Created by Precursory Slip at Frictional Interfaces. Phys Rev Lett 2013;111:164302.
- 47 [466] Taloni A, Benassi A, Sandfeld S, Zapperi S. Scalar model for frictional precursors dynamics.  
48 Scientific Reports 2014;5:8086.
- 49 [467] Scholz CH. The mechanics of earthquakes and faulting. : Cambridge university press, 2002.
- 50 [468] Amundsen DS, Trømborg JK, Thøgersen K, Katzav E, Malthe-Sørensen A, Scheibert J.  
51 Steady-state propagation speed of rupture fronts along one-dimensional frictional interfaces.  
52 Physical Review E 2015;92:032406.
- 53 [469] Chateauminois A, Frégnigny C, Olanier L. Friction and shear fracture of an adhesive contact  
54 under torsion. Phys Rev E 2010;81:026106.
- 55  
56  
57  
58  
59  
60  
61  
62  
63  
64  
65

- [470] Prevost A, Scheibert J, Debrégeas G. Probing the micromechanics of a multi-contact interface at the onset of frictional sliding. *The European Physical Journal E* 2013;36:17.
- [471] Bar Sinai Y, Brener EA, Bouchbinder E. Slow rupture of frictional interfaces. *Geophys Res Lett* 2012;39.
- [472] Bar-Sinai Y, Spatschek R, Brener EA, Bouchbinder E. Instabilities at frictional interfaces: Creep patches, nucleation, and rupture fronts. *Physical Review E* 2013;88:060403.
- [473] Kaproth BM, Marone C. Slow earthquakes, preseismic velocity changes, and the origin of slow frictional stick-slip. *Science* 2013;341:1229-32.
- [474] Trømborg JK, Sveinsson HA, Thøgersen K, Scheibert J, Malthé-Sørensen A. Speed of fast and slow rupture fronts along frictional interfaces. *Physical Review E* 2015;92:012408.
- [475] Thøgersen K, Trømborg JK, Sveinsson HA, Malthé-Sørensen A, Scheibert J. History-dependent friction and slow slip from time-dependent microscopic junction laws studied in a statistical framework. *Physical Review E* 2014;89:052401.
- [476] Grosch K. The relation between the friction and visco-elastic properties of rubber. 1963;274:21-39.
- [477] Persson BNJ, Albohr O, Tartaglino U, Volokitin AI, Tosatti E. On the nature of surface roughness with application to contact mechanics, sealing, rubber friction and adhesion. *Journal of Physics: Condensed Matter* 2005;17:R1.
- [478] Tuononen AJ. Digital image correlation to analyse stick-slip behaviour of tyre tread block. *Tribol Int* 2014;69:70-6.
- [479] Tuononen AJ. Onset of frictional sliding of rubber-glass contact under dry and lubricated conditions. *Sci Rep* 2016;6:27951.
- [480] Chateauminos A, Frétygny C. Local friction at a sliding interface between an elastomer and a rigid spherical probe. *The European Physical Journal E: Soft Matter and Biological Physics* 2008;27:221-7.
- [481] Audry M, Frétygny C, Chateauminos A, Teissere J, Barthel E. Slip dynamics at a patterned rubber/glass interface during stick-slip motions. *The European Physical Journal E: Soft Matter and Biological Physics* 2012;35:1-7.
- [482] Brörmann K, Barel I, Urbakh M, Bennewitz R. Friction on a microstructured elastomer surface. *Tribology Letters* 2013;50:3-15.
- [483] Greenwood JA, Tripp JH. Elastic contact of rough spheres. *J Appl Mech* 1967;34:153-9.
- [484] Tworzydło W, Cecot W, Oden J, Yew C. Computational micro-and macroscopic models of contact and friction: formulation, approach and applications. *Wear* 1998;220:113-40.
- [485] Brzoza A, Pauk V. Torsion of rough elastic half-space by rigid punch. *Arch Appl Mech* 2008;78:531-42.
- [486] Barquins M, Courtel R, Maugis D. Friction on stretched rubber. *Wear* 1976;38:385-9.
- [487] Frétygny C, Chateauminos A. Contact of a spherical probe with a stretched rubber substrate. *Soft Matter* 2017;13:5849-57.
- [488] Autumn K, Liang YA, Hsieh ST, Zesch W, Chan WP, Kenny TW et al. Adhesive force of a single gecko foot-hair. *Nature* 2000;405:681-5.
- [489] Varenberg M, Pugno NM, Gorb SN. Spatulate structures in biological fibrillar adhesion. *Soft Matter* 2010;6:3269-72.
- [490] Filippov A, Popov VL, Gorb SN. Shear induced adhesion: Contact mechanics of biological spatula-like attachment devices. *J Theor Biol* 2011;276:126-31.
- [491] Labonte D, Williams JA, Federle W. Surface contact and design of fibrillar 'friction pads' in stick insects (*Carausius morosus*): mechanisms for large friction coefficients and negligible adhesion. *J R Soc Interface* 2014;11:20140034.
- [492] Barthlott W, Neinhuis C. Purity of the sacred lotus, or escape from contamination in biological surfaces. *Planta* 1997;202:1-8.
- [493] Burton Z, Bhushan B. Surface characterization and adhesion and friction properties of hydrophobic leaf surfaces. *Ultramicroscopy* 2006;106:709-19.
- [494] Stempflé P, Brendlé M. Tribological behaviour of nacre—influence of the environment on the elementary wear processes. *Tribol Int* 2006;39:1485-96.
- [495] Baum MJ, Kovalev AE, Michels J, Gorb SN. Anisotropic friction of the ventral scales in the snake *Lampropeltis getula californica*. *Tribology Letters* 2014;54:139-50.

- 1 [496] Dean B, Bhushan B. Shark-skin surfaces for fluid-drag reduction in turbulent flow: a review.  
2 Philos Trans A Math Phys Eng Sci 2010;368:4775-806.
- 3 [497] Federle W, Barnes WJ, Baumgartner W, Drechsler P, Smith JM. Wet but not slippery: Boundary  
4 friction in tree frog adhesive toe pads. J R Soc Interface 2006;3:689-97.
- 5 [498] Prevost A, Scheibert J, Debrégeas G. Effect of fingerprints orientation on skin vibrations during  
6 tactile exploration of textured surfaces. Communicative & integrative biology 2009;2:422-4.
- 7 [499] Derler S, Gerhardt L. Tribology of skin: review and analysis of experimental results for the  
8 friction coefficient of human skin. Tribology Letters 2012;45:1-27.
- 9 [500] Leyva-Mendivil MF, Lengiewicz J, Page A, Bressloff NW, Limbert G. Skin microstructure is a  
10 key contributor to its friction behaviour. Tribology Letters 2017;65:12.
- 11 [501] Lakes R. Materials with structural hierarchy. Nature 1993;361:511-5.
- 12 [502] Fratzl P, Weinkamer R. Nature's hierarchical materials. Progress in Materials Science  
13 2007;52:1263-334.
- 14 [503] Yurdumakan B, Ravivikar NR, Ajayan PM, Dhinojwala A. Synthetic gecko foot-hairs from  
15 multiwalled carbon nanotubes. Chemical Communications 2005:3799-801.
- 16 [504] Lee J, Bush B, Maboudian R, Fearing RS. Gecko-inspired combined lamellar and nanofibrillar  
17 array for adhesion on nonplanar surface. Langmuir 2009;25:12449-53.
- 18 [505] Singh A, Suh K. Biomimetic patterned surfaces for controllable friction in micro-and nanoscale  
19 devices. Micro and Nano Systems Letters 2013;1:6.
- 20 [506] Murarash B, Itovich Y, Varenberg M. Tuning elastomer friction by hexagonal surface  
21 patterning. Soft Matter 2011;7:5553-7.
- 22 [507] Li N, Xu E, Liu Z, Wang X, Liu L. Tuning apparent friction coefficient by controlled patterning  
23 bulk metallic glasses surfaces. Sci Rep 2016;6:39388.
- 24 [508] Borghi A, Gualtieri E, Marchetto D, Moretti L, Valeri S. Tribological effects of surface  
25 texturing on nitriding steel for high-performance engine applications. Wear 2008;265:1046-51.
- 26 [509] Gualtieri E, Borghi A, Calabri L, Pugno N, Valeri S. Increasing nanohardness and reducing  
27 friction of nitride steel by laser surface texturing. Tribol Int 2009;42:699-705.
- 28 [510] Baum MJ, Heepe L, Fadeeva E, Gorb SN. Dry friction of microstructured polymer surfaces  
29 inspired by snake skin. Beilstein J Nanotechnol 2014;5:1091-103.
- 30 [511] Maegawa S, Itoigawa F, Nakamura T. Effect of surface grooves on kinetic friction of a rubber  
31 slider. Tribol Int 2016;102:326-32.
- 32 [512] He B, Chen W, Wang QJ. Surface texture effect on friction of a microtextured poly  
33 (dimethylsiloxane)(PDMS). Tribology Letters 2008;31:187.
- 34 [513] Tay NB, Minn M, Sinha SK. A tribological study of SU-8 micro-dot patterns printed on Si  
35 surface in a flat-on-flat reciprocating sliding test. Tribology Letters 2011;44:167.
- 36 [514] Greiner C, Schäfer M, Popp U, Gumbsch P. Contact splitting and the effect of dimple depth on  
37 static friction of textured surfaces. ACS applied materials & interfaces 2014;6:7986-90.
- 38 [515] Giraud L, Bazin G, Giasson S. Lubrication with Soft and Hard Two-Dimensional Colloidal  
39 Arrays. Langmuir 2017;33:3610-23.
- 40 [516] Capozza R, Fasolino A, Ferrario M, Vanossi A. Lubricated friction on nanopatterned surfaces  
41 via molecular dynamics simulations. Physical Review B 2008;77:235432.
- 42 [517] Burridge R, Knopoff L. Model and theoretical seismicity. Bulletin of the seismological society  
43 of america 1967;57:341-71.
- 44 [518] Capozza R, Pugno N. Effect of surface grooves on the static friction of an elastic slider.  
45 Tribology Letters 2015;58:35.
- 46 [519] Costagliola G, Bosia F, Pugno NM. Static and dynamic friction of hierarchical surfaces.  
47 Physical Review E 2016;94:063003.
- 48 [520] Costagliola G, Bosia F, Pugno NM. Hierarchical spring-block model for multiscale friction  
49 problems. ACS Biomaterials Science & Engineering 2017.
- 50 [521] Capozza R, Rubinstein SM, Barel I, Urbakh M, Fineberg J. Stabilizing stick-slip friction. Phys  
51 Rev Lett 2011;107:024301.
- 52 [522] Pugno NM, Yin Q, Shi X, Capozza R. A generalization of the Coulomb's friction law: from  
53 graphene to macroscale. Meccanica 2013;48:1845-51.
- 54 [523] Tabor D. Surface forces and surface interactions. J Colloid Interface Sci 1977;58:2-13.
- 55  
56  
57  
58  
59  
60  
61  
62  
63  
64  
65

- [524] Maugis D. Contact, adhesion and rupture of elastic solids. : Springer Science & Business Media, 2013.
- [525] Muller V, Yushchenko V, Derjaguin B. On the influence of molecular forces on the deformation of an elastic sphere and its sticking to a rigid plane. *J Colloid Interface Sci* 1980;77:91-101.
- [526] Greenwood J. Adhesion of elastic spheres. *Proceedings of the Royal Society of London A: Mathematical, Physical and Engineering Sciences* 1997;453:1277-97.
- [527] Maugis D. Adhesion of spheres: The JKR-DMT transition using a dugdale model. *J Colloid Interface Sci* 1992;150:243-69.
- [528] Greenwood JA, Johnson KL. An alternative to the Maugis model of adhesion between elastic spheres. *J Phys D* 1998;31:3279-90.
- [529] Sauer RA, Li S. An atomic interaction-based continuum model for adhesive contact mechanics. *Finite Elements Anal Des* 2007;43:384-96.
- [530] Sauer RA, Wriggers P. Formulation and analysis of a three-dimensional finite element implementation for adhesive contact at the nanoscale. *Comput Methods Appl Mech Eng* 2009;198:3871-83.
- [531] Du Y, Chen L, McGruer NE, Adams GG, Etsion I. A finite element model of loading and unloading of an asperity contact with adhesion and plasticity. *J Colloid Interface Sci* 2007;312:522-8.
- [532] Eid H, Adams G, McGruer N, Fortini A, Buldyrev S, Srolovitz D. A combined molecular dynamics and finite element analysis of contact and adhesion of a rough sphere and a flat surface. *Tribol Trans* 2011;54:920-8.
- [533] Carbone G, Mangialardi L. Adhesion and friction of an elastic half-space in contact with a slightly wavy rigid surface. *J Mech Phys Solids* 2004;52:1267-87.
- [534] Carbone G, Mangialardi L. Analysis of the adhesive contact of confined layers by using a Green's function approach. *J Mech Phys Solids* 2008;56:684-706.
- [535] Fuller K, Tabor D. The effect of surface roughness on the adhesion of elastic solids. 1975;345:327-42.
- [536] Maugis D. On the contact and adhesion of rough surfaces. *J Adhes Sci Technol* 1996;10:161-75.
- [537] Chang W, Etsion I, Bogy D. Adhesion model for metallic rough surfaces. *Journal of Tribology* 1988;110:50-6.
- [538] Sergici AO, Adams GG, Müftü S. Adhesion in the contact of a spherical indenter with a layered elastic half-space. *J Mech Phys Solids* 2006;54:1843-61.
- [539] Johnson KL, Greenwood JA. An Adhesion Map for the Contact of Elastic Spheres. *J Colloid Interface Sci* 1997;192:326-33.
- [540] Yao H, Ciavarella M, Gao H. Adhesion maps of spheres corrected for strength limit. *J Colloid Interface Sci* 2007;315:786-90.
- [541] Persson B, Tosatti E. The effect of surface roughness on the adhesion of elastic solids. *J Chem Phys* 2001;115:5597-610.
- [542] Persson BN, Scaraggi M. Theory of adhesion: role of surface roughness. *J Chem Phys* 2014;141:124701.
- [543] Persson B. Adhesion between an elastic body and a randomly rough hard surface. *The European Physical Journal E: Soft Matter and Biological Physics* 2002;8:385-401.
- [544] Yong CW, Kendall K, Smith W. Atomistic studies of surface adhesions using molecular-dynamics simulations. *Philosophical Transactions of the Royal Society A: Mathematical, Physical and Engineering Sciences* 2004;362:1915-30.
- [545] Deng Z, Smolyanitsky A, Li Q, Feng X, Cannara RJ. Adhesion-dependent negative friction coefficient on chemically modified graphite at the nanoscale. *Nature materials* 2012;11:1032-7.
- [546] Pastewka L, Robbins MO. Contact between rough surfaces and a criterion for macroscopic adhesion. *Proceedings of the National Academy of Sciences* 2014;111:3298-303.
- [547] Wu J. Numerical analyses on elliptical adhesive contact. *J Phys D* 2006;39:1899.
- [548] Bazrafshan M, de Rooij M, Valefi M, Schipper D. Numerical method for the adhesive normal contact analysis based on a Dugdale approximation. *Tribol Int* 2017;112:117-28.
- [549] Medina S, Dini D. A numerical model for the deterministic analysis of adhesive rough contacts down to the nano-scale. *Int J Solids Structures* 2014;51:2620-32.

- 1 [550] Ciavarella M. On a recent stickiness criterion using a very simple generalization of DMT theory  
2 of adhesion. *J Adhes Sci Technol* 2016;30:2725-35.
- 3 [551] Gropper D, Wang L, Harvey TJ. Hydrodynamic lubrication of textured surfaces: A review of  
4 modeling techniques and key findings. *Tribol Int* 2016;94:509-29.
- 5 [552] Greiner C, Schäfer M. Bio-inspired scale-like surface textures and their tribological properties.  
6 *Bioinspiration & biomimetics* 2015;10:044001.
- 7 [553] Elrod HG, Adams ML. A Computer Program for Cavitation and Starvation Problems 1974:37-  
8 41.
- 9 [554] Elrod HG. A cavitation algorithm. *ASME J.Lubr.Technol.* 1981;103:350.
- 10 [555] Jakobsson B, Floberg L. The finite journal bearing considering vaporization. *Transactions of*  
11 *Chalmers University of Technology* 1957;190:1-116.
- 12 [556] Olsson K. Cavitation in dynamically loaded bearing. *Trans.Chalmers Univ.of Tech, Sweden*  
13 *1957;308.*
- 14 [557] Braun M, Hannon W. Cavitation formation and modelling for fluid film bearings: a review. *Proc*  
15 *Inst Mech Eng Part J* 2010;224:839-63.
- 16 [558] Sahlin F, Almqvist A, Larsson R, Glavatskih S. Rough surface flow factors in full film  
17 lubrication based on a homogenization technique. *Tribol Int* 2007;40:1025-34.
- 18 [559] Patir N, Cheng H. An Average Flow Model for Determining Effects of Three-Dimensional  
19 Roughness on Partial Hydrodynamic Lubrication. *Journal of Lubrication Technology* 1978;100.
- 20 [560] Elrod H. A general theory for laminar lubrication with Reynolds roughness. *Journal of*  
21 *Lubrication Technology* 1979;101:8-14.
- 22 [561] Tripp J. Surface roughness effects in hydrodynamic lubrication: the flow factor method. *Journal*  
23 *of Lubrication Technology* 1983;105:458-65.
- 24 [562] Scaraggi M, Carbone G, Persson BN, Dini D. Lubrication in soft rough contacts: A novel  
25 homogenized approach. Part I-Theory. *Soft Matter* 2011;7:10395-406.
- 26 [563] Miyoshi K. *Solid lubrication fundamentals and applications.* : CRC Press, 2001.
- 27 [564] Wornyoh EY, Jasti VK, Higgs CF. A review of dry particulate lubrication: powder and granular  
28 materials. *Journal of Tribology* 2007;129:438-49.
- 29 [565] Jang J, Khonsari M. On the granular lubrication theory. 2005;461:3255-78.
- 30 [566] Haff P. Grain flow as a fluid-mechanical phenomenon. *J Fluid Mech* 1983;134:401-30.
- 31 [567] Lun C, Savage SB, Jeffrey D, Chepurniy N. Kinetic theories for granular flow: inelastic particles  
32 in Couette flow and slightly inelastic particles in a general flowfield. *J Fluid Mech*  
33 *1984;140:223-56.*
- 34 [568] Lun C, Savage S. A simple kinetic theory for granular flow of rough, inelastic, spherical  
35 particles. *J.Appl.Mech* 1987;54:47-53.
- 36 [569] Iordanoff I, Berthier Y, Descartes S, Heshmat H. A review of recent approaches for modeling  
37 solid third bodies. *Journal of Tribology* 2002;124:725-35.
- 38 [570] Heshmat H. The rheology and hydrodynamics of dry powder lubrication. *Tribol Trans*  
39 *1991;34:433-9.*
- 40 [571] Cundall PA, Strack OD. A discrete numerical model for granular assemblies. *Geotechnique*  
41 *1979;29:47-65.*
- 42 [572] Neukirchner J. Tribocorrosion and ways of prevention. *Maschinenbautechnik* 1980;29:313-6.
- 43 [573] Ahn BK, Lee DW, Israelachvili JN, Waite JH. Surface-initiated self-healing of polymers in  
44 aqueous media. *Nature materials* 2014;13:867-72.
- 45 [574] Olabisi O, Adewale K. *Handbook of thermoplastics.* : CRC press, 2016.
- 46 [575] Bao G, Suresh S. Cell and molecular mechanics of biological materials. *Nature materials*  
47 *2003;2:715-25.*
- 48 [576] Licup AJ, Munster S, Sharma A, Sheinman M, Jawerth LM, Fabry B et al. Stress controls the  
49 mechanics of collagen networks. *Proc Natl Acad Sci U S A* 2015;112:9573-8.
- 50 [577] Heepe L, Gorb SN. Biologically inspired mushroom-shaped adhesive microstructures. *Annual*  
51 *Review of Materials Research* 2014;44:173-203.
- 52 [578] Rus D, Tolley MT. Design, fabrication and control of soft robots. *Nature* 2015;521:467-75.
- 53 [579] Marx N, Guegan J, Spikes HA. Elastohydrodynamic film thickness of soft EHL contacts using  
54 optical interferometry. *Tribol Int* 2016;99:267-77.
- 55  
56  
57  
58  
59  
60  
61  
62  
63  
64  
65

- 1 [580] Hutt W, Persson B. Soft matter dynamics: accelerated fluid squeeze-out during slip. *J Chem*  
2 *Phys* 2016;144:124903.
- 3 [581] Scaraggi M, Persson B. Theory of viscoelastic lubrication. *Tribol Int* 2014;72:118-30.
- 4 [582] Putignano C, Dini D. Soft matter lubrication: does solid viscoelasticity matter? *ACS Applied*  
5 *Materials & Interfaces* 2017;Submitted.
- 6 [583] Selway N, Chan V, Stokes JR. Influence of fluid viscosity and wetting on multiscale viscoelastic  
7 lubrication in soft tribological contacts. *Soft Matter* 2017;13:1702-15.
- 8 [584] Putignano C, Carbone G, Dini D. Theory of reciprocating contact for viscoelastic solids. *Phys*  
9 *Rev E* 2016;93:043003.
- 10 [585] Hatchett C. Experiments and Observations on the Various Alloys, on the Specific Gravity, and  
11 on the Comparative Wear of Gold. Being the Substance of a Report Made to the Right  
12 Honourable the Lords of the Committee of Privy Council, Appointed to Take into Consideration  
13 the State of the Coins of This Kingdom, and the Present Establishment and Constitution of His  
14 Majesty's Mint. *Philosophical Transactions of the Royal Society of London* 1803;93:43-194.
- 15 [586] Archard JF. Contact and rubbing of flat surfaces. *J Appl Phys* 1953;24:981-8.
- 16 [587] Schirmeisen A. Wear: one atom after the other. *Nature nanotechnology* 2013;8:81-2.
- 17 [588] Meng HC, Ludema KC. Wear models and predictive equations: their form and content. *Wear*  
18 1995;181-183, Part 2:443.
- 19 [589] Binnig G, Quate CF, Gerber C. Atomic Force Microscope. *Phys Rev Lett* 1986;56:930-3.
- 20 [590] Jacobs TDB, Gotsmann B, Lantz MA, Carpick RW. On the Application of Transition State  
21 Theory to Atomic-Scale Wear. *Tribology Letters* 2010;39:257-71.
- 22 [591] Bhaskaran H, Gotsmann B, Sebastian A, Drechsler U, Lantz MA, Despont M et al. Ultralow  
23 nanoscale wear through atom-by-atom attrition in silicon-containing diamond-like carbon.  
24 *Nature Nanotechnology* 2010;5:181-5.
- 25 [592] Gotsmann B, Lantz MA. Atomistic Wear in a Single Asperity Sliding Contact. *Phys Rev Lett*  
26 2008;101:125501.
- 27 [593] Sato T, Ishida T, Jalabert L, Fujita H. Real-time transmission electron microscope observation of  
28 nanofriction at a single Ag asperity. *Nanotechnology* 2012;23:505701.
- 29 [594] Merkle AP, Marks LD. Liquid-like tribology of gold studied by in situ \TEM\. *Wear*  
30 2008;265:1864-9.
- 31 [595] Vahdat V, Grierson DS, Turner KT, Carpick RW. Mechanics of Interaction and Atomic-Scale  
32 Wear of Amplitude Modulation Atomic Force Microscopy Probes. *ACS Nano* 2013;7:3221-35.
- 33 [596] Chung K. Wear characteristics of atomic force microscopy tips: A reiew. *International Journal*  
34 *of Precision Engineering and Manufacturing* 2014;15:2219-30.
- 35 [597] Liu J, Notbohm JK, Carpick RW, Turner KT. Method for Characterizing Nanoscale Wear of  
36 Atomic Force Microscope Tips. *ACS Nano* 2010;4:3763-72.
- 37 [598] Chung K, Kim D. Fundamental Investigation of Micro Wear Rate Using an Atomic Force  
38 Microscope. *Tribology Letters* 2003;15:135-44.
- 39 [599] Ciavarella M. On the effect of wear on asperity height distributions, and the corresponding effect  
40 in the mechanical response. *Tribol Int* 2016;101:164.
- 41 [600] de Beer S, Müser MH. Viewpoint: Surface Folds Make Tears and Chips. *Physics* 2012;5:100.
- 42 [601] Filippov AE, Popov VL, Urbakh M. Mechanism of Wear and Ripple Formation Induced by the  
43 Mechanical Action of an Atomic Force Microscope Tip. *Phys Rev Lett* 2011;106:025502.
- 44 [602] Sutton D, Limbert G, Stewart D, Wood R. A functional form for wear depth of a ball and a flat  
45 surface. *Tribology letters* 2014;53:173-9.
- 46 [603] Singer IL. How third-body processes affect friction and wear. *MRS Bull* 1998;23:37-40.
- 47 [604] Singer I, Dvorak S, Wahl K, Scharf T. Role of third bodies in friction and wear of protective  
48 coatings. *Journal of Vacuum Science & Technology A: Vacuum, Surfaces, and Films*  
49 2003;21:S232-40.
- 50 [605] Molinari J-, Ortiz M, Radovitzky R, Repetto EA. Finite element modeling of dry sliding wear in  
51 metals. *Eng Comput* 2001;18:592-610.
- 52 [606] Andersson J, Almqvist A, Larsson R. Numerical simulation of a wear experiment. *Wear*  
53 2011;271:2947.
- 54  
55  
56  
57  
58  
59  
60  
61  
62  
63  
64  
65

- 1 [607] Furustig J, Dobryden I, Almqvist A, Almqvist N, Larsson R. The measurement of wear using  
2 AFM and wear interpretation using a contact mechanics coupled wear model. *Wear*  
3 2016;350:74.
- 4 [608] Lengiewicz J, Stupkiewicz S. Continuum framework for finite element modelling of finite wear.  
5 *Comput Methods Appl Mech Eng* 2012;205:178-88.
- 6 [609] Lengiewicz J, Stupkiewicz S. Efficient model of evolution of wear in quasi-steady-state sliding  
7 contacts. *Wear* 2013;303:611.
- 8 [610] Dimaki AV, Dmitriev AI, Menga N, Papangelo A, Ciavarella M, Popov VL. Fast High-  
9 Resolution Simulation of the Gross Slip Wear of Axially Symmetric Contacts. *Tribol Trans*  
10 2016;59:189-94.
- 11 [611] Akchurin A, Bosman R, Lugt PM. A Stress-Criterion-Based Model for the Prediction of the Size  
12 of Wear Particles in Boundary Lubricated Contacts. *Tribology Letters* 2016;64:35.
- 13 [612] Song H, Dikken RJ, Nicola L, Van der Giessen E. Plastic Ploughing of a Sinusoidal Asperity on  
14 a Rough Surface. *ASME.J.Appl.Mech.* 2015;82:071006,071006-8.
- 15 [613] Sun F, Van der Giessen E, Nicola L. Dry frictional contact of metal asperities: A dislocation  
16 dynamics analysis. *Acta Materialia* 2016;109:162.
- 17 [614] Stoyanov P, Romero PA, Merz R, Kopnarski M, Stricker M, Stemmer P et al. Nanoscale sliding  
18 friction phenomena at the interface of diamond-like carbon and tungsten. *Acta Materialia*  
19 2014;67:395.
- 20 [615] Pastewka L, Moser S, Gumbsch P, Moseler M. Anisotropic mechanical amorphization drives  
21 wear in diamond. *Nature Materials* 2011;10:34-8.
- 22 [616] von Lantz J, Pastewka L, Gumbsch P, Moseler M. Molecular Dynamic Simulation of Collision-  
23 Induced Third-Body Formation in Hydrogen-Free Diamond-Like Carbon Asperities. *Tribology*  
24 *Letters* 2016;63:26.
- 25 [617] Sha Z, Sorkin V, Branicio PS, Pei Q, Zhang Y, Srolovitz DJ. Large-scale molecular dynamics  
26 simulations of wear in diamond-like carbon at the nanoscale. *Appl Phys Lett* 2013;103:073118.
- 27 [618] Hu X, Martini A. Atomistic simulation of the effect of roughness on nanoscale wear.  
28 *Computational Materials Science* 2015;102:208.
- 29 [619] Hu X, Sundararajan S, Martini A. The effects of adhesive strength and load on material transfer  
30 in nanoscale wear. *Computational Materials Science* 2014;95:464.
- 31 [620] Li A, Szlufarska I. How grain size controls friction and wear in nanocrystalline metals.  
32 *Phys.Rev.B* 2015;92:075418.
- 33 [621] Eder S, Vernes A, Vorlaufer G, G. B. Molecular dynamics simulations of mixed lubrication with  
34 smooth particle post-processing. *J Phys : Cond Matter* 2011;23:175004.
- 35 [622] Mishra M, Tangpatjaroen C, Szlufarska I. Plasticity-Controlled Friction and Wear in  
36 Nanocrystalline SiC. *J Am Ceram Soc* 2014;97:1194-201.
- 37 [623] Pastewka L, Mrovec M, Moseler M, Gumbsch P. Bond order potentials for fracture, wear, and  
38 plasticity. *MRS Bull* 2012;37:493-503.
- 39 [624] Renouf M, Massi F, Fillot N, Saulot A. Numerical tribology of a dry contact. *Tribol Int*  
40 2011;44:834.
- 41 [625] Fillot N, Iordanoff I, Berthier Y. Wear modeling and the third body concept. *Wear*  
42 2007;262:949.
- 43 [626] Aghababaei R, Warner DH, Molinari J. On the debris-level origins of adhesive wear.  
44 *Proceedings of the National Academy of Sciences* 2017;114:7935-40.
- 45 [627] Reye T. Zur theorie der zapfenreibung. *Der Civilingenieur* 1860;4:235-55.
- 46 [628] Grossiord C, Varlot K, Martin J-, Le Mogne T, Esnouf C, Inoue K. MoS<sub>2</sub> single sheet  
47 lubrication by molybdenum dithiocarbamate. *Tribol Int* 1998;31:737-43.
- 48 [629] De Feo M, Minfray C, De Barros Bouchet MI, Thiebaut B, Le Mogne T, Vacher B et al. Ageing  
49 impact on tribological properties of MoDTC-containing base oil. *Tribol Int* 2015;92:126-35.
- 50 [630] Mangolini F, Rossi A, Spencer ND. In Situ Attenuated Total Reflection (ATR/FT-IR)  
51 Tribometry: A Powerful Tool for Investigating Tribochemistry at the Lubricant-Substrate  
52 Interface. *Tribology Letters* 2012;45:207-18.
- 53 [631] Gosvami NN, Bares JA, Mangolini F, Konicek AR, Yablon DG, Carpick RW. Mechanisms of  
54 antiwear tribofilm growth revealed in situ by single-asperity sliding contacts. *Science*  
55 2015;348:102.
- 56  
57  
58  
59  
60  
61  
62  
63  
64  
65



- 1 [632] Jacobs TDB, Carpick RW. Nanoscale wear as a stress-assisted chemical reaction. *Nat Nano*  
2 2013;8:108-12.
- 3 [633] Lahouij I, Dassenoy F, Vacher B, Martin J. Real Time TEM Imaging of Compression and Shear  
4 of Single Fullerene-Like MoS<sub>2</sub> Nanoparticle. *Tribology Letters* 2012;45:131-41.
- 5 [634] Campen S, Green JH, Lamb GD, Spikes HA. In Situ Study of Model Organic Friction Modifiers  
6 Using Liquid Cell AFM; Saturated and Mono-unsaturated Carboxylic Acids. *Tribology Letters*  
7 2015;57:18.
- 8 [635] Mori S, Imaizumi Y. Adsorption of Model Compounds of Lubricant on Nascent Surfaces of  
9 Mild and Stainless Steels under Dynamic Conditions. *Tribol Trans* 1988;31:449-53.
- 10 [636] Hiratsuka K, Abe T, Kajdas C. Tribocatalytic oxidation of ethylene in the rubbing of palladium  
11 against aluminum oxide. *Tribol Int* 2010;43:1659-64.
- 12 [637] Nakayama K. Mechanism of Triboplasma Generation in Oil. *Tribology Letters* 2011;41:345-51.
- 13 [638] Furlong O, Miller B, Kotvis P, Adams H, Tysoe WT. Shear and thermal effects in boundary film  
14 formation during sliding. *RSC Adv* 2014;4:24059-66.
- 15 [639] Crobu M, Rossi A, Spencer ND. Effect of Chain-Length and Countersurface on the  
16 Tribochemistry of Bulk Zinc Polyphosphate Glasses. *Tribology Letters* 2012;48:393-406.
- 17 [640] Berkani S, Dassenoy F, Minfray C, Belin M, Vacher B, Martin JM et al. Model formation of  
18 ZDDP tribofilm from a mixture of zinc metaphosphate and goethite. *Tribol Int* 2014;79:197-  
19 203.
- 20 [641] Spikes H, Tysoe W. On the Commonality Between Theoretical Models for Fluid and Solid  
21 Friction, Wear and Tribochemistry. *Tribology Letters* 2015;59:1-14.
- 22 [642] Park S, Costa KD, Ateshian GA. Microscale frictional response of bovine articular cartilage  
23 from atomic force microscopy. *J Biomech* 2004;37:1679-87.
- 24 [643] Coles JM, Blum JJ, Jay GD, Darling EM, Guilak F, Zauscher S. In situ friction measurement on  
25 murine cartilage by atomic force microscopy. *J Biomech* 2008;41:541-8.
- 26 [644] Chan S, Neu C, DuRaine G, Komvopoulos K, Reddi AH. Atomic force microscope  
27 investigation of the boundary-lubricant layer in articular cartilage. *Osteoarthritis and Cartilage*  
28 2010;18:956-63.
- 29 [645] Gispert MP, Serro AP, Colaco R, Saramago B. Friction and wear mechanisms in hip prosthesis:  
30 Comparison of joint materials behaviour in several lubricants. *Wear* 2006;260:149-58.
- 31 [646] Ebenstein DM, Kuo A, Rodrigo JJ, Reddi AH, Ries M, Pruitt L. A nanoindentation technique  
32 for functional evaluation of cartilage repair tissue. *J Mater Res* 2004;19:273-81.
- 33 [647] Li C, Pruitt LA, King KB. Nanoindentation differentiates tissue- scale functional properties of  
34 native articular cartilage. *Journal of Biomedical Materials Research Part A* 2006;78:729-38.
- 35 [648] Darling EM, Wilusz RE, Bolognesi MP, Zauscher S, Guilak F. Spatial mapping of the  
36 biomechanical properties of the pericellular matrix of articular cartilage measured in situ via  
37 atomic force microscopy. *Biophys J* 2010;98:2848-56.
- 38 [649] Stolz M, Raiteri R, Daniels A, VanLandingham MR, Baschong W, Aebi U. Dynamic elastic  
39 modulus of porcine articular cartilage determined at two different levels of tissue organization  
40 by indentation-type atomic force microscopy. *Biophys J* 2004;86:3269-83.
- 41 [650] Stolz M, Aebi U, Stoffler D. Developing scanning probe-based nanodevices—stepping out of  
42 the laboratory into the clinic. *Nanomedicine: Nanotechnology, Biology and Medicine*  
43 2007;3:53-62.
- 44 [651] Ateshian GA. The role of interstitial fluid pressurization in articular cartilage lubrication. *J*  
45 *Biomech* 2009;42:1163-76.
- 46 [652] Zappone B, Greene GW, Oroudjev E, Jay GD, Israelachvili JN. Molecular aspects of boundary  
47 lubrication by human lubricin: effect of disulfide bonds and enzymatic digestion. *Langmuir*  
48 2008;24:1495-508.
- 49 [653] Chang DP, Abu-Lail NI, Coles JM, Guilak F, Jay GD, Zauscher S. Friction force microscopy of  
50 lubricin and hyaluronic acid between hydrophobic and hydrophilic surfaces. *Soft Matter*  
51 2009;5:3438-45.
- 52 [654] Benz M, Chen N, Israelachvili J. Lubrication and wear properties of grafted polyelectrolytes,  
53 hyaluronan and hylan, measured in the surface forces apparatus. *Journal of Biomedical*  
54 *Materials Research Part A* 2004;71:6-15.
- 55  
56  
57  
58  
59  
60  
61  
62  
63  
64  
65

- [655] Dean D, Han L, Ortiz C, Grodzinsky AJ. Nanoscale conformation and compressibility of cartilage aggrecan using microcontact printing and atomic force microscopy. *Macromolecules* 2005;38:4047-9.
- [656] Limbert G. Mathematical and computational modelling of skin biophysics: a review. 2017;473:20170257.
- [657] Burns D, Breathnach S, Cox N, Griffiths CE. *Rook's Textbook of Dermatology* (4 vol. set.). 2004.
- [658] Silver FH, Siperko LM, Seehra GP. Mechanobiology of force transduction in dermal tissue. *Skin Research and Technology* 2003;9:3-23.
- [659] Leyva-Mendivil MF, Page A, Bressloff NW, Limbert G. A mechanistic insight into the mechanical role of the stratum corneum during stretching and compression of the skin. *Journal of the Mechanical Behavior of Biomedical Materials* 2015;49:197-219.
- [660] Leyva-Mendivil MF, Lengiewicz J, Page A, Bressloff NW, Limbert G. Implications of multi-asperity contact for shear stress distribution in the viable epidermis – an image-based finite element study. *Biotribology* 2017.
- [661] Zhou Z, Jin Z. *Biotribology: recent progresses and future perspectives*. *Biosurface and Biotribology* 2015;1:3-24.
- [662] Adams M, Briscoe B, Johnson S. Friction and lubrication of human skin. *Tribology letters* 2007;26:239-53.
- [663] Gerhardt LC, Strassle V, Lenz A, Spencer ND, Derler S. Influence of epidermal hydration on the friction of human skin against textiles. *J R Soc Interface* 2008;5:1317-28.
- [664] Kwiatkowska M, Franklin S, Hendriks C, Kwiatkowski K. Friction and deformation behaviour of human skin. *Wear* 2009;267:1264-73.
- [665] Wolfram L. Friction of skin. *Journal of the Society of Cosmetic Chemists* 1983;34:465-76.
- [666] Stupkiewicz S, Lewandowski MJ, Lengiewicz J. Micromechanical analysis of friction anisotropy in rough elastic contacts. *Int J Solids Structures* 2014;51:3931-43.
- [667] Geerligs M, Oomens C, Ackermans P, Baaijens F, Peters G. Linear shear response of the upper skin layers. *Biorheology* 2011;48:229-45.
- [668] Goldstein B, Sanders J. Skin response to repetitive mechanical stress: a new experimental model in pig. *Arch Phys Med Rehabil* 1998;79:265-72.
- [669] Lamers E, Van Kempen T, Baaijens F, Peters G, Oomens C. Large amplitude oscillatory shear properties of human skin. *Journal of the Mechanical Behavior of Biomedical Materials* 2013;28:462-70.
- [670] Chu Y, Dufour S, Thiery JP, Perez E, Pincet F. Johnson-Kendall-Roberts theory applied to living cells. *Phys Rev Lett* 2005;94:028102.
- [671] Li S, Sun B. *Advances in cell mechanics*. : Springer, 2012.
- [672] Borodich FM, Galanov BA, Keer LM, Suarez-Alvarez MM. Problems of adhesive contact interactions between prestressed biological cells. 2015.
- [673] Kendall K, Kendall M, Rehfeldt F. *Adhesion of cells, viruses and nanoparticles*. : Springer Science & Business Media, 2010.
- [674] Korayem MH, Rastegar Z, Taheri M. Application of Johnson-Kendall-Roberts model in nanomanipulation of biological cell: air and liquid environment. *Micro & Nano letters* 2012;7:576-80.
- [675] Lenarda P, Gizzi A, Paggi M. A modeling framework for contact, adhesion and mechano-transduction between excitable deformable cells. arXiv preprint arXiv:1707.00920 2017.
- [676] McCain ML, Lee H, Aratyn-Schaus Y, Kléber AG, Parker KK. Cooperative coupling of cell-matrix and cell-cell adhesions in cardiac muscle. *Proceedings of the National Academy of Sciences* 2012;109:9881-6.
- [677] Bueno-Orovio A, Cherry EM, Fenton FH. Minimal model for human ventricular action potentials in tissue. *J Theor Biol* 2008;253:544-60.
- [678] Hurtado DE, Castro S, Gizzi A. Computational modeling of non-linear diffusion in cardiac electrophysiology: A novel porous-medium approach. *Comput Methods Appl Mech Eng* 2016;300:70-83.
- [679] Ambrosi D, Arioli G, Nobile F, Quarteroni A. Electromechanical Coupling in Cardiac Dynamics: The Active Strain Approach. *SIAM J Appl Math* 2011;71:605-21.

- 1 [680] Wong J, Goktepe S, Kuhl E. Computational modeling of chemo- • electro- • mechanical  
2 coupling: A novel implicit monolithic finite element approach. *International journal for*  
3 *numerical methods in biomedical engineering* 2013;29:1104-33.
- 4 [681] Ruiz-Baier R, Gizzi A, Rossi S, Cherubini C, Laadhari A, Filippi S et al. Mathematical  
5 modelling of active contraction in isolated cardiomyocytes. *Mathematical Medicine and Biology*  
6 2014;31:259-83.
- 7 [682] Paggi M, Gizzi A. A Computational Framework for Nonlinear Contact between Deformable  
8 Excitable Biological Cells. 2016.
- 9 [683] Paggi M, Barber JR. Contact conductance of rough surfaces composed of modified RMD  
10 patches. *Int J Heat Mass Transfer* 2011;54:4664-72.
- 11 [684] Hol J, Cid Alfaro MV, Meinders VT, Huetink J. Advanced friction modeling in sheet metal  
12 forming. *Key Eng Mat* 2011;473:715-22.
- 13 [685] Ewen JP, Restrepo SE, Morgan N, Dini D. Nonequilibrium molecular dynamics simulations of  
14 stearic acid adsorbed on iron surfaces with nanoscale roughness. *Tribol Int* 2017;107:264-73.
- 15 [686] Tadmor EB, Ortiz M, Phillips R. Quasicontinuum analysis of defects in solids. *Philos Mag A*  
16 1996;73:1529-63.
- 17 [687] Smith E, Trevelyan D. cpl-library: CPL library with a new streamlined Interface. 2016.
- 18  
19  
20

---

21 <sup>i</sup> Despite the fact that the task set by the challenge was well-defined in scope (only elastic deformations, no shape  
22 but only a single realization of a nominally flat infinite rough surface to consider, modest adhesion, and well-  
23 detailed information including some data files to start with), still Martin Müser remarked that reaching the stage  
24 where different groups would provide results in the same units, and putting together the amount of information  
25 obtained, was not an easy task, involving more than 1,400 email exchanges.

26  
27  
28  
29  
30  
31  
32  
33  
34  
35  
36  
37  
38  
39  
40  
41  
42  
43  
44  
45  
46  
47  
48  
49  
50  
51  
52  
53  
54  
55  
56  
57  
58  
59  
60  
61  
62  
63  
64  
65

Figure(s)

# Modelling in Tribology: from Electrons to Machines

